

**Profiling the Protein Corona of Human Saliva Interacted Dietary
Particles and Understanding the Effect of Silica Particles on the
Structure and Function of Salivary α -amylase.**

By

Divya Srinivasan

**Department of Food Science and Agricultural Chemistry
Macdonald campus, McGill University,
Montreal, Quebec**

**A thesis submitted to McGill University in Partial Fulfilment of the requirements
of the degree of Master of Science**

May, 2019

©Divya Srinivasan, 2019

This thesis is dedicated to my parents, Israel Borochof, Research supervisor and my close friends who supported me throughout my journey in here.

ACKNOWLEDGEMENTS

First and foremost, I offer my sincere gratitude to my research supervisor, Dr. Saji George, who has supported me throughout my thesis with his motivation, knowledge and financial support whilst allowing me to work under his supervision.

I would like to thank Dr. Salwa Karboune, Dr. Varoujan Yaylayan and Dr. Shiv O Prasher for giving access to some of their laboratory facilities to support my research work.

I would like to thank Dr. Lorne from Proteomic platform and the services of the RIMUHC Clinical proteomics platform for proteomic analysis and PhD student MS. Debora Viera from biomass production lab to help me with some technical information in handling proteomic data.

I would also like to thank Dr. Armando Jardim from parasitology department, McGill for his technical advice and ideas in relation to my research work.

Finally, I would like to thank my colleagues Ms. Wut Hmone Phue and Ms. Iris Xu to share their hands-on experience and support me in completing some of my experiments. A special thanks to Stephanie Lacoste from Food Science department and Amanda Turiff from Bioresource Engineering department for helping me to translate my abstract in French.

AUTHOR CONTRIBUTION

D.S. designed the study and performed all the experiments. S.G. supervised and directed the projects. K.X. helped in synthesizing the citrate coated gold NPs. W.H. and K.X. worked on the physical characterization of NPs using SEM. D.S. wrote the manuscript in supervision with S.G.

TABLE OF CONTENT

TITLE.....	i
ACKNOWLEDGEMENT.....	iii
AUTHOR CONTRIBUTION.....	iv
TABLE OF CONTENTS.....	v
LIST OF TABLES.....	viii
LIST OF FIGURES.....	ix
ABBREVIATIONS.....	xii
OBJECTIVES OF RESEARCH.....	xv
CHAPTER1 LITERATURE REVIEW	1
1.1 ABSTRACT:.....	1
1.2 RÉSUMÉ :	2
1.3 OBJECTIVE:	3
1.4 INTRODUCTION:.....	4
1.5 NPS ARE ALL AROUND US: HISTORICAL ASPECT & BACKGROUND	4
1.6 WHAT MAKES NPS UNIQUE:	6
1.7 CLASSIFICATION OF NANOMATERIALS:	7
1.8 NANOTECHNOLOGY IN FOOD INDUSTRY:.....	8
1.9 IS NANOTECHNOLOGY A SAFE APPLICATION IN FOOD SECTOR?	9
1.10 NANOFOOD AND COMMONLY USED ENMS IN FOOD & FOOD PACKAGING INDUSTRY:	10
1.11 FOOD APPLICATION AND SURFACE PROPERTIES OF COMMONLY USED DIETARY NPS SiO ₂ , TiO ₂ AND Ag NPS:	12
1.11.1 Physical Properties and Surface Chemistry of Food Grade Silica:	12
1.11.2 Application of SiO ₂ in Food:	14
1.11.3 Physical Properties and Surface Chemistry of Titanium Dioxide:	14
1.11.4 Application of TiO ₂ in Food:	15
1.11.5 Physical Properties and Surface Chemistry of Nano Silver:	16
1.11.6 Application of Nano Silver in Food:.....	17
1.12 NP -PROTEIN CORONA:	19
1.12.1 Introduction:.....	19
1.12.2 What is Protein Corona:	19
1.12.3 Evolution of the Concept of NP Corona:	19
1.12.4 Current Knowledge on the Biological Identity of NPs:.....	20
1.12.5 Mechanism and Kinetics of Protein Adsorption:.....	21
1.12.6 Formation of the Protein Corona:.....	24
1.12.7 Composition of Protein Corona:	25
1.12.8 Influence of Protein Conformation on Protein Corona:	27
1.13 ANALYTICAL APPROACHES TO STUDY THE NP -PROTEIN INTERACTIONS:.....	30
1.14 CHARACTERIZATION OF PROTEIN CORONA:	31
1.14.1 Indirect Method:.....	31
1.14.2 Direct Methods:.....	33
1.15 LIMITATION OF Ex -VIVO STUDY ON CHARACTERIZING PROTEIN CORONA FORMATION:	40
1.16 ADVANCEMENT IN THE NP-PC CHARACTERIZATION:	41
1.17 EFFECT OF DIFFERENT PARAMETERS AFFECTING BIOMOLECULAR CORONA:	43
1.18 EFFECT OF PHYSIOLOGICAL CONDITION/SUSPENDING MEDIA PROPERTIES ON PROTEIN CORONA FORMATION:	45

1.18.1	Media Composition:	45
1.18.2	Exposure Time, Temperature, pH and static & Fluidic Conditions:.....	45
1.18.3	Protein Concentration:	47
1.18.4	Effect of Nanomaterial Properties on the Protein Corona Formation:	49
1.18.5	Size & Curvature:	49
1.18.6	Surface Area and NP-Protein Ratio:	50
1.18.7	Surface Properties:	51
1.19	HUMAN WHOLE SALIVA:.....	53
1.20	INTRODUCTION:.....	53
1.21	COMPOSITION AND FUNCTIONS:	53
1.21.1	Potential Challenges with Identification of Salivary Proteins:	55
1.22	THE HUMAN SALIVARY PROTEOME:.....	55
1.23	CURRENT STATUS IN SALIVARY PROTEOME DATABASE:.....	62
1.24	INTERACTION BETWEEN INGESTED DIETARY NPS AND THE GASTROINTESTINAL TRACT:.....	62
1.25	KNOWLEDGE GAP	66
1.26	HYPOTHESIS:	68
1.27	CONCLUSION.....	68
1.28	REFERENCE:	69
CHAPTER2	THE TYPE OF DIETARY NPS INFLUENCES SALIVARY PROTEIN CORONA COMPOSITION	80
2.1	ABSTRACT:.....	80
2.2	RÉSUMÉ :	ERROR! BOOKMARK NOT DEFINED.
2.3	KEY WORDS:	82
2.4	INTRODUCTION:.....	82
2.5	MATERIALS AND METHODS:.....	83
2.5.1	Materials:.....	83
2.5.2	NPs Used in the Study:	84
2.5.3	Physical Characterization:.....	84
2.5.4	Human Saliva Collection and Processing:	85
2.5.5	Preparation of Saliva Interacted Dietary Particles:.....	85
2.5.6	Desorption of Salivary Proteins from Dietary Particles:	86
2.5.7	Protein Quantification:	86
2.5.8	One Dimensional (1D) SDS PAGE:	86
2.5.9	Protein Identification by Mass Spectrometry:.....	87
2.5.10	Bioinformatic Data Analysis:.....	88
2.5.11	α -amylase Enzyme Activity by DNS Assay:.....	88
2.5.12	Turbidimetric Assay for Lysozyme Activity:	89
2.6	RESULTS:	90
2.6.1	Dietary Particles Characterization:	90
2.6.2	Protein Quantification and Analysis by 1D Gel Electrophoresis:	92
2.6.3	Proteomic Profiling of Salivary Coronal Proteins by Mass Spectrometry Analysis:.....	93
2.6.4	Comparative Analysis of the Protein Corona on Dietary Particles:	97
2.6.5	Functional Annotation of the Salivary Protein Corona:	100
2.6.6	Influence of Dietary Particles on the Enzyme Activities of α -amylase and Lysozyme in Human Saliva:	101
2.7	DISCUSSION:	102
2.8	CONCLUSION:.....	106
2.9	SUPPLEMENTARY INFORMATION.....	106
2.10	REFERENCE	108
3.	STUDIES ON THE INTERACTION OF SILICA PARTICLES ON THE SALIVARY A-AMYLASE BY MULTI-SPECTROSCOPIC METHODS.....	111

3.1	ABSTRACT:.....	111
	KEYWORDS:	111
3.2	RÉSUMÉ :	111
3.3	INTRODUCTION:.....	112
3.4	MATERIALS AND METHODS:.....	113
3.4.1	<i>Chemicals and Reagents:</i>	113
3.4.2	<i>Physical Characterization:</i>	114
3.4.3	<i>Preparation /Interaction of Silicon Dioxide Particles with α-amylase:</i>	114
3.4.4	<i>Effect of SiO_2 Particles on Enzyme Kinetics of α-amylase by DNS Method:</i>	115
3.4.5	<i>Fluorescence Spectroscopy:</i>	116
3.4.6	<i>Far- UV Circular Dichroism Spectroscopy:</i>	117
3.4.7	<i>FTIR Analysis of Protein Structure:</i>	117
3.5	RESULTS:.....	118
3.5.1	<i>Particle Characterization:</i>	118
3.5.2	<i>Enzyme Inhibition Kinetics:</i>	119
3.5.3	<i>Fluorescence Quenching Studies of α-amylase in the Presence of SiO_2 Particles:</i>	121
3.5.4	<i>FTIR Analysis:</i>	123
3.5.5	<i>CD Analysis to Study the Changes in the Secondary Structure of α-amylase upon Interaction with SiO_2 Particles:</i>	125
3.6	DISCUSSION:	127
3.7	CONCLUSION:.....	130
3.8	REFERENCE	132
	GENERAL CONCLUSION.....	134
	FUTURE PRESPECTIVE	134

LIST OF TABLES

Table 1.1 Classification of NPs based on the source and the physico chemical properties	8
Table 1.2 : Summary of analytical techniques used to characterize NP & NP-PC Complex	37
Table 1.3 Relationship between changes in the NPs physiochemical proteins and the Protein corona.....	52
Table 1.4 Major salivary protein and its functions in human saliva.....	56
Table 2.1 Summary of physical characterization of the dietary particles used in the experiment.	91
Table 2.2: Twenty most abundant salivary -coronal proteins identified in the protein corona of each dietary particle's following 1 hr of incubation with human saliva.....	98
Table 2.3(S1): Twenty most enriched proteins by fold change ≥ 2	107
Table 3.1 Physical characterization of SiO ₂ particles suspended in water and PBS buffer...	119

LIST OF FIGURES:

Figure 1.1 Schematic representation of the size of the nanomaterials relative to biomolecules and other familiar things.	5
Figure 1.2 The functionality, applicability and safety assessments of nanotechnology in food industry	9
Figure 1.3 Types of nanomaterials used for food, feed and food contact surfaces.	11
Figure 1.4 Various techniques for the synthesis of silica.	13
Figure 1.5 Crystal Structure of Anatase (on the left) and Rutile form of TiO_2 (on the right).	15
Figure 1.6 Structure of PEG -Ag NP.....	17
Figure 1.7 The evolution of the concept of NP corona	20
Figure 1.8 : Biomolecule corona models: hard & soft corona.....	20
Figure 1.9 The relationship between identity of pristine NP, biological identity and the physiological response.	21
Figure 1.10 The formation of protein corona and exchange of adsorbed proteins over time in physiological.....	25
Figure 1.11 The Biochemical interactions at the bio-nano interface. (A) Vander waals force (B) Electrostatic interaction (C) Hydrogen bonding (D) Hydrophobic interaction.	28
Figure 1.12 Effects of protein corona surrounding a NP. (A) Pre-existing or initial material characteristics contribute to corona formation in a biological environment. (B) Interactions with the NP surface causing potential alterations in protein structure and function which can give rise to possible molecular mechanisms of injury that may contribute to disease pathogenesis.	30

Figure 1.13 Techniques used to measure protein corona indirectly according to the measured parameter and then correlated with the amount of adsorbed proteins .	32
Figure 1.14 :Techniques used to measure protein corona directly according to the measured parameter and then correlated with the amount of adsorbed proteins.	34
Figure 1.15 Different factors influencing Bio-nano interaction of dietary ENMs/NPs	44
Figure 1.16 (A) Composition of Saliva; (B) Function of Saliva	54
Figure 1.17 Approximate percentage of the major classes of the salivary proteins and peptides in human saliva	61
Figure 2.1 SEM image of dietary particles obtained after drying the NP dispersion (50ppm) on the SEM stub. (A) SiO ₂ NP; (b) SiO ₂ MP; (C) TiO ₂ NP; (D) Ag NP.	90
Figure 2.2 Analysis of hard protein corona after incubation with human saliva.(A)Quantitative analysis of bound protein concentration in µg/mg of Particles: It is quantified after the desorption of proteins from particles using 2% SDS by pierce 660nm Assay; (B) changes in the bound protein pattern of whole saliva interacted with 4 different dietary particles: Particle bound proteins were separated by molecular mass via 1D -SDS-PAGE and visualized by combination of Coomassie and silver staining. The molecular weight (KDa) of reference proteins are shown in the lane MW.	92
Figure 2.3 Venn diagram shows the number of identified salivary coronal proteins associated with four different dietary particles after 1 hr incubation. (A) 4 dietary particles (B) only dietary NPs and (C) silica particles at micro and nano range. The figure clearly depicts change in the protein corona composition with respect to particle chemistry, size and shows the preferential enrichment of low abundant proteins that were not detectable in the human saliva by proteomic analysis.	93
Figure 2.4 Hierarchical clustering of the salivary proteins formed around each dietary particle.	96
Figure 2.5 comparison of top 20 abundant (A & C) and enriched proteins (B & D) on the corona profiles based on MW & pI. graph (A & B): shows the classification of coronal Proteins according to their molecular weight (MW); graph (C&D): shows the difference between	

abundant and enriched coronal profiles on the particles based on the calculated isoelectric point (pI).....	99
Figure 2.6 :Bioinformatic classification of identified salivary coronal proteins according to their protein class.	100
Figure 2.7 Influence of dietary particles on the enzyme activity of α -amylase and lysozyme in human saliva. Figure 7(A): α -Amylase activity by DNS assay with particle concentration of 2 mg/mL . The enzyme inhibitory activity is expressed as decrease in units of maltose liberated. Figure 7(B): Lysozyme activity by turbidimetric method with bacterial suspension concentration of <i>M. lysodeikticus</i> at 0.3 mg/mL with particle concentration of 1.25 mg/mL. The enzymes are incubated in the substrate for 5 min.	101
Figure 3.1 Scanning Electron Microscope (SEM) image of food grade silicon dioxide particles obtained after drying the particles suspended in water (50 ppm) on the SEM stub. (A) SiO ₂ NP and (B) SiO ₂ MP.	118
Figure 3.2 Dixon plot for enzyme kinetics with increasing concentrations of substrate (starch): (A) α -amylase interacted with SiO ₂ NP ;(B) α -amylase interacted with SiO ₂ MP. (C) Michaelis-Menton plot for Km and Vmax values of α -amylase and α -amylase interacted with SiO ₂ particles in the presence of different concentration of soluble starch.	120
Figure 3.3 Fluorescence spectra of α -amylase in the presence of SiO ₂ particles with increasing concentration from 0 to 1 mg/mL while the enzyme concentration was kept constant: (A) & (B): Fluorescence spectra and Stern-Volmer plot of α -amylase interacted with increasing concentrations of SiO ₂ NP ; (B) Fluorescence spectra and Stern-Volmer plot of α -amylase interacted with increasing concentration of SiO ₂ MP	122
Figure 3.4 Double -logarithmic plots representing the binding constant (K) and number of binding sites (n).(A) α -amylase interacted with SiO ₂ NP (B) α -amylase interacted with SiO ₂ MP.....	123
Figure 3.5 FTIR spectra of free α -amylase and SiO ₂ interacted α -amylase.(A) FTIR spectra of free α -amylase and SiO ₂ NP and MP particle interacted α -amylase and (B) Amide 1 region of α -amylase and SiO ₂ particle interacted α -amylase.	124

Figure 3.6 Far-UV CD spectra representing the changes in the secondary structure of the α -amylase and the α -amylase interacted with SiO₂ Np and MP particles. The concentration of the concentration of α -amylase and the SiO₂ Particles in the CD study was 100U/mL and 1mg/mL respectively. 126

ABBREVIATIONS:

GIT	Gastrointestinal Track
iNPs	Ingested Nanoparticles
ENMs	Engineered Nano Materials
NP	Nano Particles
SiO ₂ NP	Silicon Dioxide Nanoparticles
SiO ₂ MP	Silicon Dioxide Micron particles
TiO ₂ NP	Titanium Dioxide Nanoparticles
Ag NP	Silver Nanoparticles
EFSA	European Food Safety Authority
ZnO	Zinc Oxide
MgO	Magnesium Oxide
TEOS	Tetra Ethyl Ortho Silicate
Si-O-Si	Siloxanes
Si-OH	silanols
PVP	Poly Vinyl Pyrrolidone
DLS	Dynamic Light Scattering
DCS	Differential Centrifugal Sedimentation
TEM	Transmission Electron Microscopy
SEM	Scanning Electron Microscopy

AFM	Atomic Force Microscopy
NTA	Nanoparticle tracking analysis
NMR	Nuclear Magnetic Resonance Spectroscopy
GE	Gel Electrophoresis
FCS	Fluorescence Correlation Spectroscopy
DDLS	Depolarized DLS
ITC	Isothermal Titration Calorimetry
CD	Circular Dichroism
FT-IR	Fourier Transformed Infrared Spectrometry
SEC	Size-Exclusion Chromatography
MS-MS	Tandem Mass Spectrometry
MALDI-TOF MS	Matrix-Assisted Laser Desorption/Ionization Time-of-Flight Mass Spectrometry
ESI-MS	Electrospray Ionisation Mass Spectrometry
SPR	Surface Plasmon Resonance
FQ	Fluorescence Quenching
HAS	Human Serum Albumin
BAM	N-tert-Butylacrylamide

PTMs	Post Translational Modifications
PRPs	Proline-Rich Proteins
SMSL	Submandibular- Sublingual
DRC	Dynamic Range Compression
FFF	Field Flow Fraction
XANES	X-ray Absorption Near Edge Structure
BSA	Bovine Serum Albumin
DNS	3,5-Dinitrosalicylic Acid
DDT	Dichloro Diphenyl Trichloroethane
PDI	Poly Dispersity Index
PBS	Phosphate Buffer Saline
GO	Gene Ontology
MW	Molecular Weight
pI	Isoelectric Point
sv	Stern-Volmer
SNPs	Starch Nanoparticles

OBJECTIVES OF MY RESEARCH:

The objective of my research study is to understand the interaction of dietary particles with human salivary proteins which will be conducted in two stages.

Phase 1: To understand the protein profile of saliva interacted dietary particles (Silicon dioxide, titanium dioxide and silver particles) by using proteome analysis.

Phase 2: To understand the interaction and mechanism of inhibition of salivary enzymes (A-amylase & lysozyme) by silicon dioxide particles of nano and micron size using enzyme kinetic assay, inhibition kinetic assay and different spectrometric techniques.

Chapter1 LITERATURE REVIEW

1.1 Abstract:

We are intentionally and unintentionally exposed to several nano-sized particles through dermal, oral and pulmonary routes. Applications of nanotechnology is keep increasing in the following four key Agri-food sector that includes agriculture & farming, food processing, food packaging and nutraceutical supplements industry. These applications imply inadvertent exposure to such nanomaterials throughout our lifetime often without being aware of them. Despite the rapid development of its use in the food sector, little is known about the fate of ingested dietary NPs in the GIT (gastrointestinal track) of human body and we still require an extensive knowledge to understand the kinetics of different dietary NPs during in- vitro/in-vivo bio-nano interaction by considering all factors that could possibly influence the biological identity of the ingested nanoparticles (iNPs).

Despite the fact that oral cavity is an important portal of entry, interaction between salivary proteins and ENMs are seldom studied. Mostly the previous studies are focused on interaction between blood plasma and ENMs in an effort to understand the fate of NPs entering the blood circulation whereas a less likely event in comparison to NPs entering the oral cavity. Moreover, as the protein corona composition varies in respect to the route of exposure to the human body , it is very essential to understand the mechanism of ENMs interactions with different physiological environment and characterize the protein corona at its bio -nano interface with different combination of proteins and biological fluid representing different compartment of the GIT of Human system, to know its differences and implications for the development and risk assessment of dietary NPs.

1.2 Résumé :

Nous sommes exposés continuellement, de façon intentionnelle ou non, à plusieurs nanoparticules, que ce soit par les voies dentaires, orales ou pulmonaires, la voie orale étant la voie principale des nanoparticules. Simultanément, l'application potentielle des nanotechnologies dans les secteurs clés du domaine de l'Agro-Alimentaire ne cesse de croître, que ce soit en agriculture, en transformation alimentaire, en emballage alimentaire ou bien en suppléments nutraceutiques. Ces applications impliquent une exposition inévitable à ces nanoparticules tout au long de notre vie souvent sans même s'en rendre compte. Malgré le développement rapide de son utilisation dans le secteur alimentaire, on a peu d'information sur le sort des nanoparticules ingérées dans la diète dans le système gastro-intestinal de l'être humain. De plus, nous requérons de vastes connaissances afin de comprendre la cinétique de différentes nanoparticules ingérées dans la diète pendant l'interaction bio-nano autant *in vitro* qu'*in vivo* en considérant tous les facteurs qui peuvent possiblement influencer l'identité biologique des dites nanoparticules.

Malgré le fait que la cavité orale est une porte d'entrée importante, l'interaction entre les protéines salivaires et les nanoparticules synthétiques n'est pratiquement pas étudiée. Les études précédentes sont principalement concentrées sur l'interaction entre le plasma sanguin et les nanoparticules synthétiques dans l'optique de comprendre la destinée des nanoparticules qui entrent dans le système circulatoire, une interaction beaucoup moins probable que l'entrée de nanoparticules par la cavité buccale. De plus, alors que la «couronne» de la protéine varie en fonction de la route d'exposition au corps humain, il est essentiel de comprendre le mécanisme d'interactions des nanoparticules synthétiques avec différents environnements physiologiques et de caractériser la couronne de protéines à son interface avec différentes combinaisons de protéines et de fluides biologiques représentant différents compartiments du

système gastro-intestinal du corps humain, de connaître ses différences et ses implications pour le développement ainsi que de faire l'évaluation des risques des nanoparticules ingérées dans la diète.

1.3 Objective:

The objective of this literature is to start with the background of basic understanding of nanotechnology and its application in food industry focussing particularly on three main dietary NPs such as SiO₂, TiO₂ and Nano Silver. In most of the intravenous administration blood is considered to be the first physiological environment that an ENM encounters. However, considering dietary NPs, oral exposure and ENMs interaction with proteins/biomolecules that are majorly present saliva needs focused studies to understand the fate of iNPs. Thorough understanding of protein corona formation and characterization of ENMs with protein corona forms background information for my experiment design and rationale to support knowledge gaps in NP-saliva interactions.

Neither the bio-reactivity of the protein corona at different physiological environments been adequately evaluated nor the knowledge of exposure of dietary NPs in oral cavity investigated in detail. This review article examines current understanding and major knowledge gaps in the interaction of NP with salivary components. Topics discussed in this review are,

1. Introduction to nanotechnology applications in food and entry to oral route
2. The formation of protein corona and its possible changes in the composition in accordance with change in several factors of the ENMs physicochemical properties and the physiological mediums relevant to routes of entry.

3. Technical approaches to study the characteristics of protein corona and recent developments in the field of characterization using several techniques.
4. Human salivary proteins data source which helps to compare and predict the reliable experiment design for its interaction with ENMs.
5. Summary on the Interaction between ingested dietary NPs and the GIT (gastrointestinal track).

1.4 Introduction:

Nanotechnology is the formation and manipulation of functional materials, devices and systems through the manipulation of matter at a length scale of 1-100 nm, wherein materials shrunken to billionth of a meter (10^{-9} m) acquire considerably different material properties in comparison to their bulk counterparts [1].

Nanomaterial Definition:

According to Health Canada nanomaterial is any manufactured product, material substance, ingredient, device, system or structure to be nanomaterial if: (a) It is at or within the nanoscale in at least one spatial dimension, or (b) It is smaller or larger than the nanoscale in all spatial dimensions and exhibits one or more nanoscale phenomena [2]. "For the purposes of this definition: The term "nanoscale" means 1 to 100 nanometers, inclusive; The term "nanoscale phenomena" means properties of the product, material, substance, ingredient, device, system or structure which are attributable to its size and distinguishable from the chemical or physical properties of individual atoms, individual molecules and bulk material; and, the term "manufactured" includes engineering processes and control of matter and processes at the nanoscale." [2].

1.5 NPs are all Around Us: Historical Aspect & Background

Despite the recent explosion of NP (NP) research, synthesis and use, NPs/ENMs are not a recent innovation as the nanotechnology has been utilized throughout human history where the invention and scientific breakthrough has progressed tremendously over the years. Naturally occurring organic NP includes exosomes, lipoproteins and some viruses (Refer figure 1.1). In fact, humans are naturally exposed to NPs on a daily basis and always have been. For instance, the process of digestion in our GIT track breaks food down in to nanoscale particles for the absorption of nutrients from the food we eat.

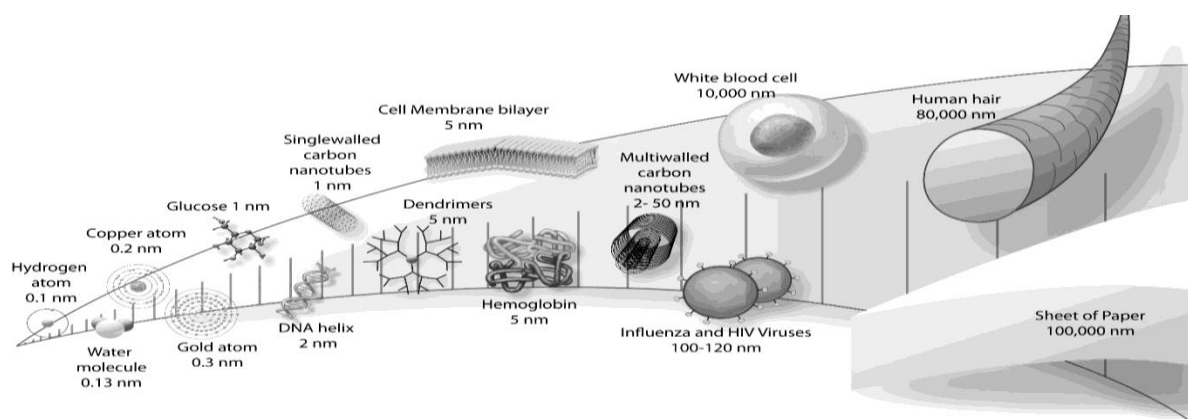


Figure 1.1 Schematic representation of the size of the nanomaterials relative to biomolecules and other familiar things.

[3].

It has also been discovered that people have used NP for their optical properties dating back to 4th century of roman times [4]. Michael Faraday's experiments on the interaction of light with gold NP dispersions are considered the beginning of modern colloid science and thus nanoscience [5] with an illustration of is evolution as mentioned below.

YEAR	HISTORY OF NANOTECHNOLOGY
1981	Scanning tunnelling electron microscope that could process single atoms.

1985	Discovery of fullerene, 60 carbon atoms in a circle (C60).
1992	Discovery of carbon nanotubes that are stronger than steel; can be used in drug delivery, energy storage, and power transmission.
1993	Discovery of quantum dots.
2000	Construction of passive NPs for applications as nano fuel cells and in products of daily use, including cosmetics.
2005	Construction of active NPs for target directed drugs and other adaptive structures.
Future	Nano systems, hierarchical nanoarchitectures, atomic devices, nano DNA-based computers, diagnostic robots, etc.

1.6 What makes NPs Unique:

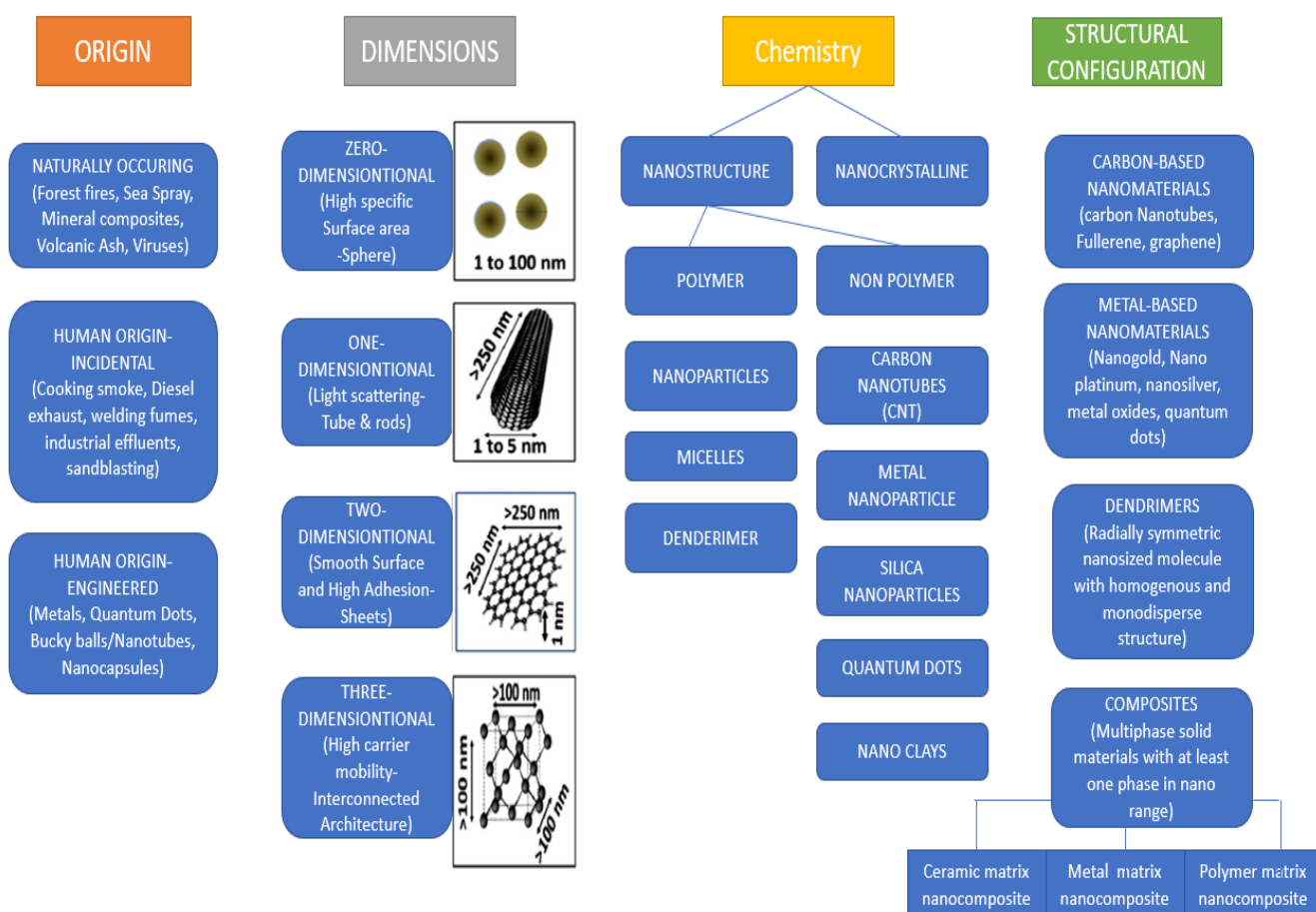
Their extremely small size and high surface area are associated with their greater strength, stability and chemical and biological activities. Therefore, nanotechnology enables development of novel materials with a wide range of potential applications which brings a combination of benefits, promises, risks, and uncertainties [6]. Two of the major factors why NPs have different properties (optical, electrical, magnetic, chemical and mechanical) than bulk material are because in this size-range quantum effects start to predominate and the surface area to volume ratio is increased [7]. The increase in the surface-area-to-volume ratio is a gradual progression as the particles get smaller which leads to that atoms on the outside of the particle will increasingly begin to dominate the one's inside the particle. This changes the individual properties of the particle and how it interacts with other materials in the surroundings. Due to which, nanotechnology-based application has improved, and in some

cases revolutionized many industrial sectors, some of which are very close to our everyday life such as the agriculture, food, medicine, pharmacy, cosmetic, and personal care.

1.7 Classification of Nanomaterials:

Different Classification of nanomaterials depending on the source and physico-chemical properties are mentioned in Table: 1.1 [8-14]. Natural and artificial nanomaterials are the major classification type which is based on the origin. Natural nanomaterials originate from animals or minerals without any human intervention or processing such as natural nanomaterials from minerals, clay and natural carbon NPs from diamond and graphite, as well as nanomaterial from space, animals such as chitin, sponge fibers, collagen etc. [14]. Intentionally produced ENMs are designed with very specific properties (i.e. size, shape, surface charge, surface area, functionalization/coatings) which may be made completely from inorganic materials such as metals (e.g. iron, silver, gold, zinc, titanium), and metal oxides (titanium dioxide, silica, zinc oxide, cerium dioxide, etc.), and other materials that include carbon (CNT), nanopolymers, fullerenes, chalcogenides (selenides or sulfides) of metals like cadmium or zinc. Moreover, ENMs are commercially available as dry powders or dispersed in liquids, usually with organic stabilizers [10].

Table 1.1 Classification of NPs based on the source and the physico chemical properties [8-14].



1.8 Nanotechnology in Food Industry:

Nanotechnology in food industry is said to be revolutionary and is giving scientists the ability to increase the functionality, efficiency, and customizability of our daily food [15]. Nanotechnology can be used in all phases of food production chain from the field with agricultural production till the industrial processing, packaging, transportation, storage, security, safety and quality [15-19]. The nanoscience that has been and is being intensively researched by experts in the field of food industry includes major four areas such as agriculture, food processing, food packaging and supplements with other innovative

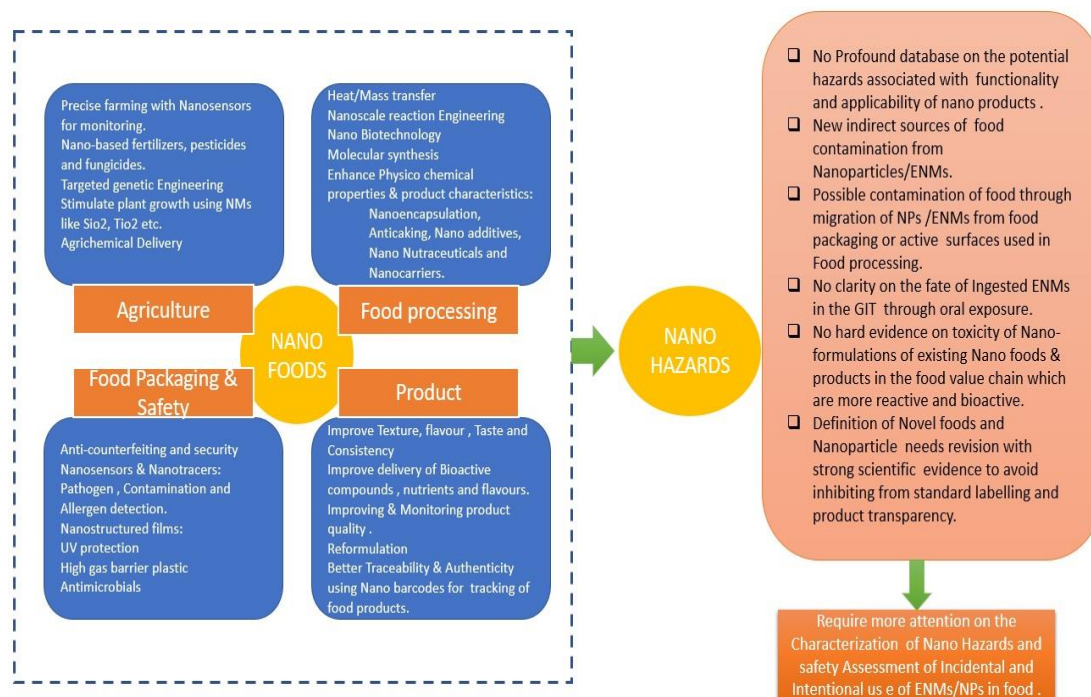


Figure 1.2 The functionality, applicability and safety assessments of nanotechnology in food industry [16, 20-24].

applications like sensory improvement, increased intestinal absorption, more efficient targeted delivery of nutrients, bioactive compounds and stabilization of active ingredients using nanosized additives as depicted in Figure 1.2. [16, 19, 21-27] .

1.9 Is Nanotechnology a Safe Application in Food Sector?

As with any new technology or novel product, a potential risk includes impacts on long term health and the environment. However, we should accept the fact that just because the material is “Nano” it does not have to be necessarily riskier than other materials or chemicals that goes in to the food causing health hazard. The use of NPs within food sector found to be used as supplements and additives that prolong shelf-life for fresh and processed foods with major focus of its application in the processing and formulation of food ingredients to form nanostructures that are claimed to offer improved taste, texture, consistency, enhanced bioavailability and allow mixing of incompatible ingredients in food matrix [28-30]. However,

the majority of the NPs in food production reported a few years ago were non-biodegradable metals and metal oxides [31]. As per the report of the inventory of nanomaterials in food, feed, and agriculture performed by European Food safety Authority (EFSA) , it showed a trend from inorganic materials to organic nanomaterials with indication of most commonly used nanomaterials are nano-encapsulates, silver, SiO₂ and TiO₂ and 55 types of nanomaterials in 12 different applications were identified with the most common application as food additives and food contact materials [32]. As per the report of Bhupinder in 2010 [33] it was noticed that the use of ENMs are not tested for the safety nor regulated its use in more than 100 food products, food packaging and contact materials currently on the market, without warning or new FDA testing .However , report from the Project on Emerging Nanotechnologies (PEN) has attempted to develop an inventory of nano enabled consumer products, has identified 117 food and beverage products use nanotechnology including food , food storage products , supplements and products used for cooking [34] .

Despite the potential benefits of nanotechnology in food supply chain from farm to fork, there are gaps in understanding the safety of its application and lack of enough evidence to prove its toxicity and health hazard to human [35]. It is clear from the above illustration (Figure:2) on the possible potential nano hazards and quality issues from the nano foods or nano products used in the food value chain. This strongly recommends considerable research and great attention towards characterization of the nano hazards and safety risk assessment of ENMs/NPs used at all stages from manufacture till exposure travelling in the food chain with a stringent regulatory surveillance [35, 36].

1.10 Nanofood and Commonly Used ENMs in Food & Food Packaging Industry:

The term “Nanofood” are differentiated from regular food products when the use of ENMs and or nanotechnology techniques & tools used during the cultivation, production, processing, or packaging of the products with wider application in improving nutrient bioavailability, improving physico chemical properties and or controlled release of the target compound in the

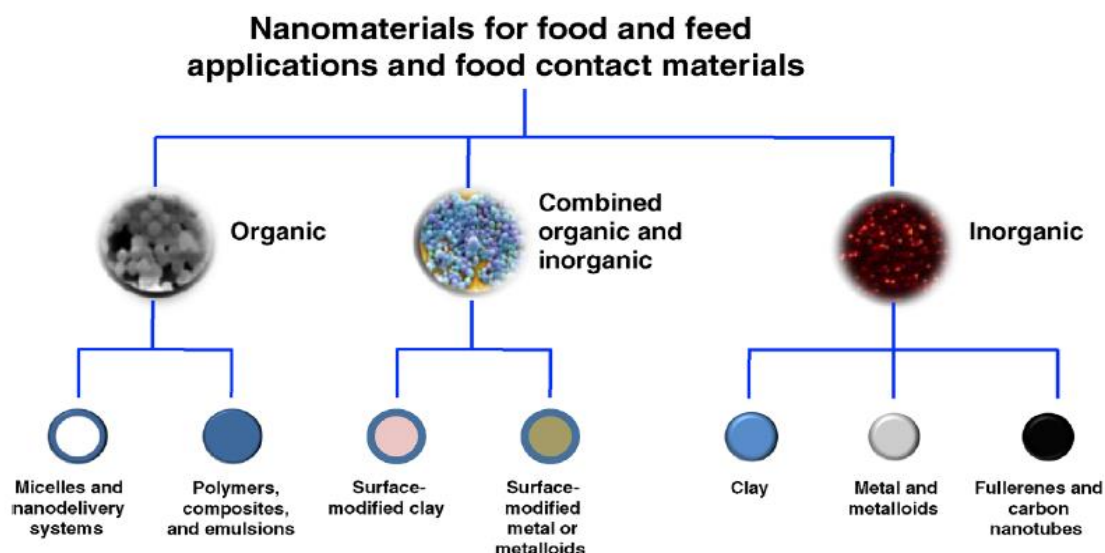


Figure 1.3 Types of nanomaterials used for food, feed and food contact surfaces. Adapted from [32] .

system through the possible techniques like nano emulsion, micelles and nanoencapsulation [16, 19, 20, 26].

In recent years, major group of ENMs [31] as showed in Figure 1.3, have attracted great interest especially organic NPs for vitamins, antioxidants, color, flavors, preservatives, and active ingredients in the food processing line and food products. Whereas, inorganic nanomaterials are used in food and food supplements and the same with polymer matrices are used in food packaging applications [37]. They help in improving the food’s flow property, colour, and stability. The effectiveness of the NPs in the food depends on its bioavailability in a system [16] [31, 32] . In food packaging, ENMs gained attention to improve the stability, flexibility and gas barrier properties of packaging, to actively utilize the antimicrobial or oxygen scavenging NP to keep food fresh longer, to add nanosensors which can detect and respond to the freshness of the package content and to make packaging biodegradable with the applicable

ENMs like silver, Zinc oxide(ZnO), magnesium oxide (MgO) for their antimicrobial properties, titanium dioxide (TiO₂) for its UV absorption properties, and nanoclay which can limit the gas permeation. [16, 19, 20, 25, 26].

1.11 Food Application and Surface Properties of Commonly Used Dietary NPs SiO₂, TiO₂ and Ag NPs:

NP are currently made out of a very wide variety of materials; inorganic particles are primarily used for two tasks. They are used as additives in food processing, like the food colours E171 titanium dioxide and E174 Silver, or as anticaking and anti-foaming agents, like E551 Silicon Dioxide, E552-559 Silicates, E529 Calcium Oxide and E530 Magnesium oxide. These substances are not necessarily defined as NPs, but it is expected that the size distribution of each substance will when used, include NPs. The most common of which is SiO₂, TiO₂ and silver NPs [7]. TiO₂(E171) is a photocatalytic disinfecting agent and a food colorant used as food whitener [18]. Silver NPs prove to be effective as antibacterial agent and hence protect the food from microbial infestation. The usage of carbon nanotubes in food packaging is limited due to its potential toxicity [18].

1.11.1 Physical Properties and Surface Chemistry of Food Grade Silica:

Silica is a porous, amorphous material composed of honey comb like porous structure consisting of SiO₂ tetrahedra covalently bonded to each other with pores of 2-50nm in diameter. The common food grade silica E551 which is a food additive is a synthetic form of amorphous silica originating from four different routes to form pyrogenic silica, precipitated silica, silica gel and colloidal silica. It can be synthesized from a silicon source such as tetraethylorthosilicate (TEOS) by the process of hydrolysis under aqueous conditions and then

condensed to form the material [38, 39]. The process is illustrated in the chemical reaction given below:

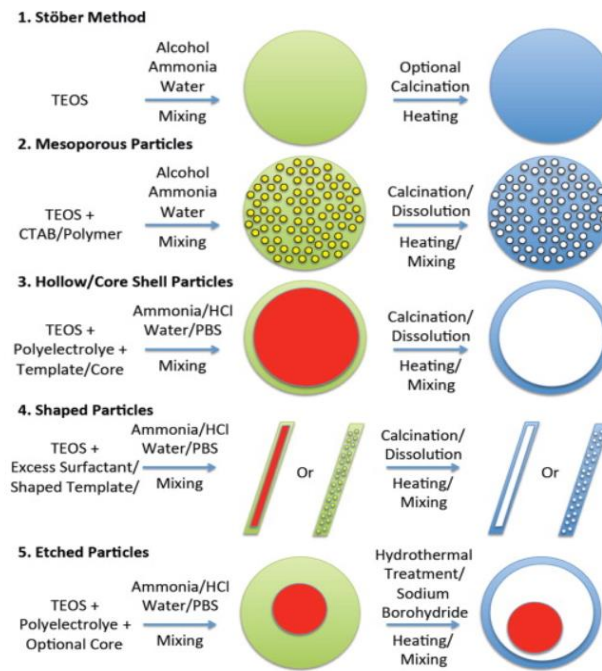
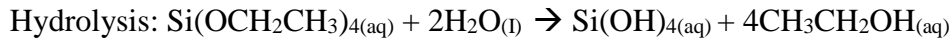


Figure 1.4 Various techniques for the synthesis of silica. Adapted from ref [39].

The size and arrangement of the pores and different surface groups in the material is generally controlled by the synthesis conditions with predominant surface groups of silanols (Si-OH) or siloxanes (Si-O-Si) and possess several unique properties such as high surface area $\geq 1000 \text{ m}^2\text{g}^{-1}$, large pore volume etc. The nano-porous structure of silica allows the surface to modify with a specific functional group which can create hydrophobic, hydrophilic or fluorophilic surfaces (Superhydrophobic coating). The hydroxyl terminated silica exhibit a large negative zeta potential at neutral and basic pH whereas, the amine terminated silica colloids yields positive zeta potential at acidic pH.

1.11.2 Application of SiO₂ in Food:

The conventional form of SiO₂ is known as the food additive E551, used in the food industry as anticaking and thickening agent in food products [15, 16, 30, 40] which helps in adsorbing the water molecules in food, thus displaying hygroscopic application. SiO₂-gallic acid NPs were used as a novel Nano antioxidants to protect against chemical ingredients based on its scavenging capacity of 2,2 diphenyl-1-picrylhydrazyl radicals [20]. These SiO₂ NP can also act as a carriers of flavors in food and non-food application through nanoencapsulation techniques [41]. The silicate NPs were also found to be used in food packaging as nanostructured films to reduce the entry of oxygen inside the packaging material and keeps the food fresh for longer time by preventing oxidation and moisture loss. The E551 Food additive are not necessarily defined as NPs, but it is expected that the size distribution of each substance will when used, include NPs. However, Several studies found that the food products including E551 contain Nano silica fraction depending on the total silica concentration, where the particle sizes were ranging from 30-200nm and it also suggest that, upon consumption of foods containing E551, the gut epithelium is most likely exposed to nanosized SiO₂ [40]. According to the recent re-evaluation report by the Scientific Committee on Food of the European Food Safety Authority (EFSA), the estimated intake of silicon derived from silica used as an additive is 20–50 mg silicon per day in a 60 kg person [42, 43]. Dekker's et al analysed food products including E551 and found that they contained silica NPs at concentrations ranging from <0.1 to 6.9 mg/g product and with particle sizes ranging from 30 to 200 nm [41].

1.11.3 Physical Properties and Surface Chemistry of Titanium Dioxide:

Titanium dioxide NPs are one of the top five types of nanomaterials used in consumer products also known as Titania. It is the naturally occurring oxide of titanium and can be purified from ilmenite ore and exists in three main forms such as rutile, anatase and brookite. However,

anatase TiO_2 has been reported to be more reactive than rutile form and each of which has unique properties and uses [44-46].

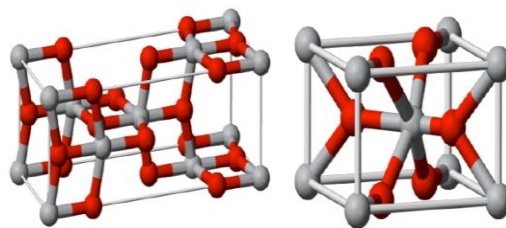


Figure 1.5 Crystal structure of Anatase (on the left) and Rutile form of TiO_2 (on the right). Adapted from [46].

Due to its stability and physical properties, TiO_2 particles are found to be used in food industry where, there are two kinds of TiO_2 particles in which the size range of 250 to 350nm called as pigmentary TiO_2 and the nano - TiO_2 with the range of under 250nm [47]. Depending on the type of synthesis , the size, shape , chemical functionalization and the crystalline state of the TiO_2 NPs will vary and moreover there are number of routes for the synthesis of TiO_2 NPs such as Sol gel method, Micelle and inverse micelle method, Sol method, Hydrothermal and solvothermal method [47, 48]. Solvothermal method found to be more reliable over other different methods because of its better size control NPs with higher crystallization and less agglomeration[49]. Titanium dioxide had been approved by USFDA and as the anatase form has been accepted as food pigment much longer than the rutile form, it seems plausible that this form is still the most used in food products as a white pigment and food colorant.

1.11.4 Application of TiO_2 in Food:

In food, titanium dioxide is widely used as a white pigment and food colorant agent and for creating a specific texture quality. Rutile TiO_2 has been reported to be the active form in food

colorants. In food packaging, smaller TiO₂ particles used in food storage due to its higher UV-blocking properties as well as nanosized TiO₂ showed good results in preventing microbial growth. The polymers are highly engineered to form nanocomposites with metal oxide NPs like TiO₂ to form a nanocomposite with TiO₂ by using LDPE as part of the composition. It is marked with E-number E171. The other dominating source of TiO₂ is toothpaste with a significant amount of >1%. In addition to that, the nanoform of TiO₂ are exposed to humans through cosmetics and sunscreens both through dermal and inhalation pathways[50]. As a food colour, the titanium dioxide particles are ideally 200-300 nm in diameter[50]. Under current legislation this is not defined as NPs (<100nm) [44, 51, 52]. However, several research studies demonstrated the presence of NP fraction in E171 and reported that approximately 36% of the number of particles in E171 were <100nm in at least one dimension [52]. The nanoform of TiO₂ is not licensed as a food additive [51].

The daily intake of titanium dioxide from food is estimated to be 5400µg/person /day and about 90 µg/kg bw/day in the United Kingdom [53]. Candies, sweets, and chewing gums found to have the highest content of titanium (0.01–1 mg titanium per serving) [50] and based on Weir et al. study [50], they have found 36% of the E171 particles are in nanosized referring 89 products, which would lead to an oral exposition between 0.07 and 1.08mg/kg bw/day of nano TiO₂. By separating titanium particles from food products, Chen et al [53], showed that more than the expected number of foods contained titanium dioxide NPs with diameters of <200 nm. The same authors also showed that the titanium dioxide in gum, more than 93% of which are NPs, easily comes out of the gum during chewing and is ingested [53].

1.11.5 Physical Properties and Surface Chemistry of Nano Silver:

Silver NPs can be produced with various sizes and shapes depending on the various synthesis and fabrication procedures. It can be functionalized with a wide range of polymers like polyvinyl pyrrolidone (PVP) and tannic acid as a capping agent for silver NPs. The particles can be functionalized with molecules to change the surface charge of the silver NPs from

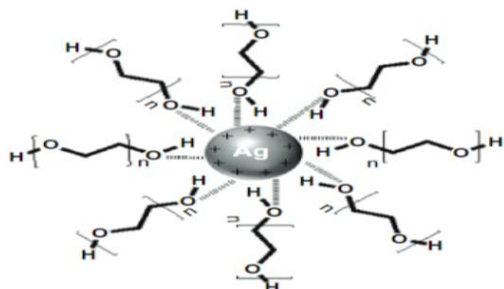


Figure 1.6 Structure of PEG -Ag nanoparticle

negative charge to a positive charge surfaces and as well as with reactive groups like amine or carboxy terminated surfaces (Refer Figure 1.6) [54]. The NP can be synthesised by physical, chemical and biological methods where, spark discharging and pyrolysis are conventionally used method whereas,

in chemical method the reduction of silver salt involve nucleation and subsequent growth with techniques like cryochemical synthesis, electrochemical reduction , thermal decomposition etc. [55]. Moreover, the surface properties of the Ag NPs change its behaviour in respect to the change in the nature of capping agent used in during the process of synthesis by chemical reduction.

1.11.6 Application of Nano Silver in Food:

The Silver NPs are widely used in the food industry due to its attractive optical, electrical, thermal and biological properties for several applications including sensing and antimicrobial agent. The antimicrobial property of the AgNPs is dependent on the size and shape by showing increased activity with decreased particle size (Higher surface area to mass ratio), where the particles get accumulated in the cell wall of the bacterial cell and form pits and catalyse the generation of ROS in bacterial cells leading to cell death through oxidative stress [55] [15]. Silver NPs are majorly used in the food contact material where number of silver containing zeolites are approved by U. S. FDA to use in food contact materials for the purpose of disinfection. At one side, the silver nanocomposites are suggested to be safer for food

packaging applications based on the detection of no significant levels of AgNPs migrated from packing materials and food contact surfaces in to the food [20]. However, there are several toxicology studies on silver NPs with growing evidence suggesting the dietary exposure of AgNPs can cross the gut epithelial cell and get absorbed to blood and reach several organs in the body causing health effects.

1.12 NP -Protein Corona:

1.12.1 Introduction:

The fate of dietary NPs was majorly studied on blood proteins (Plasma and serum protein) despite the fact that, saliva is the one of the body fluids that could encounter with NPs during the ingestion. As NP moves from one physiological compartment to another, for instance, from saliva to gastric juice its biological identity can evolve[56-58]. Adding to the fact that, each physiological environment has its own distinct set of proteins that interact in a unique way with the NPs.

1.12.2 What is Protein Corona:

Upon ingestion of dietary NPs, a combination of proteins present in the physiological medium will interact with the surface of a NP, adsorb proteins and other biomolecules such as phospholipids, sugars, nucleic acids and so on due to their nano size and high surface free energy, forming a biological coating around the NP, generally referred to as protein corona which affects the biological identity of ENMs.

1.12.3 Evolution of the Concept of NP Corona:

The importance of protein adsorption in biological interaction and responses to pristine NPs surfaces found to be evolved from the protein adsorption work by Vroman in 1962 [59]. Since after ,subsequent protein adsorption studies was carried out by different research groups where,

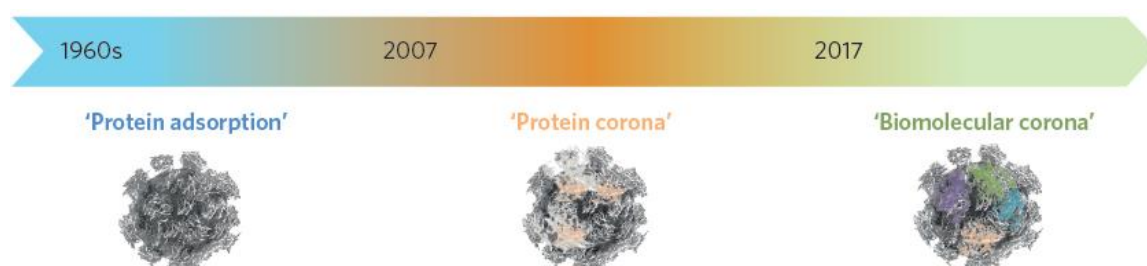


Figure 1.7 The evolution of the concept of NP corona. Adapted from [60] [61].

the concept of protein corona was proposed in 2007 by Cedervall et al, to describe the formation of protein layers on to the surface of NPs [60, 62] .

The term protein corona has been evolved to Biomolecular corona as the NPs are ingested, the surface of the NPs is altered by the adsorption of several kinds of biomolecules such as sugars, lipids and particularly proteins as well as food components in the GIT competing to form a dynamic Biomolecular corona. An original corona forms when the ingested nanomaterials come in contact with the fluid of contact at first and on subsequent translocation across the pathway, some biomolecules from the original corona may be displaced by different biomolecules in the new compartment forming a new corona. Partial displacement of the original corona by intracellular biomolecules could potentially occur at any stage along the pathway. Hence, the fact that biomolecular corona defines the biological interactions of NPs were more relevant than the protein corona in enabling Ex vivo and *in vivo* investigations [63].

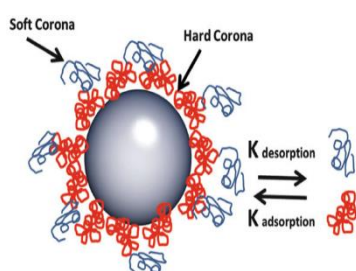


Figure 1.8 : Biomolecule corona models: Hard & Soft Corona

As referred in Figure :1.8 [64], the term “Hard protein corona” describes an inner layer of tightly bound proteins that represents the analytically accessible proteins/biomolecules constituent on the surface of NPs in a specific physiological environment and an outer rapidly exchanging layer of weakly bound proteins which is not directly interacting with the NPs called “soft corona”. The most controversial issues in the protein corona

literature is the definition and distinction of the ‘hard’ and ‘soft’ coronas. Hence, the term Biomolecule corona is used for the analytically accessible NP-Protein complexes simply as the protein corona [65].

1.12.4 Current Knowledge on the Biological Identity of NPs:

The formation of protein corona and aggregation of NPs within the physiological environment gives a new biological identity that is different from its pristine properties. From many literature and studies, it is increasingly being accepted that, biological identity of a NP is what a biological entity like cells, tissues and organs can see and interact with rather the original pristine surface of the NPs. This surface bio-transformation of NPs is therefore influencing their cellular /tissue response and toxicological profile depending on the composition of the protein corona involving in mediating further interaction with the surrounded physiological environment [58, 66, 67].

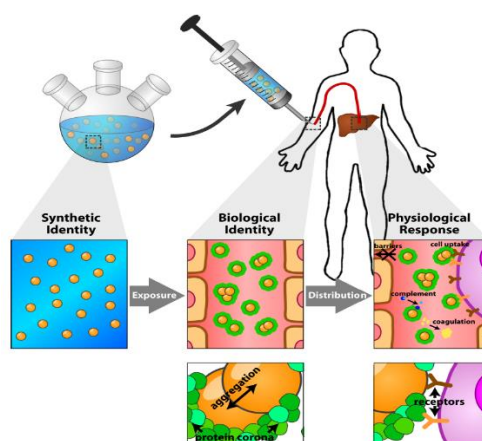


Figure 1.9 The relationship between identity of pristine NP, biological identity and the physiological response. Adapted from [68].

The above picture relates the co -relation of the three expected possible forms of NPs. Firstly, the pristine identity of the NPs is the size, shape and surface chemistry of its post-production whereas, the biological identity is the size and aggregation state of the NPs in the biological medium, along with the structure and composition of the protein corona. The physiological response is the subsequent interaction of the NPs with proteins, other biomolecules, biological barriers and different cell line in the human body.

1.12.5 Mechanism and Kinetics of Protein Adsorption:

Proteins are polypeptides with a defined conformation and carry a net surface charge depending on the pH of the surrounding medium. Adsorption of proteins at the nano-bio interface is aided by several forces such as hydrogen bonds, solvation forces, van der Waals interactions, etc. The overall protein corona complex formation is a multifactorial process and not only depends on the characteristics of the NP, but also on the interacting proteins and the medium. Specific association and dissociation rates for each protein decide longevity of their interaction with the ENMs/NPs surface. Irreversible (or at least long-term) binding of proteins on the NP leads to formation of a “hard corona” whereas quick reversible binding of proteins that have faster exchange rates defines a “soft corona” [62, 65, 69-73].

When a NP enters the physiological system, it is believed to be surrounded by high concentration of free proteins where, the proteins migrate to the ENMs Surface either by diffusion or by travelling down a potential energy gradient [61, 62, 68]. Protein adsorption occurs spontaneously only if it is thermodynamically favourable [74] [68] and every interaction between the protein and the NP occur through a portion of the protein called domain where simultaneous interaction of multiple domain of same protein with the NP surface is also expected [68]. The stability of the NP-Protein binding is dependent on the binding energy of the involved event of adsorption [68, 75, 76]. Generally, proteins that adsorb with larger binding energy will have a low probability of desorption and tend to stay associated with the surface of the NPs referred to as hard corona. On the other side, proteins that adsorb with low net binding energy will easily desorb and dissociate from the corona structure. For instance, the charged or hydrophobic NPs are more likely to form more stable interactions with proteins than the hydrophilic NPs. The rate of association and dissociation of a protein to a NP are described by the parameters K_{on} and K_{off} in which the balance between K_{on} and K_{off} determines the affinity of a protein to the NP, called dissociation constant K_d . Generally, Proteins that adsorb with a high binding energy will have low K_{off} and the value depends on the binding

energy of the NP-Protein complex. Measuring the K_{on} and K_{off} value for every single protein which compete for the binding site of the NPs in the complex physiological solution is unfeasible. As an alternative, Cedervall et al. [62] modelled total plasma protein adsorption using a biexponential function which divides protein adsorption and desorption into fast and slow components each with its value of K_{on} and K_{off} . It was noticed that, during the adsorption of plasma protein the fast component/hard corona formed in seconds while the slow component took minutes to hours for the formation. On the other side, the mean life time for the pattern of desorption is ~10 minutes for the fast component (soft corona), and ~8 hours for the slow component (hard corona). Another methodology in a time resolved manner was studied by Walczyk et al. [77], to follow lifetime of protein corona of several types of nanomaterial in plasma and figured that protein corona are sufficiently long lived and most likely to be what the cells sees rather than the nanomaterial surface.

Generally, ENMs tend to form aggregate in a solution with high ionic strength as a result of charge shielding. As the formation of hard corona occurs so fast in just seconds, it behaves to be a stabilizing layer against aggregation by particle contact. For example, the pH variance within the gastrointestinal compartments can affect aggregation status [78] and alter surface chemistry, particularly in NPs where zeta potential is highly dependent on pH and citrate stabilized gold NPs aggregate immediately in PBS but are stable in Plasma [79].

Proteins are in a continuous state of dynamic exchange when adsorbed on to the surface of the ENMs. At any time, a protein may desorb allowing other proteins of the same or different identity to interact on to the NP surface. This change in the composition of the protein corona resulting from continuous adsorption and desorption are known as the “*Vroman effect* [59, 73].” This effect takes into account that the identities of the adsorbed proteins can change over time even if the total amount of adsorbed protein remains constant. During the initial formation of

the protein corona, proteins with the highest association rates adsorb to a NP first and if these proteins have short residence times, they will be replaced with other proteins that may have slower association rates but longer residence times. This '*Vroman effect*' can be divided into "early" and "late" stages where the NPs upon entering the biological environment are rapidly adsorbed by high abundance and fast dissociation plasma proteins such as albumin, fibrinogen and IgG and later replaced by the low abundance and slow dissociation proteins by apolipoproteins [80, 81].

As it is noted that, the composition and structure of the protein corona is time dependent and changes from early stage to the late stage. Hence the characterization study of protein corona composition has to be observed on the time scale for the various investigation of the biological behaviour of the dietary NPs such phagocytosis, cellular uptake, and toxicity. Vilanova et al . [67] modelled a computational approach to understand the kinetics of corona formation for 100 nm silica NPs in a model plasma made of human serum albumin, transferrin, and fibrinogen. They were able to find the evidence of memory in the corona formation when the environment changes and proposed a mechanism that could account for this effect. Hence this memory effect can be interpreted as a consequence of how the adsorption on the NP changes the interaction of the first incubated protein with those adsorbed at later time and this approach is particularly relevant for the NPs travelling through body of different physiological medium.

1.12.6 Formation of the Protein Corona:

The simultaneous adsorption of many proteins by a combination of protein–NP and protein–protein interactions in the respective physiological medium is responsible for the formation of protein corona where each interaction will have its own binding energy.

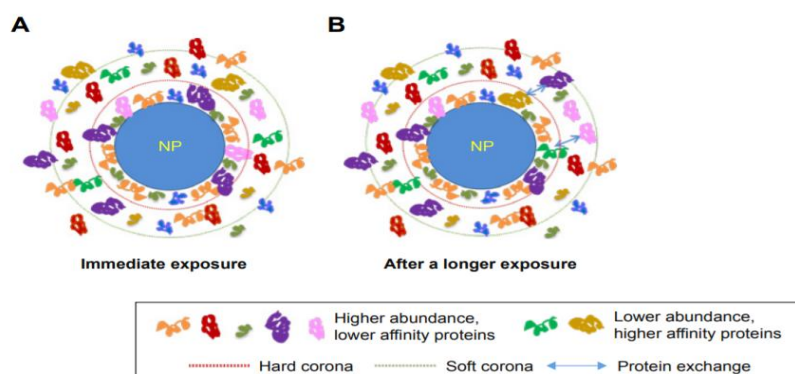


Figure 1.10 The formation of Protein corona and exchange of adsorbed proteins over time in physiological. Adapted from [82].

The dynamic process of protein adsorption and the evolution of protein corona had been extensively studied following *ex vivo* incubation of NPs with plasma where, the observation of protein corona formation is highly dependent on the incubation conditions of the NPs with biological fluid, purification protocol to separate bound protein from NPs and experimental approach employed to characterize the protein corona. However, the formation of protein corona in different physiological media and under dynamic *in vivo* conditions remains largely unexplored.

1.12.7 Composition of Protein Corona:

The major element of the biological identity of the NPs are the biomolecule corona which is unique to specific physiological environment in the human body. The physico-chemical properties of such a corona covered NP often differ significantly from those of the pristine particle formulated during manufacturing.

As the composition of the protein corona changes over time due to the competition between more than 3,700 proteins in the plasma for adsorption on the NP surface and its long and short

exchange times. In most of the cases, proteins with high abundance in the plasma are adsorbed on the surface, and over the time, they are replaced by proteins with lower concentration with higher affinity. To date investigations of protein corona composition shows that the protein corona is complex and highly individual to the nanomaterials in question and the biological medium in which they are investigated. It is also observed that, even though the blood plasma contains thousands of different proteins with different abundance, the most abundant ones need not be present in the protein corona. It is clear from the above fact that, the composition and evolution of the protein corona is not only influenced by the NPs properties but also by the properties of the physiological media [58, 68, 75, 83-85]. Based on the assumption of Lundqvist *et al*, the compositional change of NPs in different biological medium can reveal the transit history of NPs through different physiological environments [56, 86]. The prediction of the composition of corona in a complex medium still remains challenging besides knowing the properties of NPs in the bio nano interface and the other influencing factors of it [66].

All the protein corona studies are majorly performed in serum and plasma proteins which lacks the condition of true stimulation of in-vivo state where, it is believed to have difference in the composition of the corona due to various biomolecules present in the environment. This fact was proved by Lundqvist *et al* [71] by investigating the corona composition of silica NPs in plasma proteins where the result showed a distinct difference in the composition of the protein corona formed in whole blood, whole blood with EDTA, plasma and serum. Even though the source is whole blood, the model is a simplification of a *in vivo* in which other factors influencing the corona formation like the blood flow, pressure and other bio molecules in the system is missing and hence it shows complexity in determining exactly the fate of NPs after entering the biological fluid [71].

The identity and possible changes in the structure and composition of the protein corona can significantly affect the NPs fate and behaviour due to their physical and chemical interactions

with the biomolecules. Likewise, physico chemical properties of the NP such as size, shape, surface charge etc. can also define their behaviour in the biological medium.

1.12.8 Influence of Protein Conformation on Protein Corona:

Proteins are the chains of amino acids, where the sequence of the amino acids determines the protein's structure, and function. When the protein is bound to NPs to form protein corona, proteins may rearrange their structures to adapt to NPs surface and surrounding environments and the process is known as “conformational changes” [87]. As protein functions depend on their secondary and tertiary structures, the change in protein structure due to the change in the secondary and/or tertiary protein structure, which can significantly affect their functions and activities due to the dynamic changes of exposing conditions or thermodynamically favourable if it allows either charged or hydrophobic regions of proteins to interact with either hydrophobic or charged NPs [68, 75, 87]. The NP-Protein interactions are managed by certain forces such as Van der Waals Interactions, electrostatic interactions, hydrogen bonding (H-bond), hydro-phobic interactions and π - π stacking interactions where each of these forces depends on various parameters including the sizes, shapes, charges and chemical functionalities of the NP surface (Figure 1:11) [88]. H-bonding between uncharged hydrophilic parts of the protein and polar residues on the surface of the NP interactions are individually stronger than VDW, but usually less abundant in aqueous physiological environments [89].

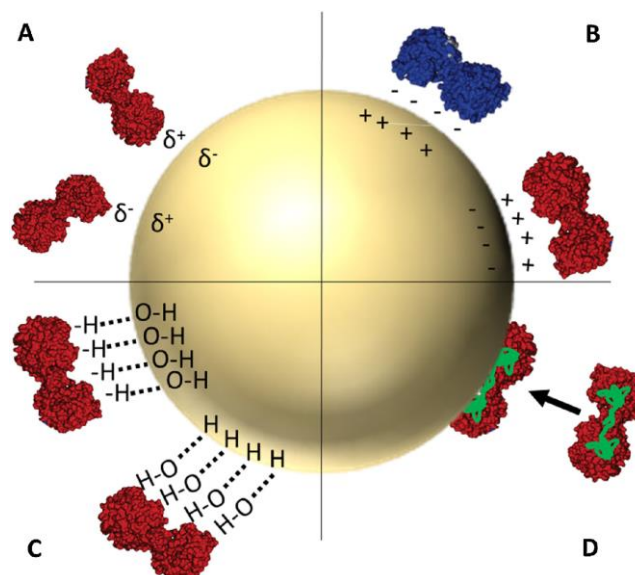


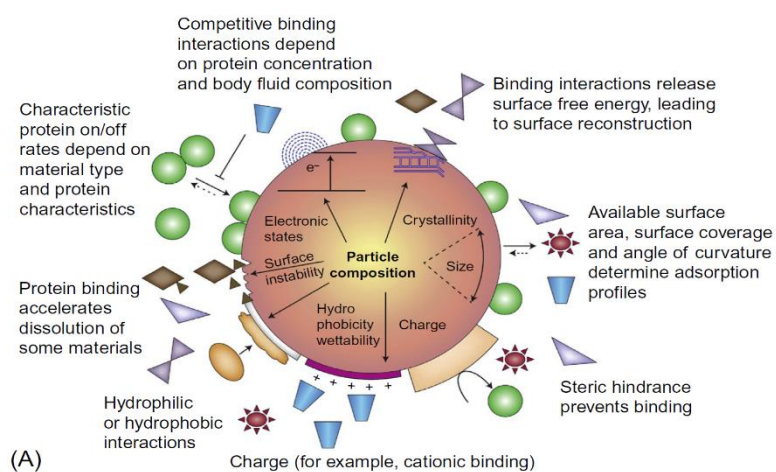
Figure 1.11 The Biochemical interactions at the bio-nano interface. (A) Vander Waals force (B) Electrostatic interaction (C) Hydrogen bonding (D) Hydrophobic interaction. Adapted from the reference [88].

The correlation between size of ENMs and proteins are the most important factors that determine the proteins structures. For example, proteins tend to stretch with NPs with sizes bigger than themselves. Whereas with smaller NPs the interaction between protein and NP may cause less structural changes [89, 90]. Even the surface charge of the NPs has a strong influence in affecting the secondary structure of proteins. For instance, gold NPs were modified with amphiphilic polymer to obtain an identical physical property with different surface charge in order to study the charge dependent interactions of ENMs. The results showed that, BSA retains its native structure with negatively charged gold NP whereas, the positively charged NP showed a conformational change of BSA with faster cellular uptake which might be caused due to the influence of change in the surface charge of the ENMs [90, 91]. Moreover, it was found that the conformational changes of proteins after desorption are usually irreversible with a noticeable pattern where hydrophobic NPs undergo higher conformational change compared to hydrophilic NPs [92]. Thus, interaction with a surface can easily disrupt the native

conformation and, therefore, the protein function which has implications for the biological impact of NPs.

Another study on pH dependent conformational change was studied by Shang et al, in the BSA protein by using different spectroscopic techniques such as UV-Visible spectrophotometer, fluorescence spectrophotometer, circular dichroism, and FTIR. It was observed that , the conformation change of the protein occur at secondary and tertiary structure level with an observation that higher pH contributed to the maximum changes at the protein structure [93].

As protein function is directly linked with the protein conformation , understanding the type of conformational change in protein upon interaction with the NPs is important. However, it's quite challenging to determine the structural change as these conformational changes could be reversible or irreversible. It is very important to study the change as the irreversible alteration of protein conformation is a recognized molecular mechanism of injury and can contribute to disease pathogenesis [94, 95] following protein dissociation from the surface of the NPs. The subsequent biological responses to the unfolded proteins are highly affected by their conformational changes. This can induce subsequent biological responses to the unfolded proteins (Figure: 1.12b) .Therefore better understanding of the consequences of the interaction with NPs on the protein conformation is essential to develop a safe use of dietary NPs [96].



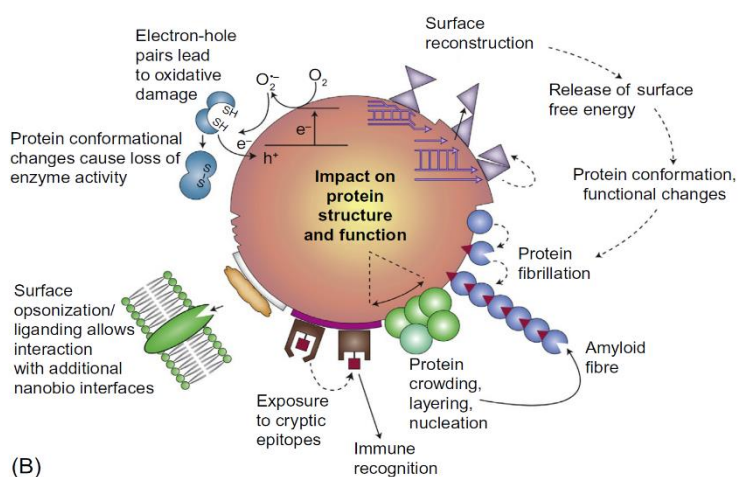


Figure 1.12 Effects of Protein corona surrounding a NP. (A) Pre-existing or initial material characteristics contribute to corona formation in a biological environment. (B) Interactions with the NP surface causing potential alterations in protein structure and function which can give rise to possible molecular mechanisms of injury that may contribute to disease pathogenesis. Adapted from the reference [89]. *The colored symbols denote many kinds of proteins, such as charged, lipophilic, conformationally flexible proteins, catalytic enzymes with sensitive thiol groups, and proteins that gather together or interact to form fibrils.

1.13 Analytical Approaches to Study the NP -Protein Interactions:

A better understanding of the biological effects of NPs requires knowledge of the binding properties of proteins that associate with the particles from realistic mixtures of proteins such as those in biological fluids in different compartment of human GI tract. However, the isolation and identification of particle-associated proteins is not a simple task, as the protein corona constantly evolves over time following Vroman's effect and also evolves as the NP transit through different compartments of human body [70, 83]. Understanding the nature of the NP-protein corona complex and its impact on NP physicochemical properties and cellular uptake is critical and important for understanding the fate of NPs in the body. In order to extend our

study in this area, we need more realistic and mechanistic approach to study and understand NP-Protein corona complexes due to the complex and dynamic nature of the biological environment. Hence, it is quite challenging to reliably characterize a protein corona for *in vivo* condition where multiple factors influence its formation and response towards the cellular response.

The protein corona can be characterized either directly or indirectly using several techniques by determining total quantity, density, thickness, composition, relative abundance of each protein, protein binding affinity, and protein conformation [82]. For instances, the adsorbed proteins can be analysed directly with mass spectrometry, Circular dichroism, etc, and can be compared with indirect techniques, based on the information about the protein corona gathered from changes in the properties of the NPs such as Size, Absorbance, Charge, temperature, Fluorescence and mass.

1.14 Characterization of Protein Corona:

1.14.1 Indirect Method:

Firstly, the basic NP dispersion characteristics such as hydrodynamic diameter, zeta potential and polydispersity index in the respective biological fluid should be measured before and after corona formation involving time kinetics along the process of corona formation. It is observed that, there is an indirect correlation between the protein corona and NPs characterization and variety of analytical techniques used in NPs characterization are now being extended to investigate protein corona indirectly via measuring changes in the properties of the underlying NPs such as changes in their size, charge, density, mass, absorbance and fluorescence (As illustrated in the Figure:1.13)

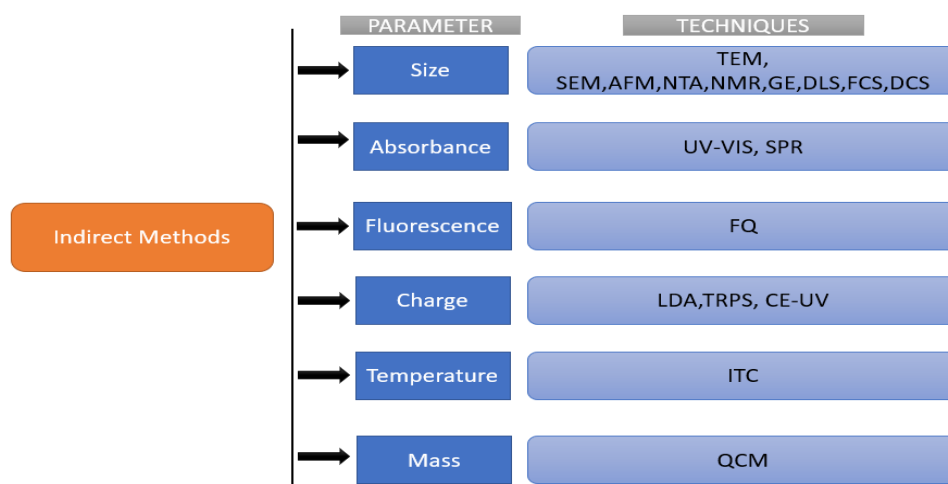


Figure 1.13 Techniques used to measure protein corona indirectly according to the measured parameter and then correlated with the amount of adsorbed proteins [97].

The dispersion properties are generally determined by Dynamic scattering Light (DLS) and by Differential Centrifugal Sedimentation (DCS). Since, most NPs are negative charged in the presence of a protein corona at physiological pH, any changes in the surface charge due to protein adsorption might lead imbalance in the electrostatic stability of the system but may also increase the steric stability of the system [76]. The information about the thickness of the protein corona and its effect on the surface charge of NPs can be collected by comparing the result of size and zeta potential measure of NPs before and after corona formation using several techniques like TEM (Transmission Electron Microscopy), SEM (Scanning Electron Microscopy), AFM (Atomic Force Microscopy), NTA (NP tracking analysis), DLS, NMR (Nuclear Magnetic Resonance Spectroscopy), GE (Gel Electrophoresis) and fluorescence correlation spectroscopy (FCS). DLS is the technique commonly used for hydrodynamic diameter [98] allowing NP size measurement based on the light scattered by them due to their Brownian motion, which is dependent on the primary size and influenced by NPs agglomeration, which results in the difference in data between DLS and TEM [99, 100]. In addition to that DLS technique is hard to apply when NPs are in the size range of proteins $\leq 10\text{nm}$, as unbound proteins may interfere the results. This can be overcome by separation of

excess unbound proteins from the biological fluid, which however result in desorption of some of the originally bound hard corona proteins to solution towards formation of a new equilibrium[97, 100, 101]. An alternate technique is depolarized DLS (DDLS) used for measuring protein corona in complex mixtures by eliminating the unwanted signals from unbound proteins [100]. TEM and Atomic force microscopy (AFM) give more clear data on the NP size, shape and the protein corona compared to DLS whereas, the zeta potential characterizes the net charge of the particle surface in the given dispersing medium providing information on the changes in the surface charge of the NPs after incubating with the biological media. The corona complex has to be studied through a approach with relevance to study different subpopulations rather the average protein corona of the multiple populations [102].

1.14.2 Direct Methods:

NP—protein interactions can be characterized through a wide range of analytical techniques such as Isothermal Titration Calorimetry (ITC), fluorescence spectroscopy, quartz crystal microbalance, Surface Plasmon Resonance (SPR), atomic force microscopy, fluorescence correlation spectroscopy, size-exclusion chromatography, infrared and Raman spectroscopies, etc. However, in general GE, LC-MS and ICP-MS can provide information about the identity of the adsorbed protein but they cannot analyse the structure of the adsorbed protein, while circular dichroism (CD) and Fourier transformed infrared spectrometry (FT-IR) found to be the common techniques used for the detection of structural changes of the adsorbed proteins.

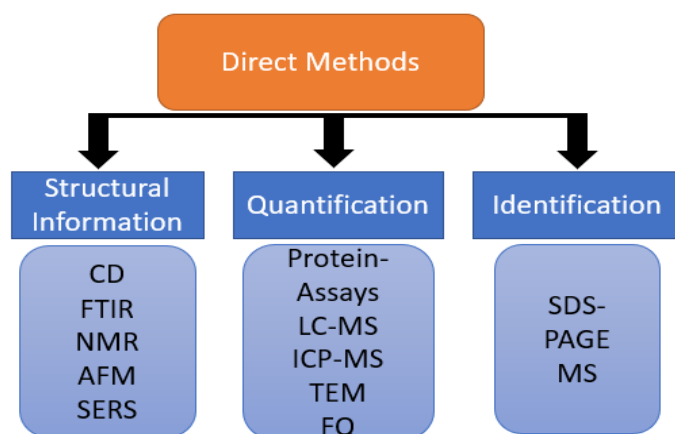


Figure 1.14 :Techniques used to measure protein corona directly according to the measured parameter and then correlated with the amount of adsorbed proteins.

The standard biochemical protein quantification assays such as Bradford or bicinchoninic acid assay can be used for the quantification of adsorbed proteins on the NPS surface. However, the most commonly used strategy for the NP -protein characterization is proteomic approach, which uses state-of-the-art MS platforms, bioinformatics and system biology tools [103], a multi -step process where, the NPs are incubated with either a single protein or in a biological fluid for a period of time before the analysis of surface adsorbed proteins. The protein -NP complex is centrifuged to remove unbound proteins and then separated and quantified using gel electrophoresis and Tandem Mass spectrometry [56, 57, 62, 71, 86, 104-106]. 1D & 2D gel Electrophoresis considered to be another common technique for the identification and qualitative determination of the protein corona composition. Currently gel free approaches like Shotgun proteomics found to be very effective, which enables to analyse complex protein mixtures in a single experiment [106-109].

The interaction between NPs and proteins can also be verified qualitatively by the physical changes of NPs in size and Zeta potential measurement. For detailed quantitative estimation of the amount of adsorbed proteins and the composition of the protein corona, the bound proteins need to be desorbed from the NPs using centrifugation techniques. However, it should be noted that centrifugation may change equilibrium status of the medium and soft corona may be lost during this purification step [97, 101]. As the centrifugation is a common method of choice due to its versatility, in the process of separating NP-protein complex from unbound proteins it introduces limitations as well. For instances, Protocols generally include washing steps to detach weakly and non-specifically bound proteins. However, these steps could be insufficient to avoid the sedimentation of large proteins and of protein aggregates together with NP–

proteins complexes thus providing false positive identifications in the protein corona composition. For this reason, additional purification strategies, such as Size-Exclusion Chromatography (SEC), magnetic separation, and microfiltration, often have to be included in the analysis protocol. It is noticed that, SEC enables the separation of large molecules and aggregates depending on the molecular size of the analytes in a potentially less perturbing way. In addition to that, most of the studies did not precisely control short period incubation times of NPs with the biological fluid of interest since, the centrifugation times (15-30 min) required to pellet the NP-PC complexes can represent an unintended exposure time, during which NPs are still in contact with the medium and can potentially resulting in the additional binding/dissociation of corona proteins [58, 83, 110]. This condition was overcome by using a featured protocol developed by Docter et al, based on sucrose cushion centrifugation technique which efficiently limits the contact time of the NPS with the biological fluid and enable the kinetic study of NPs and Protein interaction of short time periods feasible [111].

GE is always complemented with MS based proteomics to determine the identity of the proteins where, selected bands from 1D/2D SDS PAGE are recovered from the gel and analysed by tandem mass spectrometry (MS-MS), matrix-assisted laser desorption/ionization time-of-flight mass spectrometry (MALDI-TOF MS), or Electrospray Ionisation Mass Spectrometry (ESI-MS) to obtain the mass spectra of the protein fragments with existing standard protein data for quantifying the composition of the protein corona. However, chromatographic techniques coupled with MS is required and relatively accurate for the absolute quantification of the protein corona composition using techniques like size exclusion chromatography, gel filtration chromatography, LC-MS etc. For instance, most of the method applied by Cedervall et al. [62] are quite uncommon techniques with better results that includes, Size-Exclusion Chromatography (SEC), Isothermal Titration Calorimetry (ITC), and Surface Plasmon Resonance (SPR), where SEC can determine both identity of the proteins on the NPs and the rates of exchange with plasma proteins (Association time) [112]. This method is less perturbing

of protein–particle complexes than centrifugation and other approaches and moreover the same work group shows that ITC can be used to assess the stoichiometry and affinity of protein binding, and SPR studies (in which NPs are linked to gold by a thiol anchor) yield additional data on protein association/dissociation from NPs [62, 112, 113]. These techniques majorly provide information about the identity of the adsorbed proteins which generally requires purification from excess protein but they cannot analyze the structure of adsorbed proteins.

Other commonly used techniques for the detection of structural changes of proteins during the adsorption of proteins on to the surface of NPs are circular dichroism (CD) and Fourier transformed Infrared spectrometry (FT-IR). CD generally applied for the determination of secondary structure of proteins. FTIR offers higher signal-to-noise and speeds than spectrometers that use gratings and hence offers the capability of observing the critical early events when proteins interact with surfaces. Perhaps the biggest advantage of the FTIR technique over dispersive Infrared spectrometers are the precision in the wavelength which allows the subtraction of water, a strong infrared absorber, from the spectra of proteins in aqueous solutions [106, 114]. NMR spectroscopy is not a commonly used technique to study the protein corona due to the high molecular weight of most of the proteins and also due to the difficulty in interpreting the spectra of complex mixtures such as biological fluids[115]. However, the above mentioned techniques are generally used to study the interaction of specific NP-protein interactions which details the information related to structural and conformational changes of an adsorbed protein [97]. In addition to the above techniques, Fluorescence quenching (FQ) an interesting parameter based on fluorescence of proteins, since the adsorption of proteins on NPs usually leads to quenching of the native fluorescence of proteins containing tryptophan, tyrosine and phenylalanine. However, this technique has

limitations like overestimation due to the inner filter effect caused by light adsorption and or scattering [97].

In both cases of direct and indirect methods to characterize the protein corona, some techniques allow for detection of the protein corona *in situ*, while others require the removal of unbound proteins before measurements, which may however change equilibrium properties and loosely bound proteins called “soft corona” may be lost in the purification step [97, 101].

Table 1.2 : Summary of analytical techniques used to characterize NP & NP-PC Complex [72, 116].

Parameter	Analytical Technique	Description
Physical characterization of NPs		
Size & Charge	Dynamic Light Scattering	Changes in the hydrodynamic diameter of NP upon binding to proteins.
	Ultra-centrifugation	Changes in the hydrodynamic diameter of NP
Dissolution	Inductively coupled mass spectrometry	For detecting elemental composition of the nanomaterial
Shape & Structure	X Ray Diffraction	Determination of crystalline structure
	Electron microscopy	Visualisation of NP structure
Surface Area	Braunauer Emmet Teller method	Measures specific surface area using adsorption of gas on the surface

De-Agglomeration	Ultrasonication	Uses sound energy to disrupt large aggregates of NP
Thickness	DLS, Differential centrifugal sedimentation (DCS), Size exclusion chromatography (SEC), Transmission Electron microscopy(TEM)	DLS is useful for in -situ experiments and TEM applied to study the thickness which requires counter staining.
Density	Calorimetric Protein Assays	
NP Protein Interaction		
Protein Binding Affinity	Isothermal calorimetry (ITC)	To measure binding constant, thermodynamic parameters of NP-protein interactions
	Fluorescence correlation spectroscopy	Measures change in fluorescence spectra due to NP-protein interaction
	UV–vis spectroscopy	Measures change in absorption spectra due to NP-protein interaction
	Quartz crystal balance	Detects change in mass at the oscillating quartz surface due to NP-protein interaction
	Surface Plasmon resonance	Detects change in oscillation of electrons on a metal surface due to NP-protein interaction

	Atomic force microscopy	Gives surface profile of the nanomaterial
	Fluorescence correlation spectroscopy	Binding characteristics depending on fluctuation in fluorescence
	Size Exclusion Chromatography	Isolation of bound protein can be performed and the strength of the protein interaction can be assessed.
	Particle Size and Distribution (TEM & DLS)	Plasma protein corona structure examination. Particle's dispersibility & Zeta potential before and after protein corona formation on NPs.
Identity & Quantity of Protein Corona	1D-polyacrylamide gel electrophoresis (PAGE) and 2D PAGE	Identification of proteins in corona on NPs. The order of protein adsorbed onto the surface of NPs can be determined.
	Protein Assay (BSA quantification & Bradford)	Half-max protein adsorption. Hill slope for protein adsorption.
	Capillary Electrophoresis	Analysis of NP-Protein interaction with high degree of resolution.
	LC-MS-MS, MALDI-TOF	Efficient separation of bound plasma proteins and Identification of protein/peptide sequence. Accurate molecular weight distribution.

NP Surface Induced conformational change in Protein Structure		
Protein structural changes after binding	Circular Dichroism spectroscopy	Measures changes in secondary structure of proteins depending on chiral properties of proteins
	Fourier transformed infrared spectroscopy	Measures adsorption of amide bonds in the proteins to derive structural change
	Fluorescence Quenching	
	Raman spectroscopy	Studies molecular vibrations to predict structure
	Nuclear Magnetic Resonance	Relies on magnetic properties of atomic nuclei to predict structure
NP-Cellular Interactions		
NP uptake	Confocal microscopy	Visualization of fluorescent NPs <i>in vitro</i>
	Confocal micro Raman spectroscopy	Visualization of fluorescent NPs <i>in vitro</i>

1.15 Limitation of *Ex -vivo* study on Characterizing Protein Corona Formation:

Based on the few recent *in vivo* study of protein corona formation, Chen et al [117] and Hadjidemetriou [118], attempted to test whether protein corona formed in *ex vivo* were replaceable *in vivo* and the result showed that the gel electrophoresis of the recovered NP-Corona complex demonstrated a significant loss of the fluorescently labelled proteins, suggesting a kinetically unstable corona [117]. And *in vivo* protein corona from blood stream

differed in composition and morphology in comparison to the one formed *ex vivo* [118]. Furthermore, the blood flow dynamics, interaction with circulating and endothelial lining cells, or immune responses and the wider variety of molecular species in the true biological environment are some of the factors that cannot be mimicked by *ex vivo* studies. As per the studies presented in references [60, and 119], protein adsorption on to NPs is highly dynamic and the abundance corona proteins found to fluctuate over time due to the process of competitive exchange of proteins. These observations clearly indicate a difference between coronas forming *ex vivo* and *in vivo*.

1.16 Advancement in the NP-PC Characterization:

As our current methodologies require the isolation of the NP-PC complex from the biological fluid for the subsequent characterization which can compromise some bound proteins due to harsh treatment, which can further modify the NP-PC composition [101, 120]. We need highly sophisticated methods to characterize the molecular details on the surface of NPs as they evolve and modified *in situ* in the presence of the biomolecules from the environment in which they are exposed. In order to acquire the molecular information in a realistic biological scenario, a recent study by Lo Giudice et al., has introduced flow – cytometry technique for single protein-NP model and *in situ* multiplexing epitope mapping of NP-Protein complex and hard corona using intense fluorescent reporter binders to map out the availability of such recognition fragments, allowing for a rapid and meaningful biological characterization [121]. Whereas, in another study by Lara et al., they suggested that the “labelling” of NPs by biomolecular adsorption processes can allow for multiple pathways in biological processes by using immune-mapping technique to quantify epitope presentations which was studies in two major proteins in the serum corona in order to identify key protein recognition motifs and link them to specific cell-receptor interactions [122].

A database framework was developed using multivariate approach by Walkey et al., to predict the interaction of NPs with biological systems by protein corona Fingerprinting strategy, where they characterized serum protein corona fingerprint formed around a library of 105 surface modified gold particles model is applicable for across different NP classes, however distinct model may be required and the database need extensive experiment and validation to find the biological data of different physiological fluids [123]

Depending on the type of selected analytical technique, the evaluation of the protein corona characterization will differ. A significant difference in the corona composition and characterization based on the type of technique applied where, the Human serum Albumin (HAS) was measured by Isothermal Titration calorimetry (ITC) , while there was no trace of HAS when evaluated by SDS-PAGE [124] . In another experiment, Single particle ICP -MS with appropriate single particle data processing tool found to be used to characterize metal and metal oxide NPS even at low concentrations in a complex media [125] .Hence, it is critical to choose suitable technique to accurately characterize protein corona properties since protein corona is highly influential to the changes in the physicochemical properties and biological identity of the NPs.

It is evident that, a considerable progress has been made towards the characterization of corona and protein identification through increased sensitivity of chromatography and mass spectrometry techniques [106, 126] with the use of tandem mass spectrometry (MS/MS), matrix-assisted laser desorption/ionization time-of-flight mass spectrometry (MALDI-TOF MS), or electrospray ionisation mass spectrometry (ESI-MS). The composition of the protein corona can be obtained by comparing the mass spectra of the recorded protein fragments with the existing database like Sequest, Mascot, etc. However, for an absolute quantitative analysis of protein corona, chromatographic technique has to couple with Mass spectrometer, for example LC-MS-MS. However, these techniques have limitations that experimental

conditions are crucial and their lack of homogeneity in the processing protocol and data interpretation can create a difference which makes difficult the comparison between studies from the literature. In addition to that, the composition of the protein corona on a given NPs at a given time, depends on the concentration and kinetic properties of the proteins found in the biological fluid such as plasma, serum, saliva etc. Hence, it is significant to not only determine the identity of proteins adsorbed on to the surface of the NPs, but also understand the binding affinities and stochiometries. In a recent study by Kelly et al., had demonstrated a promising approach to identify the spatial location of the proteins, their functional motifs, and their binding sites using differential centrifugal sedimentation and various imaging techniques to investigate the microscopic organization on a particle by particle basis to map the protein binding and to study the molecular description of the biological identity of NPs [127].

Some of the downside of the current techniques used for the characterization of the protein corona are; Firstly, most studies apply *in vitro* models of physiological condition of human system where plasma/serum used as a model for the blood protein adsorption and interaction study. However, neither models fully represent the real time *in vivo* condition [128]. Secondly, many techniques measure an ensemble average of the adsorbed proteins and cannot distinguish individual proteins within the corona where those techniques are well suited for single protein interaction study. Hence, there is a significant need for new experimental strategies to use combination of different analytical techniques to study the protein corona with structural detail, molecular resolution and within a physiological environment of interest [72] [97] [129].

1.17 Effect of Different Parameters Affecting Biomolecular Corona:

As the Protein adsorption occurs at the interface between the ENMs/NPs and the physiological environment. We need to understand that, not only the NPs material, size and the surface properties been shown to play a role in determining the composition of the protein corona but also Several others factors (Figure: 1.14) [89, 130, 131] are considerable to affect the manner by which NPs interact with biomolecules and composition of the protein corona formed. As the NP-Protein interaction occurs at the Bio-Nano interface, the physicochemical properties of NPs and the biological environment and its conditions are vital parameters governing protein corona formation [63]. Moreover, on the other side protein corona being the highly focussed and still investigated parameter to understand the biological identity of the NPS. However, it is not the only relevant feature of the

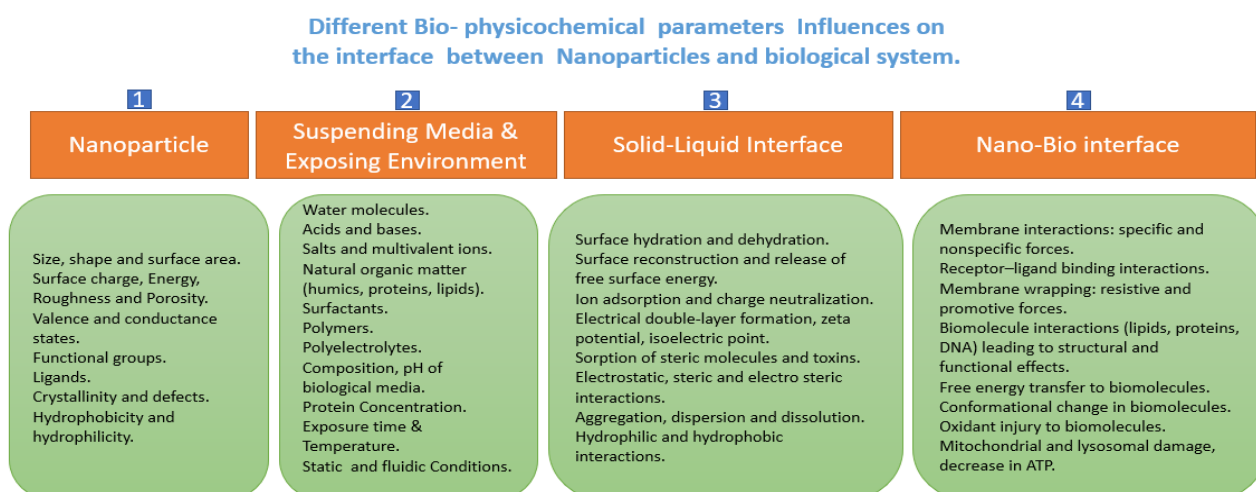


Figure 1.15 Different factors influencing bio-nano interaction of dietary ENMs/NPs

bio-interface of the NPs because it comprises the dynamic physicochemical interactions, kinetics and thermodynamic exchanges between nanomaterial surfaces and the surfaces of biological components like proteins, membranes, phospholipids, endocytic vesicles, organelles, DNA and biological fluids in the physiological medium of the human system [87, 88, 96, 132-137]. In addition to that there are emerging studies on non-protein corona such as lipid corona and natural organic matter corona whose formation and physicochemical factors regulating these type of NPC are currently less understood [63, 138]. Therefore, analyzing and

understanding each of these ignored parameters with meaningful characterization of the protein corona evolution and formation are essential to understand the fate of NPs and to know their consequence cellular responses for the risk assessment of NPs.

1.18 Effect of Physiological Condition/Suspending Media Properties on Protein

Corona Formation:

1.18.1 Media Composition:

The biological fluid with different protein components strongly affects protein corona composition and its properties. From the studies [139, 140] it was observed that the same Silica NPs responded to behave with different biological outcomes, when exposed to cells in the presence and absence of serum containing media. Serum proteins adsorbed to silica NP surface showed reduced interaction with cells, resulting in lower cellular uptake of silica NPs in the media supplemented with serum compared with media with no serum addition [139]. Thus, the different exposure conditions not only affect the uptake levels but also result in differences in the intracellular NP location and impact on cells.

1.18.2 Exposure Time, Temperature, pH and static & Fluidic Conditions:

The exposure time is considered to be another important factor which determines quality and quantity of proteins adsorbed onto NP surface [56, 58, 67, 76, 105]. From many kinetic studies conducted, it was noticed that, protein corona formed immediately when ENMs comes in contact with the physiological environment. For example, just within 30 sec of contact with human plasma, nearly 300 proteins will be bound on to the NPs surface [58]. In the initial stage, high abundant low affinity proteins adsorb on to the NP surface which later are displaced by the low abundant high affinity proteins. The exchange of adsorbed proteins over time significantly modifies the abundance of proteins that bind on a different time scale. Hence,

resulting in different protein corona patterns. Additionally, the exposure time enhances the quantity of total adsorbed protein [141] and an evolution from loosely bound protein toward an irreversible attached protein corona was observed as duration of exposure evolved [76].

The temperature is one of the not investigated but another important factor influencing the changes in the protein corona pattern [135]. From the study by Bhogale et al [142], it was observed that, the quantity of proteins adsorbed on to copper NP increased when the incubation temperature increased from 15°C, 27°C, and 37°C to 42°C. Hence, for a real time simulation conditions considering the temperature of the *In vitro* experiment is very important since it can facilitate a change in the NP-Protein interaction leading to changes to the bio distribution and bioavailability of NPs [87]. Yet another study [143], showed the effect of incubating temperature on the corona formation with gold NPs. If the corona formation is influenced by the temperature, then the body temperature ranging from 35°C to 39°C can influence the cellular uptake of NPs.

pH & Ionic Strength: The change of environment temperature and pH can alter the particle characteristics by changing the size and size distribution through aggregation which in-turn leading to difference in the pattern of the resulting protein corona. The stability of the NPs especially metal, metal oxides and ENM with ionisable surface modifiers can be affected by the pH and the ionic strength of the dispersing medium by affecting the surface charge properties and also begin to decrease when pH values are close to the IEP. The ionic strength of the medium influences the corona formation by decreasing the amount of adsorption of organic matter on to NPs which happens in the presence of high amount monovalent salts [144]. Whereas, in the presence of equally charged ions like phosphates and sulphates had lowered the adsorption of NOM due to the competition for the charged sides on the surface of the NPs [145]. Normally ingested NPs will undergo different compartment of biological fluids with different pH such as blood (neutral pH), Saliva (pH 6.8-7.0), Stomach (pH 1.2-2.0) small

Intestine (6.0-7.4), intracellular fluid (pH 6.8), and lysosome (pH 4.5–5) which may alter protein binding affinity [87]. Thus, the factor need to be considered while characterizing protein corona to represent the *in vivo* GIT condition of human system.

Most of the *in vitro* studies on characterizing protein corona were often performed under static conditions. Ingested NPs entering the GIT can interact with the physiological media under various shear stresses in the hydrodynamic body condition considering the physiological condition. The fact is that, the protein corona of NPs under dynamic fluidic conditions will be different from the one investigated in the static condition. This makes the comparison and correlation of the finding less accurate. For example, NPs injected through intravenous route and react with blood proteins showed difference in NP interaction with the media under various shear stress where, at 40 cm/sec speed the PEG coated liposomes carried more negative charge in the dynamic condition compared to the static counterpart indicating difference of binding protein components and each protein quantity [146].

1.18.3 Protein Concentration:

The pattern of the protein corona changes with difference in the protein concentration, for example the Silica NPs showed different protein adsorption and corona pattern when incubated with increasing plasma concentration explaining the concept of Vroman's effect by allowing competitive binding of proteins facilitating the desorption of high abundant protein with low binding affinity [87] and from different studies it is considered that the total amount of proteins clearly increases with increasing percentage of plasma concentration [84] [113] which is most likely because of more proteins of the same type bind at higher concentrations. However, all ENMs are not necessarily behave and show the same observation. For example, silica NPs showed a slight decrease in the total bound protein with higher plasma concentration[84]. Another interesting observation were noticed with respect to the function of protein concentration that, higher levels of protein adsorption occur on hydrophobic flat surfaces than

on the hydrophilic NPs and also this evolving trend may indicate that the most abundant proteins are progressively displaced by those with a higher affinity [147] .

As most of the *In vitro* study are generally with low protein concentration, Monopoli et al. figured out that the thickness of hard protein corona around NPs decreases with decrease in the plasma concentration which indicates invitro studies of NP -protein Interaction cannot always predict the behaviour of the NPs in the physiological system of human [132]. Another study by Pablo et al , [101] adopted an analytical model called “Hill model” to describe how proteins bound on to NPs influence the adsorption of further proteins from the solution on to the same NP. They insisted meaning full characterization of protein corona by considering equilibrium dissociation and kinetic coefficient to understand the protein binding data where the concentration of protein plays an important role in quantifying the equilibrium and kinetic properties. They outlined the fact, when the concentration of protein is more than the concentration of the NPs, most of the proteins remain in the solution since NPs are already saturated with proteins and thus any further addition of proteins will remain unbound where only small fraction of the protein attaches to the NPs and very hard to detect. However, in certain scenarios have to be investigated under saturated conditions of NPs. Moreover, the optimum situation to possibly analyze free proteins as well as bound protein, is when the NPs have to be half saturated with proteins on average where the amount of free proteins and bound proteins will be in the same range.

During an *in vivo* journey of ingested NPs, they would be exposed to a variety of biological fluids travelling the GIT of human system, which contain different protein composition and concentration resulting different protein corona. Even different routes of administration of NPs and pathways lead to various corona compositions. Thus , the interaction study of different NPs with protein concentration gradient which could evolve the actual NPs pathway in the human body need more attention and understanding in knowing its biological response [134].

We can obtain wide range of different outcomes just by changing the environment. In addition to the differences that could arise between in-vivo and in-vitro data's, differences in the above parameters also influence the protein interaction with NPs which need attention while doing characterization studies in order to compare and correlate the experimental finding with the real-world scenario of human physiological system. Hence, it is essential to evaluate Protein - NP interactions in a biomimetic environment which mimics *in vivo* physiological conditions to more accurately predict the fate of NPs *in vivo*.

1.18.4 Effect of Nanomaterial Properties on the Protein Corona Formation:

NPs once ingested will enters the physiological environment and react with proteins where the extent of these interaction with the formation of protein corona depends on the physicochemical factors of the NPs such as surface chemistry, topography, surface curvature etc.

1.18.5 Size &Curvature:

The influence of size and curvature on the protein corona was observed by several studies, it was observed that an increasing surface curvature of the NP will tend to lower the affinity of a protein to NPs interaction due to decrease in the area of interaction and tend to undergo fewer changes in conformation than those adsorbed to less curved surfaces, which is why the composition of the protein corona is not the same for similar ENMs/NPs with different sizes [113, 132]. Moreover, the highly curved surfaces of NPs decrease protein–protein interactions due to increase in the angle of deflection between adsorbed proteins [148]. From the study [149, 150], the greater loss of A-helix structure for lysozyme protein on SiO₂ NPs was observed and Cytochrome- c retains a more native conformation on 4 nm compared to 15 and 35 nm SiO₂ NPs. This may be due to lesser protein -protein interaction and larger thermodynamic barrier to protein spreading on more highly curved NPs [151]. In contrast, Fibrinogen shows larger structural defect on smaller SiO₂ NPs over larger NPs [152]. This suggest the tendency

of the smaller NPs to hold the native conformation of the proteins is not only based on the curvature but also dependent on the protein orientation and stability of protein-protein interaction. Moreover, the exact influence of surface curvature on the composition of the corona is not clear where no such comprehensive study of different physiological proteins adsorption study on to wide range of dietary NPs in the 10-100 nm size range. Another study by Cedervall et al. [62] used NPs from 200nm to 70 nm with various hydrophobicity's to investigate the NP-Protein interaction on their surfaces and they showed a distinct difference in the protein coverage on the NPs where large NPs showed larger degree of protein coverage and also claimed the curvature of small NPs induce suppression of protein adsorption. Hence both NPs size and surface composition of NPs are important in defining the composition of the protein corona.

1.18.6 Surface Area and NP-Protein Ratio:

The tendency of NP to deagglomerate or agglomerate is strongly influenced by parameters like pH, Ionic stability and presence of proteins in the biological fluid, thereby the particle agglomeration behaviour will be different for varying NP-Protein ratios [153]. Thus, the NP surface might be dependent on the protein concentration present in the dispersing fluid which also influence the pattern of protein affinity and resulting protein corona. Moreover, the concentration of the NP: protein ratio also has significant influence on the binding affinity of the proteins.

Lundqvist et al. [113] studied the NP-Protein interaction at several NP-Protein ratios in order to investigate the protein binding pattern and to optimize the characterization of corona at the bio- Nano interface and suggested 2.8 mL of plasma per m² particle surface for 50 and 100nm, which is considered to be a necessary step before characterizing the protein corona using centrifugation technique to separate NP-Protein complex from unbound proteins. Another study [154] investigated the effect of NP-Protein ratio, where the number of proteins (Human

Transferrin) bound per NP is decreased by increasing the protein concentration thereby decreasing the NP-Protein ratio (r) and hence more energy is transferred to each bound proteins on the NPs resulting in stronger binding and higher conformational change.

1.18.7 Surface Properties:

In general NPs with hydrophobic or charged surfaces tend to adsorb more proteins, and denature them to a greater extent than those with neutral and hydrophilic surfaces [155]. For example, it was observed that, total protein adsorption from plasma increases with increase in the negative charge density and hydrophobicity of the polystyrene NPs and it was found that proteins denature in the presence of charged ligands, either positive or negative, but the neutral ligands keep the natural structure of proteins [62, 155-157]. From another study, it was observed that the albumin adsorption on N-tert-butylacrylamide (BAM) copolymer NPs was higher on the hydrophobic surface over hydrophilic counterpart despite having same protein affinity to the NPs [128]. This suggest, the affinity of the proteins to NPs with uniform surface chemistry tend to increase with increasing charge density and hydrophobicity. On the other hand, NPs with anionic and or cationic surfaces tend to preferentially adsorb basic or acidic plasma proteins, respectively. For example, anionic and cationic polystyrene NPs preferentially adsorb plasma proteins with $pI > 5.5$ (IgG) and $pI < 5.5$ (Albumin) respectively [157, 158]. ZnO, TiO₂, and SiO₂ NPs showed different set of adsorbed plasma proteins despite having nearly identical surface charge density [159]. However, we can't describe protein corona only based on considering few factors of NPs. For instance, despite having same surface charge with different functional groups showed different adsorption pattern where more $\alpha 1$ -acid glycoprotein, ApoJ, and ApoA-I, but less IgG and albumin adsorbed on to $N(CH_3)_3$ functionalized polystyrene NPs compared to NH₂ functionalized NPs [159]. The other purpose of doing pre-coating and surface functionalization of NPs is to optimize the protein corona composition and to decrease the protein adsorption on to NPs. For example, a study on

functionalization of CNT and SiO₂ NPS with Pluronics F127 showed a reduction in adsorption of serum proteins. The observed effect of various parameters which could possibly affect the composition, thickness, and conformation of the protein corona with its layers are summarized in Table 1.3.

Table 1.3 Relationship between changes in the NPs physiochemical proteins and the Protein corona [136] [68] [87]:

NP Physicochemical Parameter	The observed Effect on the Protein Corona
Size	<ol style="list-style-type: none"> 1. Bigger the size, larger the degree of protein coverage 2. Smaller size increases corona thickness and decreases conformational changes of the adsorbed protein on to NPs. 3. Evolution of composition and relative abundance of adsorbed protein.
Shape	<ol style="list-style-type: none"> 1. Higher protein adsorption on to NPs in nanorods over nanospheres.
Surface Charge	<ol style="list-style-type: none"> 1. Charge NPs affects the composition of formed protein corona. 2. Charged NPs have high cell internalization and faster opsonization rates than electrically neutral NPs. 3. Positively Charged NPs are incorporated by the cells at much faster rate in high numbers than negatively charged NPs. 4. Does not change the identity of the adsorbed proteins. <p>Highly charged surface</p> <ol style="list-style-type: none"> 1. Increase the density and Thickness of the protein corona 2. Increase the affinity & conformational change of the protein. <ul style="list-style-type: none"> • Protein conformation: positive >negative > neutral
Smoothness/Roughness	<ol style="list-style-type: none"> 1. Surface roughness greatly minimizes repulsive interaction and influences the amount of protein, but not the protein identity.
Hydrophobicity	<p>Higher Hydrophobic NPs</p> <ol style="list-style-type: none"> 1. Increase the thickness of the protein corona 2. Increase the affinity of the proteins to the NPs 3. Increase the protein conformational change 4. Increase the opsonization rate
Higher surface Curvature	<ol style="list-style-type: none"> 1. Increase the corona Thickness 2. Decrease the affinity and protein conformational change. 3. Does not change the identity of the adsorbed proteins
Higher Protein Concentration in the physiological environment	<ol style="list-style-type: none"> 1. Higher Thickness 2. Change in the identity of the adsorbed proteins
Higher NP Concentration Lower NP-Protein Ratio	<ol style="list-style-type: none"> 1. Increase the protein Conformational change

Evidently the size, curvature, surface charge and arrangement of surface functional groups are the major determinants for the NP-Protein interaction. However, the coherent picture of how the composition and the kinetic of corona formation varies with respect to factors such as NPs

size, charge, hydrophobicity, exposure time, protein concentration, stability etc. Therefore, a thorough knowledge and understanding of protein -NP complex and its interaction with careful characterization of biomolecular corona considering all the influencing factors will lead to predict and govern the *in vivo* fate of ingested NPs including biodistribution, bioavailability responses and toxicity. needs more attention and clarity on the area of quantitative characterization.

1.19 Human whole Saliva:

1.20 Introduction:

Human saliva is a mixture of secretions from multiple salivary glands, including the parotid, submandibular, sublingual, and other minor glands lying beneath the oral mucosa[160] [161, 162]. The saliva is slightly acidic with pH of 6.35 to 6.85 and the specific gravity ranges between 1.002 to 1.012 .Saliva is hypotonic in reference to plasma [163]. Most humans produce roughly 0.5 to 1.0 litre of saliva per day while the flow rate of unstimulated and stimulated saliva are approximately 0.3 to 0.4 mL/min and 1.5 to 2.0ml/min respectively [164]. The quality of the saliva vary between individuals ,as well as between stimulated and unstimulated saliva[162, 165].

1.21 Composition and Functions:

Human saliva is composed mainly of water, a variety of electrolytes, mucus, white blood cells, epithelial cells, glycoproteins, enzymes (such as amylase and lipase), antimicrobial agents such as secretory IgA and lysozyme proteins and nitrogenous products [160-162, 165]. The major functions of the human salivary secretions are host defense, digestion and protective functions which includes tissue coating, lubrication, humidification, immunological activity, anti- (Bacterial, Viral, Fungal) activity, digestive enzymes, bolus formation and taste [160, 162, 165, 166]. The composition and function of the human saliva are depicted in fig: 15 (a) & (b).

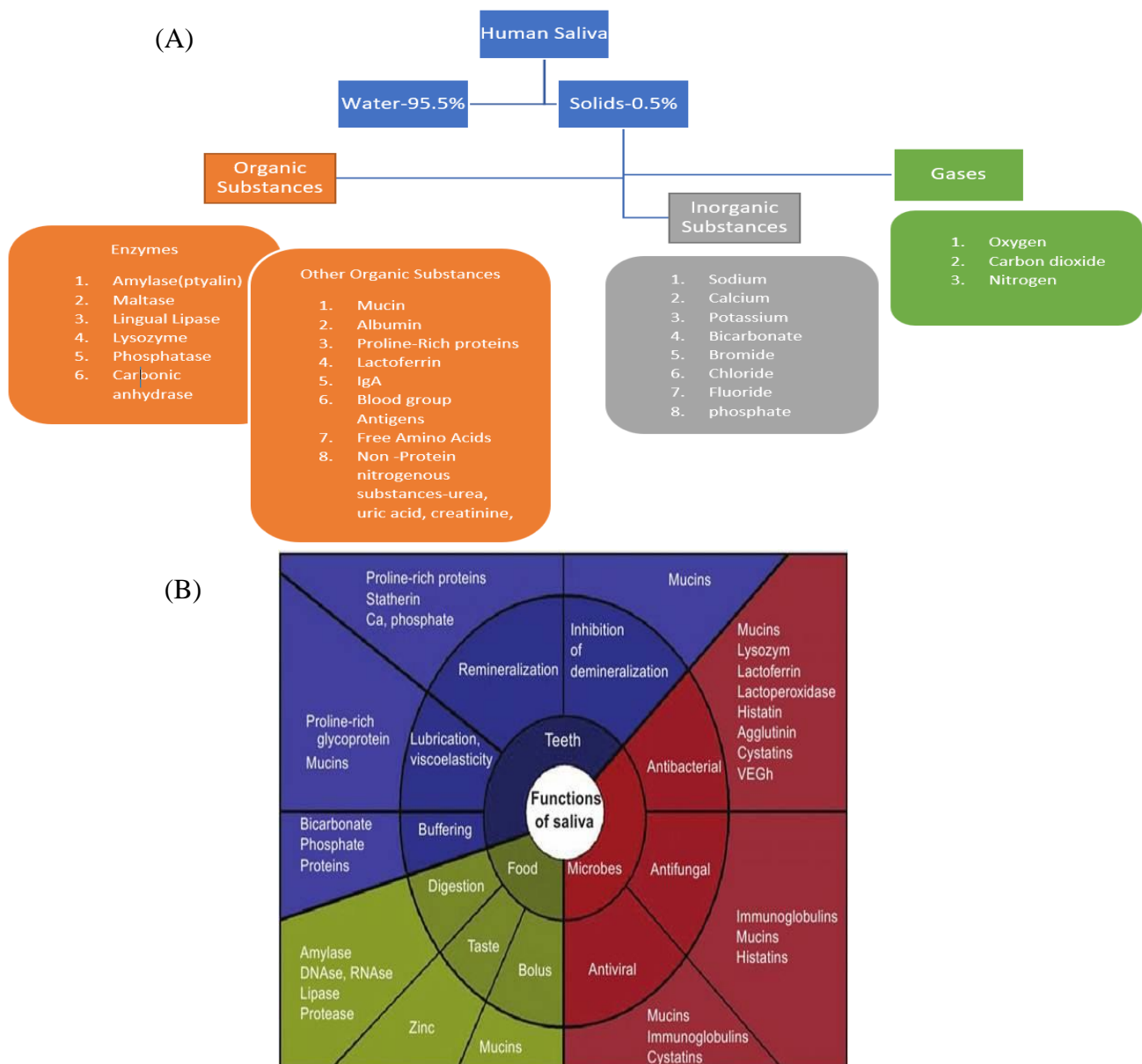


Figure 1.16 (A) Composition of saliva; (B) Function of saliva .Adapted from the reference [160, 165, 167] .

1.21.1 Potential Challenges with Identification of Salivary Proteins:

In complex protein mixtures such as saliva, proteins have different physicochemical characteristics and a wide concentration dynamic range. Generally, the presence of high abundant protein will obscure the low abundant proteins in the electrophoretic gel. The A-amylase in the saliva itself contributes to almost 60% of total salivary proteome which obscures the analysis of low abundant proteins. Salivary A-amylase can be depleted using starch column and allows the analysis of low abundant proteins [108, 168, 169]. Moreover, the identification of protein in saliva is challenging due to the high content of mucins, cellular debris, bacteria, high proteolytic activity and limited functional characterisation of specific salivary peptides and proteins which are highly polymorphic and undergo Post Translational Modifications (PTMs) leading to large inter-individual and intra-individual variations [107, 168, 170]. The composition of the saliva can also be affected by many other physiological factors like salivary flow rate, type of saliva whether stimulated or unstimulated, nature and duration of the stimulus and the diet and fluid intake [171]; hence it is important to minimise these variables by requesting volunteers to refrain from eating or drinking one hour prior to donating saliva sample to obtain similar baseline values and to report the salivary protein concentrations. In addition to the above-mentioned drawback, a study from Esser et al [172], has demonstrated that protein degradation may occur during and after sample collection. Thus, it is important to minimize the changes that could happen to saliva post collection in order to ensure to analyze the true salivary proteome by reducing the processing time between sample collection to storage and letting the samples to store immediately at freezing temperature ($<-20^{\circ}\text{C}$) to maintain the stability of the sample preventing from protein degradation [171, 172].

1.22 The Human Salivary Proteome:

Human saliva contains a large array of proteins and peptides that help maintain homeostasis in the oral cavity. Despite various biochemical and mass spectrometry techniques available for the proteomic analysis, many salivary proteins are still unknown. From several physiological studies on saliva, it was concluded that salivary acinar cells synthesize and secrete nearly all the salivary proteins using a complex array of ion pumps and channels at the cell surface. The group of enzymes such as amylase, peroxidase and others including proline-rich proteins (PRPs), histatins are mainly produced by parotid acinar cells. whereas, the sublingual and submandibular Parotid acinar cells produce mucins, enzymes and elongate polypeptides as like sublingual and parotid glands. [109, 173, 174].

The major salivary protein families which are structurally related proteins form a significant portion of total protein concentration in saliva that includes proline rich proteins (Acidic & Basic), amylase, High molecular weight glycoprotein MUC5B, Low-molecular weight glycoprotein MUC7, Agglutinin, cystatins, histatins and statherins [175] [176]. The salivary proteome contains a larger proportion (14.5%) of low-molecular-weight proteins (< 20 kDa) and the highest fraction of proteins range in the size between 20 and 40 kDa (26%) with the total percentage of the saliva proteins of molecular weight less than 60 kDa is 65%, whereas its only 36% with the plasma [177]. The highly abundant salivary proteins are majorly proline-rich proteins, amylase and mucins including other proteins as mentioned in the below summary Table:1.4. [178, 179] and the major salivary protein percentage are illustrated in figure 1.16.

Table 1.4 Major salivary protein and its functions in human saliva:

HUMAN SALIVA-MAJOR SALIVARY PROTEIN & ITS FUNCTIONS

Protein	Source	Function	MW	Modifications/Isoform	Conc in whole saliva (µg/mL)
Amylase	Parotid gland	<p>Digestion – Hydrolyzes starches (i.e. amylose, amylopectin, maltose, glucose) by catalyzing hydrolysis of alpha 1-4 glycosidic linkages in starch.</p> <p>Protection – Selective binding of oral microorganisms, preventing bacterial attachment and aiding bacterial clearance.</p>	53-57 kDa	<p>Glycosylated and</p> <p>Un-glycosylated isoforms</p>	<p>380-500- Whole saliva</p> <p>650-2600- Paraotid.</p>
Histatins	Major salivary glands -parotid, submandibular-sublingual (SMSL) and minor salivary glands (sublingual)	<p>Short distinct functional domains determine histanins biological functions.</p> <p>Anti-fungal, Anti -Bacterial.</p>	3-6 kDa	<p>Histatins exist in 3 major isoforms (Histatin 1, 3, and 5).</p> <p>Major forms of histatin undergo proteolytic cleavage to form minor forms of histatin</p>	<p>2-30- whole saliva.</p> <p>30-55- parotid</p> <p>13-70 - SMSL</p>

Mucins	Primarily sublingual and minor mucous glands	Provides salivary viscoelasticity and lubrication. Protection – physical barrier from bacterial protease activity, helps regulate bacterial and fungal colonization by selectively modulating adhesion of microorganisms to oral tissue surface.	120-1000 kDa (Glycosylation account for 40-80% of mass)	Two structurally distinct species of mucins secreted by salivary glands – MG1 (oligomeric) and MG2 (monomeric) Glycosylation –high carbohydrate content largely on serine and threonine residues	MG1=10-500- Whole saliva. MG2= 10-200 - whole saliva.
Statherins	Produced by Acinar cells	Inhibit the spontaneous precipitation of calcium phosphate salts from the supersaturated concentrations present in saliva.	5380 Da	Phosphoproteins rich in tyrosine, glutamine, and proline	2-12- Whole saliva. 16-147 Parotid. 20-150- SMSL.

Cystatins	Isolated from submandibular secretions	Inhibit crystal growth of calcium phosphate salts (10 times weaker than statherin)	14 kDa	SN, S, and S1 isoforms. Exist in phosphorylated and un-phosphorylated forms.	240-280 - whole saliva. 1.6-4.0-Paratid. 92-280-SMSL.
Carbonic Anhydrases	Submandibular and parotid glands	Protection – involved in salivary pH regulation	42 kDa	7 isozymes and several homologous carbonic anhydrase-related proteins Can be glycosylated	4.6
Peroxidases	GCF and neutrophil granulocytes and salivary glands	Antibacterial action	78-280 kDa	2 major forms found in saliva - Myeloperoxidase and Lactoperoxidase	1-5
Proline rich proteins	Whole saliva, Parotid, SMSL	Acidic PRPs -Maintain calcium homeostasis in oral cavity Glycosylated PRPs-As Lubricants		PRPs are classified as acidic, basic and glycosylated	90-180- whole saliva

		Basic PRPs-TO bind Tannins to prevent its toxic effect in the GIT.			230-1251-Parotid 270-1335-SMSL.
sIgA (Salivary Immunoglobulin)	Whole saliva, Parotid, SMSL	It represents the main adaptive immune mechanism in the oral cavity.	29 kDa		19-439-whole saliva 20-230-Parotid 41-56-SMSL.
Lactoferrin	Primarily Whole saliva including Parotid and SMSL	It is a Multifunctional protein with anti-bacterial, anti-viral, anti-inflammatory activity and modulation of the immune response.	80 kDa		194-Whole saliva 12-Parotid 13-SMSL.
Lysozyme	Parotid and SMSL	It lyses the cell wall of bacteria by the process of Hydrolysis	14.4 kDa		7-Parotid. 21-SMSL

IgG					0.4-14.4- Whole saliva
Albumin		Transporter Protein, negative acute -phase protein, pH buffer.			29-238- Whole saliva

The mucosal surface protection is conferred by components such as lysozyme, cystatins, immunoglobulins, lactoferrin, and histatins, which can destroy or inhibit the growth of microorganisms in the oral cavity [109] [180] [174]. The immunoglobulin and albumin present in the human plasma/serum make up to 60-80% of the total weight and the most abundant proteins in plasma represent 99% of the total protein content of plasma. whereas, for whole saliva the top 20 most abundant protein represent only ~40% of the salivary proteins [181] [177].

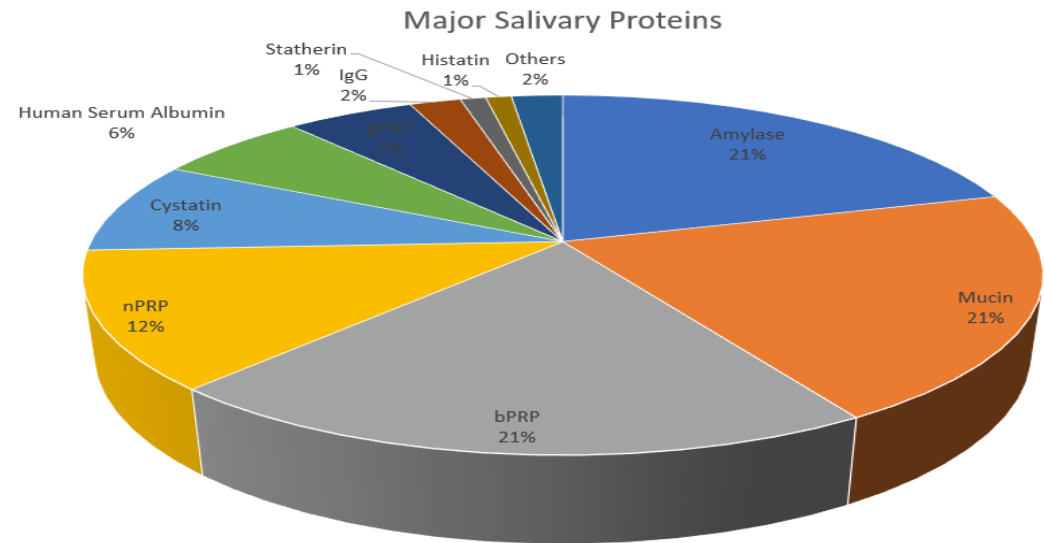


Figure 1.17 Approximate percentage of the major classes of the salivary proteins and peptides in Human saliva [178, 182, 183].

1.23 Current Status in Salivary Proteome Database:

Identification of total salivary proteins are largely dependent on the method of selection. Recent advancement in mass spectrometry-based proteomics provide a better platform in identifying and quantifying wide range of proteins and peptides. Till date 1381 proteins were reported in saliva using advanced proteomic approaches with improving analytical sensitivity [178]. As per the observation, lower the presence of abundance protein, the ease in identifying low abundant proteins in the complex biological sample [184]. Hence, diverse protein and peptide fractionation methods coupled with mass spectrometry techniques have been demonstrated for maximizing proteome coverage and to avoid the high abundant proteins from obscuring the detection of low lower concentration proteins which will allow the detection and characterization of both high abundant and low abundant proteins [169, 170, 185] .

An interesting study by Yan et al. on comparing the proteome of human plasma and saliva using peptide fractionation method with Mass spectrometry technique, documented a total of 1939 salivary proteins in whole and ductal saliva. 597 proteins out of 3020 proteins identified in human plasma are also found in human saliva [170] .

Another study by Bandhakavi et al [186] , used hexapeptide libraries for Dynamic Range Compression (DRC) coupled with 3D peptide fractionation and identified 2340 proteins in Human whole saliva and of which ~27% of the whole saliva proteins are found in blood plasma. Despite the large number of known proteins identified so far, deeper and comprehensive studies are necessary, in order to understand the correlations, with high sensitivity and specificity between salivary proteins and ingested NPs through dietary source [175].

1.24 Interaction between Ingested Dietary NPs and the Gastrointestinal Tract:

The ever-growing exploitation of nanotechnology in food, feed and food packaging industry is likely to increase the oral exposure of dietary NPs. Many food products contain appreciable levels of ENMs and Dietary NPs of diameter <100nm that may be either intentionally or unintentionally (Contamination/migration from food contact materials) added which are expected to be ingested and pass through the GIT [187]. Moreover, NPs can be ingested from other sources like cosmetics, medicine etc. As the ingested NPs move through different compartments of GIT (such as mouth, stomach, small intestine, and large intestine) they are exposed to several changes [187] during the journey :

1. pH and Ionic strength
2. Surface active components (Bile salts, phospholipids, fatty acids, proteins)
3. Digestive Enzymes (Amylase, protease, lipase etc)
4. Biopolymers (proteins, mucins)
5. Biological surfaces (Tongue, stomach, Intestine)
6. Intestinal Microbiota (Colonic bacteria)
7. Complex Flow

As a result, the above changes may alter the ingested NPs properties as they travel through the GIT , thereby causing difference in the pattern of protein binding and the resulting protein corona which will influence their effects on cell /tissues uptake and its biodistribution [188]. Hence it is important to consider the condition of GIT in GIT fate studies of NPs to understand whether they are digested, dissolved or absorbed by the intestinal cells or reach the colon [187].

When NPs are mixed with food while preparation or processing, get exposed to various mechanical forces, shear stress and temperature profile which can affect the properties of the added NPs/ENMs and also the food components. Another interesting fact and question about

the influence of food matrix on dietary NPs is the consideration of physical dispersion of the added NPs in the food medium interface like for instances, whether NPs dispersed in lipid, water, protein or oil-water-protein interface and its respective changes in the NPs properties are less explored in the study of characterization & toxicity of NPs [189]. The properties of the pristine dietary NPs would undergo appreciable alterations in the properties of the NPs before entering the GIT. Therefore, it is very important to characterize the NPs within the food matrix in the beginning of the experiment before any further investigation on the interaction of respective NPs fate in GIT. Moreover, in order to understand the fate of ingested NPs in the GIT, we need to develop new methods with techniques like SP-ICP-MS, Field Flow Fraction (FFF), X-ray absorption near edge structure (XANES) and SERS for complete characterization of NPs in complex media such as food matrix or GIT. In addition to that, *in vivo* studies of human digestion process are practically difficult to sample the digesta from different sections of the GIT, while animal models strongly differ from the human GIT. *In vitro* models considered to be relatively easy, less expensive which allows to process number of trials, easy sampling with high reproducibility. Several studies were initiated on the *In vitro* static models of the digestion process to understand the influence of GIT on NPs such as AgNPs, SiO₂, TiO₂, and ZnO NPs etc.[188, 190-193] . In order to be more realistic in the observation, enumerating the *in vitro* dynamic digestion models is required which include physical process(chewing, mixing) and reproduce continuous changes of the luminal conditions to precisely mimic the *in vivo* conditions [194].

The GIT condition can impact the property of iNPs (ingested NPs) by influencing the agglomeration state and the stability of the NPs at different GIT regions and also impact their passage through the mucus layer that coats the intestinal lining including their transport into and across the epithelium cells [195]. Further , the behaviour of iNPs in the presence of food matrix during the digestion process is key question that need more attention , however some

studies suggest that the presence of digestive enzymes and food components modifies the fate of iNPs during *in vitro* digestion process [196], while a recent study [197] on AgNPs with food matrix formed less aggregates during digestion in GIT and concluded the food components could act as a colloidal stabilizers.

Walczak et al, observed that, the iNPs are protected from degradation in the presence of enzymes and led to the formation of clusters composed of AgNPs and chlorine [193]. The activity of enzymes in the GIT may also alter some of the NPs such as those that are composed of starch, lipids, proteins, or nucleic acids that may subject to digestion [195, 196]. Moreover, Amylase, lipase, nuclease, pepsin and other proteases can remove the surface covering of iNPs with adsorbed molecules and have an incidence on the kinetic of the dynamic corona [196].

The pH varies in different compartment of GIT from 1-7.5, while the pH is slightly acidic to neutral in the buccal cavity(saliva) and the small intestine and is more acidic in the stomach, thereby causing NP agglomeration due to the effect of change in pH and ionic strength on the surface of iNPs. Indeed, zeta potential modification by ionic salts may influence the electrostatic repulsion [198]. For example, the surface electrostatic repulsion of TiO₂ disappears in increased electrolyte concentration leading to particle aggregation [199] and the same observation noted for SiO₂ in the presence of food matrix [78]. In addition to aggregation metal based NPs in acidic environment will lose its stability due to decrease in the zeta potential and may be dissolve in the environment releasing silver ions which then react with chloride to form in-soluble silver chloride[193] .

The major observation of many previous studies on the fate of iNPs in GIT is the use of static *in vitro* cellular model system ignoring the potential influence of the GIT environmental conditions while characterizing NP-biomolecular corona complex. Common *in vitro* cellular approaches have significant deficiencies which may lead to erroneous result and misleading

conclusion about the impact of iNPs on their fate in the GIT and ADME properties. For instances, the pristine NP suspensions are incubated with model intestinal cells rather than passing them through GIT model first. In addition to that the interfacial properties and agglomeration state of the iNPs are not physiologically relevant and may be different from what the intestinal cells would see in real life [187, 196].

We need better understanding on the fate of iNPs in the GIT and how different types of organic (Lipid, Protein etc) and inorganic NPs (TiO₂, SiO₂, Ag etc) behave within the human gastrointestinal tract (GIT), and how the food matrix and the physiological environment changes their physicochemical properties and influence their gastrointestinal fate during the digestion process, by considering the complex physicochemical and physiological condition and possible transformation of the ingested NPs and the biomolecular corona as they pass through the human GIT [198].

1.25 Knowledge Gap

At present much of the concern about the safe use of nanotechnology in food sector is the lack of toxicology data to conclude the safety of the nanofood over other conventional counterparts. At present, there is not much information regarding the metabolism, biotransformation of dietary NPs/ENMs ingested through food and dietary supplements in human.

One of the key questions about the safety of Dietary NPs ingestion is about their impact on the oro-gastrointestinal route. As the oral cavity represents the first portal of entry for the food to begin its digestion process and is known to rapidly interact with the NPs and hence, there is a higher possibility of the NP-biomolecular and cellular interaction in the buccal cavity. Unlike NP- blood proteome study, no much data and investigation for the NP-saliva proteome interaction and its biological response in the buccal cavity for different combination of salivary proteins and dietary NPs.

Moreover, when dietary NPs are consumed along with the food, it may have different impact on the GIT fate based on the nature of the food matrix in which the NPs are dispersed, the physico-chemical properties of the pristine NPs and the nature of the physiological medium in the GIT of human system. Therefore, the biological identity of the type of NPs and its cellular response may change depending on the above-mentioned factors. Considering the above fact, our knowledge of the biomolecular corona is still not comprehensive and we need information on protein corona formation at different compartment of the GIT system and the interaction study of different combinations of proteins and NPs has to be investigated in detail to gain broad understanding in ensuring the safety of a particular Dietary NPs that are intentionally added in to the food products.

As it is evident, a change in the biological media can influence the biological identity of the ingested NPs, it is very critical to understand the influence of Dietary NPs at every stage of the GIT system and subsequently

1. To investigate the presence, dissolution, agglomeration state and release of materials in the nano-size range from food containing dietary NPs and food additives with NP fraction like Silica and TiO_2 (E 551 and E 271) during human digestion is a key question for the safety assessment of these NPs.
2. Most of the studies investigating the influence of protein binding on the uptake of NPs were conducted using either incubating NPs with individual proteins or with whole blood/serum/plasma.
3. Most of the toxicity studies of the NPs have been with pristine NPs ignoring the change in biological identity of NPs during their interaction with biological fluids. This will have a significant impact on the conclusion to suggest and ensure the safety of any dietary NPs /ENM s.

1.26 Hypothesis:

1. We hypothesize that the size and the surface chemistry of the NPs influence the salivary protein corona.
2. We hypothesize that the function of A-amylase is altered due to its conformational change occurred during its interaction with dietary NPs.

1.27 Conclusion

It is noted that, many factors influence the biological response and ADME behavior of the ingested NPs depending on the route of ingestion and the matrix in which the NPs are dispersed. Moreover, it is not just the physicochemical properties of a pristine NP that influence the composition and kinetics of biomolecular corona but also the type of biological fluid and composition of the fluid at every compartment of the GIT system. Hence, it is very critical to consider the above factors in order to investigate the fate and the biological properties and responses of the respective ingested NPs characterization followed by cellular uptake study of the iNPs.

1.28 REFERENCE:

1. Bhushan, B., *Introduction to nanotechnology*, in *Springer handbook of nanotechnology*. 2017, Springer. p. 1-19.
2. Bleeker, E.A., et al., *Considerations on the EU definition of a nanomaterial: science to support policy making*. *Regulatory toxicology and pharmacology*, 2013. **65**(1): p. 119-125.
3. Yokel, R.A. and R.C. MacPhail, *Engineered nanomaterials: exposures, hazards, and risk prevention*. *Journal of Occupational Medicine and Toxicology*, 2011. **6**(1): p. 7.
4. Freestone, I., et al., *The Lycurgus cup—a roman nanotechnology*. *Gold Bulletin*, 2007. **40**(4): p. 270-277.
5. Edwards, P.P. and J.M. Thomas, *Gold in a Metallic Divided State—From Faraday to Present-Day Nanoscience*. *Angewandte Chemie International Edition*, 2007. **46**(29): p. 5480-5486.
6. Hulla, J., S. Sahu, and A. Hayes, *Nanotechnology: History and future*. *Human & experimental toxicology*, 2015. **34**(12): p. 1318-1321.
7. Holister, P., et al., *Nanoparticles*. *Technology White Papers*, 2003. **3**(1-11).
8. Borm, P.J., et al., *The potential risks of nanomaterials: a review carried out for ECETOC*. *Particle and fibre toxicology*, 2006. **3**(1): p. 11.
9. Buzea, C., I.I. Pacheco, and K. Robbie, *Nanomaterials and nanoparticles: Sources and toxicity*. *Biointerphases*, 2007. **2**(4): p. MR17-MR71.
10. Stone, V., et al., *Nanomaterials for environmental studies: classification, reference material issues, and strategies for physico-chemical characterisation*. *Science of the total environment*, 2010. **408**(7): p. 1745-1754.
11. Bhatia, S., *Nanoparticles types, classification, characterization, fabrication methods and drug delivery applications*, in *Natural Polymer Drug Delivery Systems*. 2016, Springer. p. 33-93.
12. Bhushan, B., *Springer handbook of nanotechnology*. 2010: Springer Science & Business Media.
13. Buzea, C. and I. Pacheco, *Nanomaterials and their Classification*, in *EMR/ESR/EPR Spectroscopy for Characterization of Nanomaterials*, A.K. Shukla, Editor. 2017, Springer India: New Delhi. p. 3-45.
14. Thomas, S., et al., *Thermal and rheological measurement techniques for nanomaterials characterization. Volume 3*. 2017.
15. Higashisaka, K., Y. Yoshioka, and Y. Tsutsumi, *Applications and Safety of Nanomaterials Used in the Food Industry*. *Food Safety*, 2015. **3**(2): p. 39-47.
16. Chaudhry, Q., et al., *Applications and implications of nanotechnologies for the food sector*. *Food additives and contaminants*, 2008. **25**(3): p. 241-258.
17. Ireland, F., *The Relevance for Food Safety of Applications of Nanotechnology in the Food and Feed Industries*. The Food Safety and Authority of Ireland (FSAI), Abbey, 2008.
18. Pradhan, N., et al., *Facets of nanotechnology as seen in food processing, packaging, and preservation industry*. *BioMed research international*, 2015. **2015**.
19. Rashidi, L. and K. Khosravi-Darani, *The applications of nanotechnology in food industry*. *Critical reviews in food science and nutrition*, 2011. **51**(8): p. 723-730.
20. He, X. and H.-M. Hwang, *Nanotechnology in food science: functionality, applicability, and safety assessment*. *Journal of food and drug analysis*, 2016. **24**(4): p. 671-681.
21. Fraceto, L.F., et al., *Nanotechnology in agriculture: which innovation potential does it have?* *Frontiers in Environmental Science*, 2016. **4**: p. 20.
22. Rai, M. and A. Ingle, *Role of nanotechnology in agriculture with special reference to management of insect pests*. *Applied microbiology and biotechnology*, 2012. **94**(2): p. 287-293.

23. Robinson, D., *Value chains as a linking-pin framework for exploring governance and innovation in nano-involved sectors: illustrated for nanotechnologies and the food packaging sector*. European Journal of Law and Technology, 2011. **2**(3).
24. Singh, T., et al., *Application of nanotechnology in food science: Perception and overview*. Frontiers in microbiology, 2017. **8**: p. 1501.
25. Sen, S. and Y. Pathak, *Nanotechnology in Nutraceuticals: Production to Consumption*. 2016: CRC Press.
26. Ranjan, S., et al., *Nanoscience and nanotechnologies in food industries: opportunities and research trends*. Journal of Nanoparticle Research, 2014. **16**(6): p. 2464.
27. Duncan, T.V., *Applications of nanotechnology in food packaging and food safety: barrier materials, antimicrobials and sensors*. Journal of colloid and interface science, 2011. **363**(1): p. 1-24.
28. Hsieh, P.Y.-H. and J.A. Ofori, *Innovations in food technology for health*. Asia Pacific Journal of Clinical Nutrition, 2007. **16**(S1): p. 65-73.
29. Weiss, J., P. Takhistov, and D.J. McClements, *Functional materials in food nanotechnology*. Journal of food science, 2006. **71**(9).
30. Organization, W.H., *FAO/WHO expert meeting on the application of nanotechnologies in the food and agriculture sectors: potential food safety implications: meeting report*. 2010: World Health Organization.
31. Smolkova, B., et al., *Nanoparticles in food. Epigenetic changes induced by nanomaterials and possible impact on health*. Food and Chemical Toxicology, 2015. **77**(Supplement C): p. 64-73.
32. Peters, R., et al., *Inventory of Nanotechnology applications in the agricultural, feed and food sector*. EFSA Supporting Publications, 2014. **11**(7).
33. Sekhon, B.S., *Food nanotechnology – an overview*. Nanotechnology, Science and Applications, 2010. **3**: p. 1-15.
34. Center, W.W., *The Project on Emerging Nanotechnologies: Consumer Product Inventory*. 2015.
35. Tsuji, J.S., et al., *Research strategies for safety evaluation of nanomaterials, part IV: risk assessment of nanoparticles*. Toxicological sciences, 2005. **89**(1): p. 42-50.
36. Kandlikar, M., et al., *Health risk assessment for nanoparticles: A case for using expert judgment*. Journal of Nanoparticle Research, 2007. **9**(1): p. 137-156.
37. Axelos, M.A.V. and M.H.v.d. Voorde, *Nanotechnology in agriculture and food science*. 2017.
38. Rao, K.S., et al., *A novel method for synthesis of silica nanoparticles*. Journal of colloid and interface science, 2005. **289**(1): p. 125-131.
39. Liberman, A., et al., *Synthesis and surface functionalization of silica nanoparticles for nanomedicine*. Surface Science Reports, 2014. **69**(2): p. 132-158.
40. Martirosyan, A. and Y.-J. Schneider, *Engineered Nanomaterials in Food: Implications for Food Safety and Consumer Health*. International Journal of Environmental Research and Public Health, 2014. **11**(6): p. 5720-5750.
41. Dekkers, S., et al., *Presence and risks of nanosilica in food products*. Nanotoxicology, 2011. **5**(3): p. 393-405.
42. Organization, W.H., *Evaluation of Certain Food Additives and Contaminants: Eightieth Report of the Joint FAO/WHO Expert Committee on Food Additives*. Vol. 80. 2016: World Health Organization.
43. Additives, E.Panel o.F., et al., *Re-evaluation of silicon dioxide (E 551) as a food additive*. EFSA Journal, 2018. **16**(1): p. e05088-n/a.
44. Peters, R.J.B., et al., *Characterization of Titanium Dioxide Nanoparticles in Food Products: Analytical Methods To Define Nanoparticles*. Journal of Agricultural and Food Chemistry, 2014. **62**(27): p. 6285-6293.
45. de Jong, W.H., et al., *Engineered Nanoparticles and Food: Exposure, Toxicokinetics, Hazards and Risks*, in *Nanotechnologies in Food*. 2017. p. 200-227.

46. Bourikas, K., C. Kordulis, and A. Lycourghiotis, *Titanium dioxide (anatase and rutile): surface chemistry, liquid–solid interface chemistry, and scientific synthesis of supported catalysts*. Chemical reviews, 2014. **114**(19): p. 9754-9823.
47. Chen, X. and S.S. Mao, *Titanium dioxide nanomaterials: synthesis, properties, modifications, and applications*. Chemical reviews, 2007. **107**(7): p. 2891-2959.
48. Vijayalakshmi, R. and V. Rajendran, *Synthesis and characterization of nano-TiO₂ via different methods*. Archives of Applied Science Research, 2012. **4**(2): p. 1183-1190.
49. Yang, H.G., et al., *Solvothermal synthesis and photoreactivity of anatase TiO₂ nanosheets with dominant {001} facets*. Journal of the American Chemical Society, 2009. **131**(11): p. 4078-4083.
50. Weir, A., et al., *Titanium Dioxide Nanoparticles in Food and Personal Care Products*. Environmental Science & Technology, 2012. **46**(4): p. 2242-2250.
51. Aguilar, F., et al., *Re-evaluation of titanium dioxide (E 171) as a food additive*. EFSA JOURNAL, 2016. **14**(9).
52. Rompelberg, C., et al., *Oral intake of added titanium dioxide and its nanofraction from food products, food supplements and toothpaste by the Dutch population*. Nanotoxicology, 2016. **10**(10): p. 1404-1414.
53. Chen, X.X., et al., *Characterization and preliminary toxicity assay of nano-titanium dioxide additive in sugar-coated chewing gum*. Small, 2013. **9**(9-10): p. 1765-1774.
54. Jazayeri, S.D., et al., *Gene expression profiles in primary duodenal chick cells following transfection with avian influenza virus H5 DNA plasmid encapsulated in silver nanoparticles*. International journal of nanomedicine, 2013. **8**: p. 781.
55. Zhang, X.-F., et al., *Silver Nanoparticles: Synthesis, Characterization, Properties, Applications, and Therapeutic Approaches*. International Journal of Molecular Sciences, 2016. **17**(9): p. 1534.
56. Lundqvist, M., et al., *The Evolution of the Protein Corona around Nanoparticles: A Test Study*. ACS Nano, 2011. **5**(9): p. 7503-7509.
57. Saptarshi, S.R., A. Duschl, and A.L. Lopata, *Interaction of nanoparticles with proteins: relation to bio-reactivity of the nanoparticle*. Journal of Nanobiotechnology, 2013. **11**: p. 26-26.
58. Tenzer, S., et al., *Rapid formation of plasma protein corona critically affects nanoparticle pathophysiology*. Nature nanotechnology, 2013. **8**(10): p. 772-781.
59. Vroman, L., *Effect of adsorbed proteins on the wettability of hydrophilic and hydrophobic solids*. Nature, 1962. **196**(4853): p. 476-477.
60. Hadjidemetriou, M. and K. Kostarelos, *Nanomedicine: Evolution of the nanoparticle corona*. Nature Nanotechnology, 2017. **12**(4): p. 288-290.
61. Westmeier, D., et al., *Bio–Nano Interactions*, in *Adverse Effects of Engineered Nanomaterials (Second Edition)*. 2017, Elsevier. p. 1-12.
62. Cedervall, T., et al., *Understanding the nanoparticle–protein corona using methods to quantify exchange rates and affinities of proteins for nanoparticles*. Proceedings of the National Academy of Sciences, 2007. **104**(7): p. 2050-2055.
63. Monopoli, M.P., et al., *Biomolecular coronas provide the biological identity of nanosized materials*. Nature nanotechnology, 2012. **7**(12): p. 779.
64. Rahman, M., et al., *Nanoparticle and Protein Corona*, in *Protein-Nanoparticle Interactions: The Bio-Nano Interface*, M. Rahman, et al., Editors. 2013, Springer Berlin Heidelberg: Berlin, Heidelberg. p. 21-44.
65. Docter, D., et al., *The nanoparticle biomolecule corona: lessons learned - challenge accepted?* Chemical Society Reviews, 2015. **44**(17): p. 6094-6121.
66. Westmeier, D., R.H. Stauber, and D. Docter, *The concept of bio-corona in modulating the toxicity of engineered nanomaterials (ENM)*. Toxicology and applied pharmacology, 2016. **299**: p. 53-57.

67. Vilanova, O., et al., *Understanding the Kinetics of Protein–Nanoparticle Corona Formation*. ACS Nano, 2016. **10**(12): p. 10842-10850.
68. Walkey, C.D. and W.C. Chan, *Understanding and controlling the interaction of nanomaterials with proteins in a physiological environment*. Chemical Society Reviews, 2012. **41**(7): p. 2780-2799.
69. Lundqvist, M., I. Sethson, and B.-H. Jonsson, *Protein adsorption onto silica nanoparticles: conformational changes depend on the particles' curvature and the protein stability*. Langmuir, 2004. **20**(24): p. 10639-10647.
70. Forest, V. and J. Pourchez, *The nanoparticle protein corona: The myth of average*. Nano Today, 2016. **11**(6): p. 700-703.
71. Lundqvist, M., et al., *The nanoparticle protein corona formed in human blood or human blood fractions*. PloS one, 2017. **12**(4): p. e0175871.
72. Saptarshi, S.R., A. Duschl, and A.L. Lopata, *Interaction of nanoparticles with proteins: relation to bio-reactivity of the nanoparticle*. Journal of Nanobiotechnology, 2013. **11**(1): p. 26.
73. Slack, S.M. and T.A. Horbett, *The Vroman effect: a critical review*. 1995, ACS Publications.
74. Norde, W., *Protein adsorption at solid surfaces: A thermodynamic approach*. Pure and applied chemistry, 1994. **66**(3): p. 491-496.
75. Walkey, C.D., et al., *Nanoparticle size and surface chemistry determine serum protein adsorption and macrophage uptake*. Journal of the American Chemical Society, 2012. **134**(4): p. 2139-2147.
76. Casals, E., et al., *Time Evolution of the Nanoparticle Protein Corona*. ACS Nano, 2010. **4**(7): p. 3623-3632.
77. Walczyk, D., et al., *What the cell “sees” in bionanoscience*. Journal of the American Chemical Society, 2010. **132**(16): p. 5761-5768.
78. Peters, R., et al., *Presence of nano-sized silica during in vitro digestion of foods containing silica as a food additive*. ACS nano, 2012. **6**(3): p. 2441-2451.
79. Dobrovolskaia, M.A., et al., *Interaction of colloidal gold nanoparticles with human blood: effects on particle size and analysis of plasma protein binding profiles*. Nanomedicine: Nanotechnology, Biology and Medicine, 2009. **5**(2): p. 106-117.
80. Green, R., et al., *Competitive protein adsorption as observed by surface plasmon resonance*. Biomaterials, 1999. **20**(4): p. 385-391.
81. Dell'Orco, D., et al., *Modeling the time evolution of the nanoparticle-protein corona in a body fluid*. PloS one, 2010. **5**(6): p. e10949.
82. Nguyen, V.H. and B.-J. Lee, *Protein corona: a new approach for nanomedicine design*. International Journal of Nanomedicine, 2017. **12**: p. 3137-3151.
83. Monopoli, M.P., et al., *Biomolecular coronas provide the biological identity of nanosized materials*. Nature nanotechnology, 2012. **7**(12): p. 779-786.
84. Monopoli, M.P., et al., *Physical– chemical aspects of protein corona: relevance to in vitro and in vivo biological impacts of nanoparticles*. J. Am. Chem. Soc, 2011. **133**(8): p. 2525-2534.
85. Gebauer, J.S., et al., *Impact of the nanoparticle–protein corona on colloidal stability and protein structure*. Langmuir, 2012. **28**(25): p. 9673-9679.
86. Lundqvist, M., *Nanoparticles: Tracking protein corona over time (vol 8, pg 701, 2013)*. Nature Nanotechnology, 2013. **8**(11): p. 806-806.
87. Van Hong Nguyen, B.-J.L., *Protein corona: a new approach for nanomedicine design*. International journal of nanomedicine, 2017. **12**: p. 3137.
88. Mahmoudi, M., et al., *Emerging understanding of the protein corona at the nano-bio interfaces*. Nano Today, 2016. **11**(6): p. 817-832.
89. Nel, A.E., et al., *Understanding biophysicochemical interactions at the nano–bio interface*. Nature materials, 2009. **8**(7): p. 543.
90. Hühn, D., et al., *Polymer-coated nanoparticles interacting with proteins and cells: focusing on the sign of the net charge*. Acs Nano, 2013. **7**(4): p. 3253-3263.

91. Koegler, P., et al., *The influence of nanostructured materials on biointerfacial interactions*. Advanced drug delivery reviews, 2012. **64**(15): p. 1820-1839.
92. Foroozandeh, P. and A.A. Aziz, *Merging Worlds of Nanomaterials and Biological Environment: Factors Governing Protein Corona Formation on Nanoparticles and Its Biological Consequences*. Nanoscale Research Letters, 2015. **10**: p. 221.
93. Shang, L., et al., *pH-dependent protein conformational changes in albumin: gold nanoparticle bioconjugates: a spectroscopic study*. Langmuir, 2007. **23**(5): p. 2714-2721.
94. Dawson, K.A., A. Salvati, and I. Lynch, *Nanotoxicology: nanoparticles reconstruct lipids*. Nature nanotechnology, 2009. **4**(2): p. 84.
95. Ehrenberg, M.S., et al., *The influence of protein adsorption on nanoparticle association with cultured endothelial cells*. Biomaterials, 2009. **30**(4): p. 603-610.
96. Mahmoudi, M., et al., *Protein– nanoparticle interactions: opportunities and challenges*. Chemical reviews, 2011. **111**(9): p. 5610-5637.
97. Carrillo-Carrion, C., M. Carril, and W.J. Parak, *Techniques for the experimental investigation of the protein corona*. Current Opinion in Biotechnology, 2017. **46**: p. 106-113.
98. Sasidharan, A., J.E. Riviere, and N.A. Monteiro-Riviere, *Gold and silver nanoparticle interactions with human proteins: impact and implications in biocorona formation*. Journal of Materials Chemistry B, 2015. **3**(10): p. 2075-2082.
99. Fischer, K. and M. Schmidt, *Pitfalls and novel applications of particle sizing by dynamic light scattering*. Biomaterials, 2016. **98**: p. 79-91.
100. Balog, S., et al., *Characterizing nanoparticles in complex biological media and physiological fluids with depolarized dynamic light scattering*. Nanoscale, 2015. **7**(14): p. 5991-5997.
101. Del Pino, P., et al., *Protein corona formation around nanoparticles—from the past to the future*. Materials Horizons, 2014. **1**(3): p. 301-313.
102. Monopoli, M.P., et al., *Formation and Characterization of the Nanoparticle–Protein Corona*, in *Nanomaterial Interfaces in Biology: Methods and Protocols*, P. Bergese and K. Hamad-Schifferli, Editors. 2013, Humana Press: Totowa, NJ. p. 137-155.
103. Lai, Z.W., et al., *Emerging techniques in proteomics for probing nano–bio interactions*. ACS nano, 2012. **6**(12): p. 10438-10448.
104. Barbero, F., et al., *Formation of the Protein Corona: The Interface between Nanoparticles and the Immune System*. Seminars in Immunology, 2017. **34**(Supplement C): p. 52-60.
105. Barrán-Berdón, A.L., et al., *Time Evolution of Nanoparticle–Protein Corona in Human Plasma: Relevance for Targeted Drug Delivery*. Langmuir, 2013. **29**(21): p. 6485-6494.
106. Capriotti, A.L., et al., *Analytical Methods for Characterizing the Nanoparticle–Protein Corona*. Chromatographia, 2014. **77**(11): p. 755-769.
107. Xiao, X., et al., *Comparative proteomic analysis of the influence of gender and acid stimulation on normal human saliva using LC/MS/MS*. PROTEOMICS-Clinical Applications, 2017.
108. Madden, R.D., J.R. Sauer, and J.W. Dillwith, *A proteomics approach to characterizing tick salivary secretions*. Experimental & applied acarology, 2004. **32**(1-2): p. 131-141.
109. Vitorino, R., et al., *Identification of human whole saliva protein components using proteomics*. Proteomics, 2004. **4**(4): p. 1109-1115.
110. Monopoli, M.P., F.B. Bombelli, and K.A. Dawson, *Nanobiotechnology: nanoparticle coronas take shape*. Nature nanotechnology, 2011. **6**(1): p. 11.
111. Docter, D., et al., *Quantitative profiling of the protein coronas that form around nanoparticles*. Nature protocols, 2014. **9**(9): p. 2030.
112. Lynch, I. and K.A. Dawson, *Protein-nanoparticle interactions*. Nano Today, 2008. **3**(1): p. 40-47.
113. Lundqvist, M., et al., *Nanoparticle size and surface properties determine the protein corona with possible implications for biological impacts*. Proceedings of the National Academy of Sciences, 2008. **105**(38): p. 14265-14270.

114. Chittur, K.K., *FTIR/ATR for protein adsorption to biomaterial surfaces*. Biomaterials, 1998. **19**(4): p. 357-369.
115. Assfalg, M., et al., *The study of transient protein–nanoparticle interactions by solution NMR spectroscopy*. Biochimica et Biophysica Acta (BBA)-Proteins and Proteomics, 2016. **1864**(1): p. 102-114.
116. Yallapu, M.M., et al., *Plasma Proteins Interaction with Curcumin Nanoparticles: Implications in Cancer Therapeutics*. Current drug metabolism, 2013. **14**(4): p. 504-515.
117. Chen, F., et al., *Complement proteins bind to nanoparticle protein corona and undergo dynamic exchange in vivo*. Nature nanotechnology, 2017. **12**(4): p. 387-393.
118. Hadjidemetriou, M., et al., *In vivo Biomolecule Corona around Blood-Circulating, Clinically Used and Antibody-Targeted Lipid Bilayer Nanoscale Vesicles*. ACS Nano, 2015. **9**(8): p. 8142-8156.
119. Hadjidemetriou, M., Z. Al-Ahmady, and K. Kostarelos, *Time-evolution of in vivo protein corona onto blood-circulating PEGylated liposomal doxorubicin (DOXIL) nanoparticles*. Nanoscale, 2016. **8**(13): p. 6948-6957.
120. Di Silvio, D., et al., *Technical tip: high-resolution isolation of nanoparticle–protein corona complexes from physiological fluids*. Nanoscale, 2015. **7**(28): p. 11980-11990.
121. Lo Giudice, M.C., et al., *In situ characterization of nanoparticle biomolecular interactions in complex biological media by flow cytometry*. Nature Communications, 2016. **7**: p. 13475.
122. Lara, S., et al., *Identification of Receptor Binding to the Biomolecular Corona of Nanoparticles*. ACS Nano, 2017. **11**(2): p. 1884-1893.
123. Walkey, C.D., et al., *Protein Corona Fingerprinting Predicts the Cellular Interaction of Gold and Silver Nanoparticles*. ACS Nano, 2014. **8**(3): p. 2439-2455.
124. Winzen, S., et al., *Complementary analysis of the hard and soft protein corona: sample preparation critically effects corona composition*. Nanoscale, 2015. **7**(7): p. 2992-3001.
125. Peters, R., et al., *Single particle ICP-MS combined with a data evaluation tool as a routine technique for the analysis of nanoparticles in complex matrices*. Journal of Analytical Atomic Spectrometry, 2015. **30**(6): p. 1274-1285.
126. Michalski, A., et al., *Mass spectrometry-based proteomics using Q Exactive, a high-performance benchtop quadrupole Orbitrap mass spectrometer*. Molecular & Cellular Proteomics, 2011. **10**(9): p. M111. 011015.
127. Kelly, P.M., et al., *Mapping protein binding sites on the biomolecular corona of nanoparticles*. Nature nanotechnology, 2015. **10**(5): p. 472-479.
128. Lindman, S., et al., *Systematic investigation of the thermodynamics of HSA adsorption to N-iso-propylacrylamide/N-tert-butylacrylamide copolymer nanoparticles. Effects of particle size and hydrophobicity*. Nano letters, 2007. **7**(4): p. 914-920.
129. Li, L., et al., *Analytical strategies for detecting nanoparticle–protein interactions*. Analyst, 2010. **135**(7): p. 1519-1530.
130. Capjak, I., et al., *How protein coronas determine the fate of engineered nanoparticles in biological environment*. Archives of Industrial Hygiene and Toxicology, 2017. **68**(4): p. 245-253.
131. Docter, D., et al., *The nanoparticle biomolecule corona: lessons learned—challenge accepted?* Chemical Society Reviews, 2015. **44**(17): p. 6094-6121.
132. Monopoli, M.P., et al., *Physical– chemical aspects of protein corona: relevance to in vitro and in vivo biological impacts of nanoparticles*. Journal of the American Chemical Society, 2011. **133**(8): p. 2525-2534.
133. Tenzer, S., et al., *Nanoparticle Size Is a Critical Physicochemical Determinant of the Human Blood Plasma Corona: A Comprehensive Quantitative Proteomic Analysis*. ACS Nano, 2011. **5**(9): p. 7155-7167.
134. Ghavami, M., et al., *Plasma concentration gradient influences the protein corona decoration on nanoparticles*. Rsc Advances, 2013. **3**(4): p. 1119-1126.

135. Mahmoudi, M., et al., *Temperature: the "ignored" factor at the nanobio interface*. ACS nano, 2013. **7**(8): p. 6555-6562.
136. Rahman, M., et al., *Nanoparticle and protein corona*, in *Protein-nanoparticle interactions*. 2013, Springer. p. 21-44.
137. Zanganeh, S., et al., *Chapter 3 - Protein Corona: The Challenge at the Nanobiointerfaces A2 - Mahmoudi, Morteza*, in *Iron Oxide Nanoparticles for Biomedical Applications*, S. Laurent, Editor. 2018, Elsevier. p. 91-104.
138. Hu, G., et al., *Physicochemical properties of nanoparticles regulate translocation across pulmonary surfactant monolayer and formation of lipoprotein corona*. ACS nano, 2013. **7**(12): p. 10525-10533.
139. Lesniak, A., et al., *Effects of the Presence or Absence of a Protein Corona on Silica Nanoparticle Uptake and Impact on Cells*. ACS Nano, 2012. **6**(7): p. 5845-5857.
140. Gräfe, C., et al., *Intentional formation of a protein corona on nanoparticles: serum concentration affects protein corona mass, surface charge, and nanoparticle–cell interaction*. The international journal of biochemistry & cell biology, 2016. **75**: p. 196-202.
141. Maiorano, G., et al., *Effects of cell culture media on the dynamic formation of protein–nanoparticle complexes and influence on the cellular response*. ACS nano, 2010. **4**(12): p. 7481-7491.
142. Bhogale, A., et al., *Comprehensive studies on the interaction of copper nanoparticles with bovine serum albumin using various spectroscopies*. Colloids and Surfaces B: Biointerfaces, 2014. **113**: p. 276-284.
143. Mahmoudi, M., et al., *Variation of protein corona composition of gold nanoparticles following plasmonic heating*. Nano letters, 2013. **14**(1): p. 6-12.
144. Khan, S.S., A. Mukherjee, and N. Chandrasekaran, *Impact of exopolysaccharides on the stability of silver nanoparticles in water*. Water research, 2011. **45**(16): p. 5184-5190.
145. Erhayem, M. and M. Sohn, *Stability studies for titanium dioxide nanoparticles upon adsorption of Suwannee River humic and fulvic acids and natural organic matter*. Science of the Total Environment, 2014. **468**: p. 249-257.
146. Palchetti, S., et al., *The protein corona of circulating PEGylated liposomes*. Biochimica et Biophysica Acta (BBA) - Biomembranes, 2016. **1858**(2): p. 189-196.
147. Caracciolo, G., et al., *Evolution of the Protein Corona of Lipid Gene Vectors as a Function of Plasma Concentration*. Langmuir, 2011. **27**(24): p. 15048-15053.
148. Hill, H.D., et al., *The role radius of curvature plays in thiolated oligonucleotide loading on gold nanoparticles*. ACS nano, 2009. **3**(2): p. 418-424.
149. Vertegel, A.A., R.W. Siegel, and J.S. Dordick, *Silica nanoparticle size influences the structure and enzymatic activity of adsorbed lysozyme*. Langmuir, 2004. **20**(16): p. 6800-6807.
150. Shang, W., et al., *Cytochrome c on silica nanoparticles: influence of nanoparticle size on protein structure, stability, and activity*. Small, 2009. **5**(4): p. 470-476.
151. Gagner, J.E., et al., *Effect of gold nanoparticle morphology on adsorbed protein structure and function*. Biomaterials, 2011. **32**(29): p. 7241-7252.
152. Roach, P., D. Farrar, and C.C. Perry, *Surface tailoring for controlled protein adsorption: effect of topography at the nanometer scale and chemistry*. Journal of the American Chemical Society, 2006. **128**(12): p. 3939-3945.
153. Schulze, C., et al., *Not ready to use—overcoming pitfalls when dispersing nanoparticles in physiological media*. Nanotoxicology, 2008. **2**(2): p. 51-61.
154. Mahmoudi, M., et al., *Irreversible changes in protein conformation due to interaction with superparamagnetic iron oxide nanoparticles*. Nanoscale, 2011. **3**(3): p. 1127-1138.
155. Lynch, I. and K.A. Dawson, *Protein-nanoparticle interactions*. Nano today, 2008. **3**(1-2): p. 40-47.

156. Roach, P., D. Farrar, and C.C. Perry, *Interpretation of protein adsorption: surface-induced conformational changes*. Journal of the American Chemical Society, 2005. **127**(22): p. 8168-8173.
157. Gessner, A., et al., *Influence of surface charge density on protein adsorption on polymeric nanoparticles: analysis by two-dimensional electrophoresis*. European journal of pharmaceuticals and biopharmaceutics, 2002. **54**(2): p. 165-170.
158. Gessner, A., et al., *Functional groups on polystyrene model nanoparticles: influence on protein adsorption*. Journal of Biomedical Materials Research Part A, 2003. **65**(3): p. 319-326.
159. Deng, Z.J., et al., *Differential plasma protein binding to metal oxide nanoparticles*. Nanotechnology, 2009. **20**(45): p. 455101.
160. de Almeida, P.D.V., et al., *Saliva composition and functions: a comprehensive review*. J contemp dent pract, 2008. **9**(3): p. 72-80.
161. Tiwari, M., *Science behind human saliva*. Journal of Natural Science, Biology, and Medicine, 2011. **2**(1): p. 53-58.
162. Edgar, W., *Saliva: its secretion, composition and functions*. British dental journal, 1992. **172**(8): p. 305-312.
163. Sembulingam, K. and P. Sembulingam, *Essentials of medical physiology*. 2012: JP Medical Ltd.
164. Muddugangadhar, B.C., et al., *A clinical study to compare between resting and stimulated whole salivary flow rate and pH before and after complete denture placement in different age groups*. The Journal of the Indian Prosthodontic Society, 2015. **15**(4): p. 356-366.
165. Humphrey, S.P. and R.T. Williamson, *A review of saliva: normal composition, flow, and function*. The Journal of prosthetic dentistry, 2001. **85**(2): p. 162-169.
166. Schenkels, L.C.P.M., E.C.I. Veerman, and A.V. Nieuw Amerongen, *Biochemical Composition of Human Saliva in Relation To Other Mucosal Fluids*. Critical Reviews in Oral Biology & Medicine, 1995. **6**(2): p. 161-175.
167. Van Nieuw Amerongen, A., J. Bolscher, and E. Veerman, *Salivary proteins: protective and diagnostic value in cariology?* Caries research, 2004. **38**(3): p. 247-253.
168. Lamy, E., et al., *Protein electrophoresis in saliva study*, in *Electrophoresis*. 2012, InTech.
169. Huang, C.-M., *Comparative proteomic analysis of human whole saliva*. Archives of Oral Biology, 2004. **49**(12): p. 951-962.
170. Yan, W., et al., *Systematic comparison of the human saliva and plasma proteomes*. PRCA PROTEOMICS - Clinical Applications, 2009. **3**(1): p. 116-134.
171. Schulz, B.L., J. Cooper-White, and C.K. Punyadeera, *Saliva proteome research: current status and future outlook*. BBTN Critical Reviews in Biotechnology, 2013. **33**(3): p. 246-259.
172. Esser, D., et al., *Sample Stability and Protein Composition of Saliva: Implications for Its Use as a Diagnostic Fluid*. Biomarker insights, 2008. **3**: p. 25-27.
173. Amado, F.M., et al., *Proteomics of Human Saliva*, in *Proteomics of Human Body Fluids*. 2007, Springer. p. 347-376.
174. Thongboonkerd, V., *Proteomics of human body fluids: principles, methods, and applications*. 2008: Springer Science & Business Media.
175. Siqueira, W.L. and C. Dawes, *The salivary proteome: challenges and perspectives*. PROTEOMICS-Clinical Applications, 2011. **5**(11-12): p. 575-579.
176. Helmerhorst, E. and F. Oppenheim, *Saliva: a dynamic proteome*. Journal of dental research, 2007. **86**(8): p. 680-693.
177. Loo, J., et al., *Comparative human salivary and plasma proteomes*. Journal of dental research, 2010. **89**(10): p. 1016-1023.
178. Huq, N.L., et al., *A Review of the Salivary Proteome and Peptidome and Saliva-derived Peptide Therapeutics*. International Journal of Peptide Research and Therapeutics, 2007. **13**(4): p. 547-564.

179. Schulz, B.L., J. Cooper-White, and C.K. Punyadeera, *Saliva proteome research: current status and future outlook*. Critical reviews in biotechnology, 2013. **33**(3): p. 246-259.
180. Yao, Y., et al., *Identification of protein components in human acquired enamel pellicle and whole saliva using novel proteomics approaches*. Journal of Biological Chemistry, 2003. **278**(7): p. 5300-5308.
181. Björhall, K., T. Miliotis, and P. Davidsson, *Comparison of different depletion strategies for improved resolution in proteomic analysis of human serum samples*. Proteomics, 2005. **5**(1): p. 307-317.
182. Messina, I., et al., *Facts and artifacts in proteomics of body fluids. What proteomics of saliva is telling us?* Journal of separation science, 2008. **31**(11): p. 1948-1963.
183. Scarano, E., et al., *Proteomics of saliva: personal experience*. Acta Otorhinolaryngologica Italica, 2010. **30**(3): p. 125.
184. Bandhakavi, S., et al., *Hexapeptide libraries for enhanced protein PTM identification and relative abundance profiling in whole human saliva*. Journal of proteome research, 2011. **10**(3): p. 1052-1061.
185. Ghafouri, B., C. Tagesson, and M. Lindahl, *Mapping of proteins in human saliva using two-dimensional gel electrophoresis and peptide mass fingerprinting*. Proteomics, 2003. **3**(6): p. 1003-1015.
186. Bandhakavi, S., et al., *A dynamic range compression and three-dimensional peptide fractionation analysis platform expands proteome coverage and the diagnostic potential of whole saliva*. Journal of proteome research, 2009. **8**(12): p. 5590-5600.
187. McClements, D.J., et al., *The role of the food matrix and gastrointestinal tract in the assessment of biological properties of ingested engineered nanomaterials (iENMs): State of the science and knowledge gaps*. NanoImpact, 2016. **3**: p. 47-57.
188. Böhmert, L., et al., *Analytically monitored digestion of silver nanoparticles and their toxicity on human intestinal cells*. Nanotoxicology, 2014. **8**(6): p. 631-642.
189. Yada, R.Y., et al., *Engineered nanoscale food ingredients: evaluation of current knowledge on material characteristics relevant to uptake from the gastrointestinal tract*. Comprehensive Reviews in Food Science and Food Safety, 2014. **13**(4): p. 730-744.
190. Braakhuis, H.M., et al., *Progress and future of in vitro models to study translocation of nanoparticles*. Archives of toxicology, 2015. **89**(9): p. 1469-1495.
191. Lefebvre, D.E., et al., *Utility of models of the gastrointestinal tract for assessment of the digestion and absorption of engineered nanomaterials released from food matrices*. Nanotoxicology, 2015. **9**(4): p. 523-542.
192. Peters, R., et al., *Presence of Nano-Sized Silica during In vitro Digestion of Foods Containing Silica as a Food Additive*. ACS Nano, 2012. **6**(3): p. 2441-2451.
193. Walczak, A.P., et al., *Behaviour of silver nanoparticles and silver ions in an in vitro human gastrointestinal digestion model*. Nanotoxicology, 2012. **7**(7): p. 1198-1210.
194. Torres-Escribano, S., et al., *Comparison of a static and a dynamic in vitro model to estimate the bioaccessibility of As, Cd, Pb and Hg from food reference materials Fucus sp. (IAEA-140/TM) and Lobster hepatopancreas (TORT-2)*. Science of The Total Environment, 2011. **409**(3): p. 604-611.
195. Bellmann, S., et al., *Mammalian gastrointestinal tract parameters modulating the integrity, surface properties, and absorption of food-relevant nanomaterials*. Wiley Interdisciplinary Reviews: Nanomedicine and Nanobiotechnology, 2015. **7**(5): p. 609-622.
196. Laloux, L., M. Polet, and Y.-J. Schneider, *Interaction between Ingested-Engineered Nanomaterials and the Gastrointestinal Tract: In vitro Toxicology Aspects*. Nanotechnology in Agriculture and Food Science, 2017.
197. Lichtenstein, D., et al., *Impact of food components during in vitro digestion of silver nanoparticles on cellular uptake and cytotoxicity in intestinal cells*. Biological chemistry, 2015. **396**(11): p. 1255-1264.

198. Fröhlich, E. and E. Roblegg, *Models for oral uptake of nanoparticles in consumer products*. Toxicology, 2012. **291**(1): p. 10-17.
199. Zhou, D., et al., *Influence of material properties on TiO₂ nanoparticle agglomeration*. PLoS One, 2013. **8**(11): p. e81239.

CHAPTER 2

The type of dietary NPs influences salivary protein corona composition

In chapter 2 we investigated the interaction of human saliva with the dietary particles at proteomic level, in order to understand the influence of size and surface chemistry of the NPs on the Salivary protein corona composition. Our project was approved by the McGill University Research Ethics Board (REB File #:10-0618). All the work presented here with respect to proteomic profiling using LC-MS/MS was conducted in proteomic platform at MUHC. To our knowledge, this is the first study to capture the interaction of salivary proteome with dietary particles through a qualitative and quantitative approach.

This chapter is co-authored by Wut Hmone Phue, Ke Xu and Dr. Saji George. It is planned for submission in Journal of NanoImpact.

Chapter2 THE TYPE OF DIETARY NPs INFLUENCES SALIVARY PROTEIN CORONA COMPOSITION

2.1 Abstract:

While NPs (NPs) are copiously incorporated into different food products, the protein corona profile of saliva interacted dietary NPs and its potential influence on the function of proteins involved have received little attention in the past. In this study the most widely used NPs such as food grade silicon dioxide (SiO₂), titanium dioxide (TiO₂) and emerging NP with application in food industry- silver (Ag) were interacted with human saliva. These particles were characterized for their physicochemical properties in their pristine state and after interacting with saliva. Analysis of the protein corona composition of saliva interacted dietary particles were carried by employing 1D gel electrophoresis and LC-MS/MS. We observed a net decrease in the negative surface charge and change in agglomeration size in saliva interacted NPs. Significant differences in corona composition, and protein abundance were noted among the tested particles. Several proteins with vital functions in digestion and host protections were found to be enriched on the surface of particles. For instance, Lysozyme, Lactoferrin, Apolipoprotein B100 & E, and Annexin A2 were the most enriched proteins on NPs of SiO₂. In order to verify if the binding of proteins have any effect on their function, we tested the amylase and lysozyme activities of saliva in the presence and absence of NPs of SiO₂ and TiO₂. Our results showed that these particles could compromise the enzymes function wherein NPs of SiO₂ showed the highest effect. Overall, our study, identified salivary proteins involved in the protein corona of dietary particles and showed that vital functions of saliva such as digestion and antimicrobial properties could be partially affected by NP-Protein interactions in saliva.

2.2 Résumé :

Alors que les nanoparticules (NPs) sont copieusement incorporées dans différents produits alimentaires, le profil de la couronne de protéines salivaire interagit avec les NPs originaires de la diète. L'influence potentielle des NPs par rapport à la fonction des protéines impliquées n'ont reçu que peu d'attention dans le passé. Dans cette étude, les NPs les plus couramment retrouvées dans l'alimentation telles que le silicone alimentaire (SiO_2) et le dioxyde de titane (TiO_2) ainsi qu'une NP émergente qui possède des applications dans le domaine alimentaire soit l'argent alimentaire (Ag) ont tous été mises en contact avec de la salive humaine. Ces particules étaient caractérisées pour leur propriété physicochimique sous leur forme intacte et après avoir interagit avec la salive humaine. L'analyse de la composition de la couronne de protéines des molécules de salive ayant interagit avec les particules d'origine alimentaire ont été réalisés par électrophorèse 1D avec gel et par LC-MS/MS. On a observé une décroissance nette de la charge négative de surface ainsi qu'un changement de taille des agglomérations dans la salive ayant interagit avec les NPs. Des différences significatives dans la composition de la couronne de protéines et dans l'abondance de protéines ont été notées parmi les particules à l'étude. Plusieurs protéines avec des fonctions vitales de digestion et de protection de l'hôte ont été retrouvées enrichies à la surface des particules. Par exemple, Lysozyme, Lactoferrine, Apolipoprotéine B100 & E et Annexine A2 étaient les protéines les plus enrichies sur les NPs de SiO_2 . Afin de vérifier si la liaison de protéines avaient un effet quelconque sur leur fonction, on a testé l'activité de l'amylase et la lysozyme de la salive dans la présence et l'absence de NPs de SiO_2 et de TiO_2 . Nos résultats ont montré que ces particules pouvaient compromettre la fonction des enzymes, l'effet le plus important étant celui avec les NPs de SiO_2 . Globalement, notre étude identifie les protéines salivaires impliqués dans la couronne des protéines des particules originaires de la diète et démontre que certaines fonctions vitales de la salive telles que la digestion et les propriétés antimicrobiennes peuvent être affectées par l'interaction protéine-nanoparticule dans la salive.

Mots clés : Nanoparticules, diète, protéines salivaires, couronne de protéines, amylase salivaire, spectrométrie de masse.

2.3 Key words:

NPs, dietary, Salivary proteins, Protein corona, Mass spectrometry, salivary amylase.

2.4 Introduction:

Nanoparticles (NPs) are widely applied in the cosmetic, food and nutraceutical industry for improving stability, quality, bioavailability of active ingredients and overall function of the final product [1-3]. The ever increasing use of NPs in food and consumer products lead to human exposure through oral route [4]. Upon entry in to human body and encounter with biological fluids, the surface of the NPs will be decorated with wide range of biomolecules- generally referred to as “corona”. Surface corona plays an importance role in the biological identity of NPs that influence their fate and transport in the body [5, 6]. The concept of protein corona was extensively studied for plasma proteins interacted NPs because of its relevance to therapeutic interventions through injected NPs mediated delivery systems [7-9]. While, daily human exposure to NPs through oral route is estimated to be 10^{12} - 10^{14} [10], studies addressing the interaction of NPs with proteins of relevance to gastro-intestinal system are scarce [4]. Knowledge on the protein corona of ingested NPs is essential to understand the fate of NPs in the body and its effect on protein function.

Human saliva is a complex mixture of proteins and minerals and has several physiological roles which helps in maintaining homeostasis in the oral cavity. Saliva is constituted by secretions from multiple salivary glands and is composed of water, electrolytes, mucus, white blood cells, epithelial cells, glycoproteins, nitrogenous products, enzymes (such as amylase and lipase), antimicrobial agents such as secretory IgA and lysozyme proteins[11].Major functions of the

human saliva are host defense, nutrient digestion and protective functions which includes tissue coating, lubrication, humidification, immunological activity, anti-(Bacterial, viral, Fungal) activity, digestive enzymes, bolus formation and taste perception[11, 12]. The potential of NPs to interfere with vital functions of saliva is expected given the proven inhibitory action of NPs such as TiO_2 and SiO_2 on trypsin [13] and lysozyme [14], respectively.

In this study we investigated food grade silica (SiO_2) particles (nano and micron size), titanium dioxide (TiO_2) and citrate coated Silver (Ag) NPs to understand (1) the qualitative and quantitative differences in the protein corona of saliva interacted particles and (2) to verify if the interaction of particles with salivary enzymes (lysozyme and amylase) compromise their function. We report the difference in type and relative abundance of proteins associated with hard corona of saliva interacted particles (SiO_2 MP, SiO_2 NP, TiO_2 NP, Ag) and that dietary particles could compromise the vital functions of saliva such as digestion of starch and antimicrobial activity. To our knowledge, this is the first study reporting the interaction of dietary NPs with human saliva, which point towards potential health implications of exposure to dietary NPs.

2.5 Materials and Methods:

2.5.1 Materials:

Bovine serum albumin (BSA), 3,5-Dinitrosalicylic acid, maltose monohydrate, soluble potato starch, Lysozyme from chicken egg white (L6876), iodoacetic acid, DDT (dichlorodiphenyltrichloroethane) and *Micrococcus lysodeikticus* ATTC no.4698 were purchased from Sigma Aldrich (St. Louis, Missouri, United States). The pierce 660 nm protein assay kit was supplied by Thermo-Fisher Scientific (Scotia court, Ontario, Canada). Sodium dodecyl sulphate -polyacrylamide gel electrophoresis (SDS-PAGE) chemicals and protein

standards were purchased from Bio-Rad laboratories (Mississauga, Ontario, Canada) and Trypsin was obtained from Promega MS grade). Solvents used for LC-MS/MS orbitrap were MS grade. For all the experiment the stock solution and buffer (PBS buffer -0.01 M, pH 7.4) were prepared according to the standard laboratory procedures using Milli-Q reagent grade water (MilliQ, Millipore, Canada).

2.5.2 NPs Used in the Study:

The food grade silicon dioxide particles (SiO_2) in nano size (AEROSIL 200F) and micron size (SIPERNAT 22) were obtained from Evonik Corporation (NJ, United States). Titanium dioxide NP -Anatase (TiO_2) were purchased from Sigma Aldrich (Canada).

The Citrate coated Ag NPs (Citrate-AgNPs) were synthesized according to the protocol reported earlier [15]. Briefly, 1 mM aqueous solution of silver nitrate with the capping agent (10 mM trisodium citrate solution) in the ratio of 2:1 were mixed together. The mixture was vortexed for 2 min and wrapped with aluminium foil and incubated in water bath for 3 hrs at 70°C until the color of the mix changed to greenish yellow. The resulting mixture was centrifuged for 30 min at 14,000 rpm and the pellets were washed twice by re-suspending in deionized water and centrifugation. Washed NP pellet was re-suspended in deionized water for further use. Pellet obtained from 5 mL of the solution containing washed NPs were freeze dried and weighed for obtaining the concentration of NPs (weight/mL).

2.5.3 Physical Characterization:

The average size, polydispersity index (PDI) and surface charge of particles were characterized by Scanning Electron Microscopy (SEM), Dynamic Light Scattering (DLS) and zeta potential measurement, respectively. The hydrodynamic diameter and the zeta potential of NPs dispersed in buffer (PBS) and saliva (Incubated for 1 hr at 37 °c) were determined using a

Nanobrook omni instrument (Brookhaven's, New York), at 25°C at a concentration of 50 µg/ml [8, 16-18]. Samples prepared for the DLS were loaded in to a pre-rinsed folded capillary cell for the zeta potential measurement with an applied voltage of 100 V. For SEM analysis (Hitachi, SEM-SU8230, japan) samples (5µl of 50 ppm NP dispersion) were dropped on the SEM stub, dried at room temperature for overnight and were examined at 50 KV accelerating voltage without coating [19].

2.5.4 Human Saliva Collection and Processing:

Saliva samples (unstimulated whole saliva) were obtained from healthy volunteers in accordance with a standard protocol [20] after obtaining institutional REB. To prevent the proteolytic degradation of the salivary proteins, collection tubes were placed on ice during collection. The saliva collected from each individual was vortexed for 20 Sec and centrifuged at 8000 rpm for 10 min to remove the debris. The clear supernatant from each tube were pooled (to minimize inter-individual variation of the saliva composition). The pooled saliva was transferred to eppendorf tubes and centrifuged at 12,000 g for 10 min and the supernatant was collected. Upon completion of processing, all processed saliva samples were stored at -18°C for further analysis. The protein concentration of the saliva was quantified with the Bradford assay (Bradford dye reagent, Alfa Aesar, United States).

2.5.5 Preparation of Saliva Interacted Dietary Particles:

Fifty µL of NPs stock in buffer (10 mg/mL) were transferred in to the 450 µl of saliva (total volume of 500 µl at a concentration of 2 mg/mL) and incubated at 37°C for 1 hr under constant shaking at 100 rpm. Saliva samples without NPs were prepared in identical way with equal volume of being buffer added instead of NPs suspension. After incubation, the particles were separated from the supernatant by centrifugation at 12,000 rpm for 30 min. The pellet was

resuspended in 500 μ l of PBS buffer and centrifuged again to pellet the bound protein-particle complexes. Subsequently, the particle pellet was resuspended in PBS buffer and washed by three centrifugation steps at 12,000 rpm for 15 min and were suspended in 50 μ l of SDS sample buffer (2% SDS, 5% β -mercaptoethanol, 10% glycerol and 62.5 mM Tris-HCl)[21].

Due to the agglomeration in aqueous medium, the calculation of total surface area for the NPs was not practical for dosimetry. Therefore, the weight/volume was used for the dosimetry of particles [18].

2.5.6 Desorption of Salivary Proteins from Dietary Particles:

For 1D-GE, the proteins bound to particles were eluted by boiling the particle-proteins complex with SDS sample buffer. For this, the particle-protein pellet was mixed with 50 μ l of SDS sample buffer and was boiled for 5 min at 95 °C. The supernatant with desorbed proteins from the particle were separated by centrifuging at 12,000g for 10 min. The collected sample was used for bound protein quantification and 1D-GE. Whereas, for the proteomic analysis using LC-MS/MS, the proteins were eluted from the particles by boiling the pellet particle complex with Laemmli buffer.

2.5.7 Protein Quantification:

The amounts of proteins bound to particles were quantified after desorption of proteins from NPs using 2% SDS by pierce assay. Briefly, 20 μ l of the sample were mixed with 200 μ l of pierce 660nm assay reagent, incubated at room temperature for 10 min with gentle shaking and the absorbance was read at 660 nm using spectra max i3x plate reader (soft max pro 7.0.3, Molecular Devices, USA) [9]. BSA (Sigma Albumin, Bovine) was used as a standard and blank readings were made with particles that were not interacted with saliva.

2.5.8 One Dimensional (1D) SDS PAGE:

The particles collected after the interaction with saliva were mixed with 50 μ l of SDS sample buffer. We used gradient SDS-PAGE for visualizing the protein bands. For this, 20 μ L of particle suspension was loaded on to a polyacrylamide gel with 4% acrylamide concentration for stacking gel and a resolving gel with gradient of acrylamide concentration of 8-12%. The gels were run using gel electrophoresis unit (Bio-Rad, model 3000xi) at a constant voltage of 50 V for 4 hrs. The resulting gel was stained with Coomassie brilliant blue stain followed by silver staining (Bio-Rad) with gentle agitation. A combined Coomassie blue-silver stain method was followed to increase the sensitivity of the detectable salivary proteins. All experiments were conducted in triplicates to ensure the reproducibility of the general pattern and band intensities on the 1D gels.

2.5.9 Protein Identification by Mass Spectrometry:

We performed LC-MS/MS mass spectrometry analysis using 3000HPLC- orbitrap fusion MS (Thermo Scientific, Canada). Briefly, the pelleted particle-protein complexes obtained from the last centrifugation step in corona preparation were resuspended and incubated in Laemmli buffer and the protein solution (40 μ L) was loaded onto a single stacking gel band. Subsequently, the stacked proteins were reduced with 10 mM DTT, alkylated with iodoacetic acid and then digested with trypsin in accordance with the standard protocol for in-gel digestion [22]. The resulting peptides were re-solubilized in 0.1% aqueous formic acid and 2% acetonitrile and were loaded onto a Thermo Acclaim Pepmap (Thermo, 75 μ M ID X 2cm C18 3 μ M beads) precolumn and then onto an Acclaim Pepmap Easy spray (Thermo, 75 μ M X 15cm with 2 μ M C18 beads) analytical column separation using a Dionex Ultimate 3000 uHPLC at 220 nL/min with a gradient of 2-35% organic acid (0.1% formic acid in acetonitrile) over 2 hrs. Peptides were analyzed using a Thermo Orbitrap Fusion mass spectrometer operating at 120,000 resolution (FWHM in MS1, 15,000 FWHM for MS/MS) with HCD sequencing of all

peptides with a fold change of 2 or above. The raw data were converted into *.mgf format (Mascot generic format), searched using Mascot 2.3 against human sequences (Swissport 2018). The database search results were loaded onto Scaffold Q+ Scaffold_4.7.2 (Proteome Sciences) for spectral counting, statistical treatment and data visualization. To reduce the impact of possible false positive identifications, only 501 proteins (359 from saliva and 142 from incubated particles with saliva) with 2 or more peptides quantified were considered.

2.5.10 Bioinformatic Data Analysis:

The proteomic data from ScaffoldTM was used in bioinformatic tools such as Expasy, Pantherdb, Bioinformatics.psb, perseus for the analysis of isoelectric point, gene ontology classification, Venn diagram and cluster analysis respectively. The theoretical isoelectric point for the selected list of proteins was calculated using tools available from Expasy.org (https://web.expasy.org/compute_pi/). To describe the gene function, the GO (gene ontology) data which includes molecular function, biological function, protein class and pathway were analysed using Scaffold and Panther tools (<http://www.pantherdb.org/>).

To identify the overlap and the unique protein gene list, we used bioinformatic webtool from Ugent (<http://bioinformatics.psb.ugent.be/webtools/Venn/>). The cluster analysis and statistical analysis for the genes corresponding to the identified proteins were analysed using Perseus software (<http://www.biochem.mpg.de/5111810/perseus>). Fold change value was calculated in ScaffoldTM by comparing it with control sample (Human Saliva) and the Z score for all the genes with fold change ≥ 2 were calculated in Perseus software for cluster analysis.

2.5.11 α -amylase Enzyme Activity by DNS Assay:

The α -amylase activity was measured in the presence of SiO_2 and TiO_2 particles at a concentration of 2 mg/mL of particles in whole saliva. Saliva without particle were considered as control. Briefly, the effect of particle on α -amylase activity was studied by incubating the saliva (180 μL) and particle (20 μL) at a concentration of 2 mg/mL for 1 hr. The substrate was mixed with 1% NaCl in the ratio of (4:1) and incubated at 37°C for 5-10 min to equilibrate the reaction mixture. Subsequently, 0.2 mL of the substrate (1% soluble potato starch) was added in to the saliva -particle mixture and incubated for 5 min followed by addition of 0.2 ml of DNS reagent (dye) and place it in a heating block for 15 min. After boiling, the eppendorf tubes were cooled in ice bath and were added with 0.9ml of deionized water. The tubes are centrifuged at 12,000 rpm for 10 min to pull down the particles and 200 μl of each of the sample was pipetted in the microplate and the absorbance was read at 540 nm. The released sugar in the test sample and control was calculated and compared. All experiments were performed at least three times with triplicate samples.

2.5.12 Turbidimetric Assay for Lysozyme Activity:

Turbidimetric assay based on the lysis of gram-positive *Micrococcus lysodeikiticus* bacterial cells was used for the measurement of the salivary lysozyme activity [23]. The substrate (freeze dried bacterial cells) was prepared at a concentration of 0.30 mg/mL using phosphate buffer. The test sample containing 30 μL of saliva and 30 μL of dietary particles (2.0 mg/mL) were pre-incubated for 1hr in 96 well plate. The wells were then added with 170 μL of substrate solution (bacterial cell suspension). The mixture was incubated for additional 5 min before the absorbance was read at 450 nm using a plate reader. Thirty μL of saliva sample added with 30 μl PBS buffer served as the control. All experiments were repeated 3 times with triplicate sample in each test.

2.6 Results:

2.6.1 Dietary Particles Characterization:

The dietary particles used in this experiment were characterized prior to their interaction with human saliva to assess their size, shape, hydrodynamic diameter and surface charge (ζ potential). Particle characterization were performed in MQ water, PBS buffer and whole saliva by using scanning electron microscopy (SEM), dynamic light scattering (DLS) and zeta potential measurements as shown in Table 1 and Figure 2.1. According to the suppliers, the primary particles sizes of SiO₂ NP, SiO₂ MP and TiO₂ NPs were 12 nm, 110 μ m and \sim 44 μ m, respectively. However, SEM analysis showed that size of primary particles constituting the aggregates are 25nm, 70nm, 150nm and 50 nm for SiO₂ NP, SiO₂ MP, TiO₂ NP and Ag NP respectively, which are largely in agreement with the data supplied by the supplier except for SiO₂ MPs (Figure 2.1).

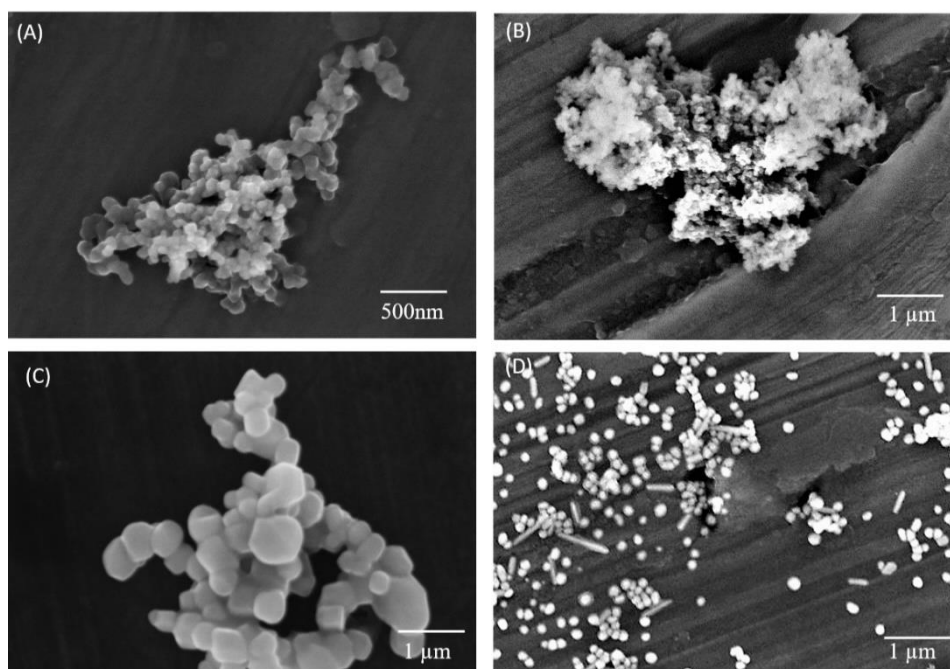


Figure 2.1 SEM image of dietary particles obtained after drying the NP dispersion (50ppm) on the SEM stub. (A) SiO₂ NP; (b) SiO₂ MP; (C) TiO₂ NP; (D) Ag NP.

All particles agglomerated to certain extent in saliva, except for SiO₂ NPs which was comparable to the size of particles dispersed in water. A significant increase in particle size was observed for titanium dioxide and Ag NPs due to the agglomeration in PBS buffer and saliva (>100nm).

The polydispersity index (PDI) value found to be higher in PBS and lower in saliva for all the particles except SiO₂ MPs. None of the particles had a PDI value less than 0.05 suggesting that these particles were not monodispersed. All these particles exhibited negative zeta potential in PBS and saliva. The zeta potential value for all the particles in saliva showed a decrease in the net negative zeta potential (Table 2.1). TiO₂ NPs showed significant decrease from the initial negative charge -43.14 mV to -13.1 mV.

Table 2.1 Summary of physical characterization of the dietary particles used in the experiment.

Dietary particles	Suspended in water			Suspended in PBS buffer			Suspended in whole Saliva		
	Effective diameter by number (nm)	PDI	Zeta Potential (mV)	Effective diameter by number (nm)	PDI	Zeta Potential (mV)	Effective diameter by number (nm)	PDI	Zeta Potential (mV)
SiO ₂ NP	50.53±15.10	0.32±0.082	-25.95±0.788	55.62±16.94	0.37±0.20	-26.47±5.62	27.43±4.56	0.28±0.01	-20.05±1.61
SiO ₂ MP	41.78±4.05	0.34±0.11	-20.13±2.63	41.96±24.10	0.25±0.03	-28.54±2.76	235.59±100.41	0.54±0.34	-17.77±0.96
TiO ₂ NP	422.86±13.41	0.13±0.014	-32.61±0.92	321.70±173.49	0.72±0.02	-43.14±2.90	291.76±384.43	0.20±0.07	-13.67±0.79
Ag NP	57.06±7.57	0.50±0.08	-20.40±5.01	54.44±9.92	0.42±0.14	-10.61±2.92	26.97±5.13	0.362±0.02	-14.33±3.81

Summary of physical characterization of the dietary particles used in the experiment. Effective diameter by number in (nm); Poly dispersity index-PDI; and Zeta potential (ZP) in mV of all the four dietary particles measured when dispersed in buffer and human whole saliva incubated

for 1 hr at 37°C. Measurements were made in PBS or human saliva with a concentration of 20µg/mL. Values are mean ± SD from three independent experiment

2.6.2 Protein Quantification and Analysis by 1D Gel Electrophoresis:

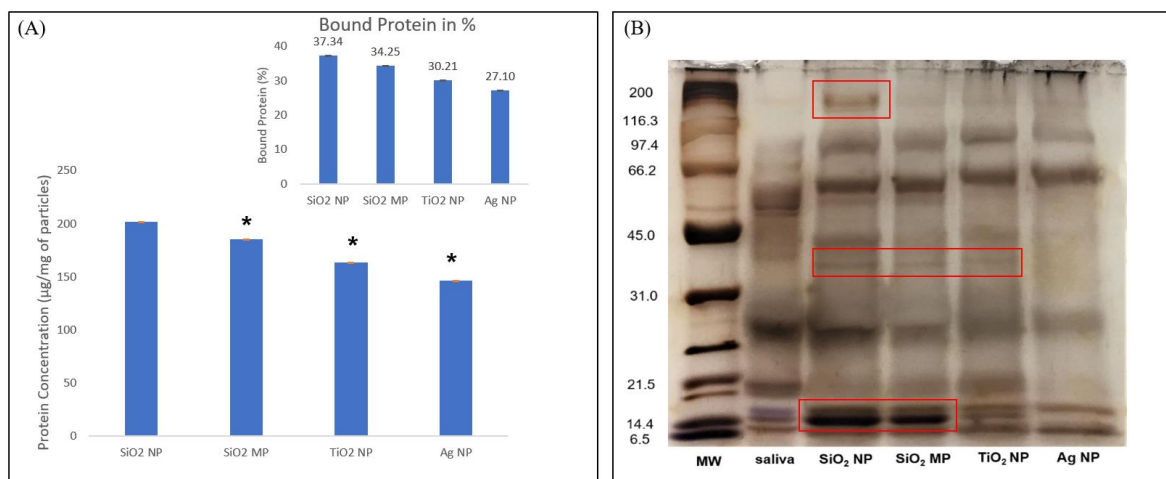


Figure 2.2A shows the amount of proteins bound onto the surface of particles. The total amount of adsorbed protein was significantly higher in SiO₂ NPs in comparison to TiO₂ and Ag NPs, and SiO₂ MPs. The data suggested 20-40% depletion of total proteins from saliva when particles are interacted at a concentration likely to be encountered during consumption of food commodities contain manufactured NPs.

Figure 2.2 Analysis of hard protein corona after incubation with human saliva.(A)Quantitative analysis of bound protein concentration in µg/mg of Particles: It is quantified after the desorption of proteins from particles using 2% SDS by pierce 660nm Assay; (B) changes in the bound protein pattern of whole saliva interacted with 4 different dietary particles: Particle bound proteins were separated by molecular mass via 1D -SDS-PAGE and visualized by combination of Coomassie and silver staining. The Molecular Weight (KDa) of reference proteins are shown in the lane MW.

Figure 2.2B shows 1D-PAGE of salivary proteins retrieved from the pellet of dietary particles incubated in human saliva for 1 hour (lane 3-6) and proteins from human whole saliva (lane 2). The difference in band intensities suggested differences in the relative abundance of proteins in tested particles. As such NPs of SiO₂ showed the highest number of protein bands and the bands were darker in comparison to protein bands obtained from other particles. The enrichment of proteins on the surface of particles were observed as new bands (red box in figure 2.2(B)) which were absent in the control lane 2 (human saliva).

2.6.3 Proteomic Profiling of Salivary Coronal Proteins by Mass Spectrometry

Analysis:

The profile of protein coronas on the surface of the dietary particles after 1 hr of incubation in human saliva were investigated using LC-MS/MS. A total of 737 unique salivary proteins were identified, in which 498 were identical to the whole saliva and the remaining 239 proteins were unique to saliva interacted particles suggesting possible enrichment of specific proteins on the surface of particles. The detailed list of the identified salivary coronal proteins is provided in the supplementary data as Excel file.

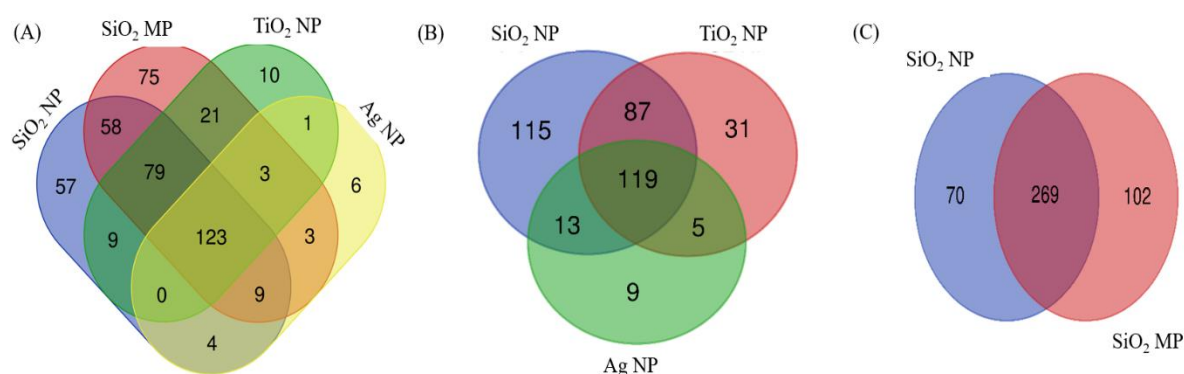


Figure 2.3 Venn diagram shows the number of identified salivary coronal proteins associated with four different dietary particles after 1 hr incubation. (A) 4 dietary particles (B) only dietary

NPs and (C) silica particles at micro and nano range. The figure clearly depicts change in the protein corona composition with respect to particle chemistry, size and shows the preferential enrichment of low abundant proteins that were not detectable in the human saliva by proteomic analysis.

The difference in the composition of the salivary protein corona around the dietary particles are evident from the Venn diagram shown in figure 2.3A , total of 351,379,255, and 157 salivary proteins were identified in the coronas on SiO₂ NPs, SiO₂ MPs, TiO₂ NPs and Ag NPs, respectively (Figure 2.3A). It was found that 119 protein were common to all the particles surface irrespective of the size and chemistry. Number of distinct proteins present in the coronas of SiO₂ NPs, TiO₂ NPs and Ag NPs were 115, 31 and 9, respectively (Figure 2.3B).

The relative abundance of the proteins is illustrated in figure 2.4A as a heap map. Hierarchical cluster analysis showed a significant difference in the abundance of proteins present on different particles. Based on GO analysis the total protein gene expression could be clustered in to 5 categories. Cluster 1 has 14 genes, most of which are highly abundant in SiO₂ NPs followed by Ag NPs while, almost none with TiO₂ NPs. Cluster 2 represent protein genes that are significantly abundant on Ag NPs but with minimal presence on TiO₂ and SiO₂ NPs. Cluster 3 represents genes of protein that are mainly abundant on TiO₂ NPs. Similarly, cluster 4 grouped genes of proteins that are mainly abundant on SiO₂ MPs and some of the protein genes from this cluster were also found on SiO₂ and TiO₂ NPs. The last class of the cluster grouped the genes of protein that are highly abundant on the surface of SiO₂ NPs. Figure 2.4B represents the fold enrichment of the salivary proteins on the particles surface. We observed a significant enrichment of salivary proteins on particle surface which were close to or below the detection limit in the whole saliva. Overall, 168, 131, 80 and 72 protein genes found to be significantly enriched on the dietary particles of SiO₂ NP, SiO₂ MP, TiO₂ NP and Ag NP respectively with

fold enrichment of ≥ 2 . The heatmap displaying fold enrichment was clustered in to 5 groups. Each cluster represents a unique pattern of protein enrichment in respective particle. Cluster 4 was found to be the major cluster with 118 protein which are constituted by either less abundant high affinity or high abundant high affinity proteins of saliva. For instance, lysozyme and lactoferrin were high abundant proteins that showed higher affinity for SiO₂ NPs and SiO₂ MPs with 3.6 & 3.2-fold enrichment from the human saliva. On the other hand, Annexin is a low abundant protein in saliva which was found to be enriched ~ 5.5-fold by all the tested particles.

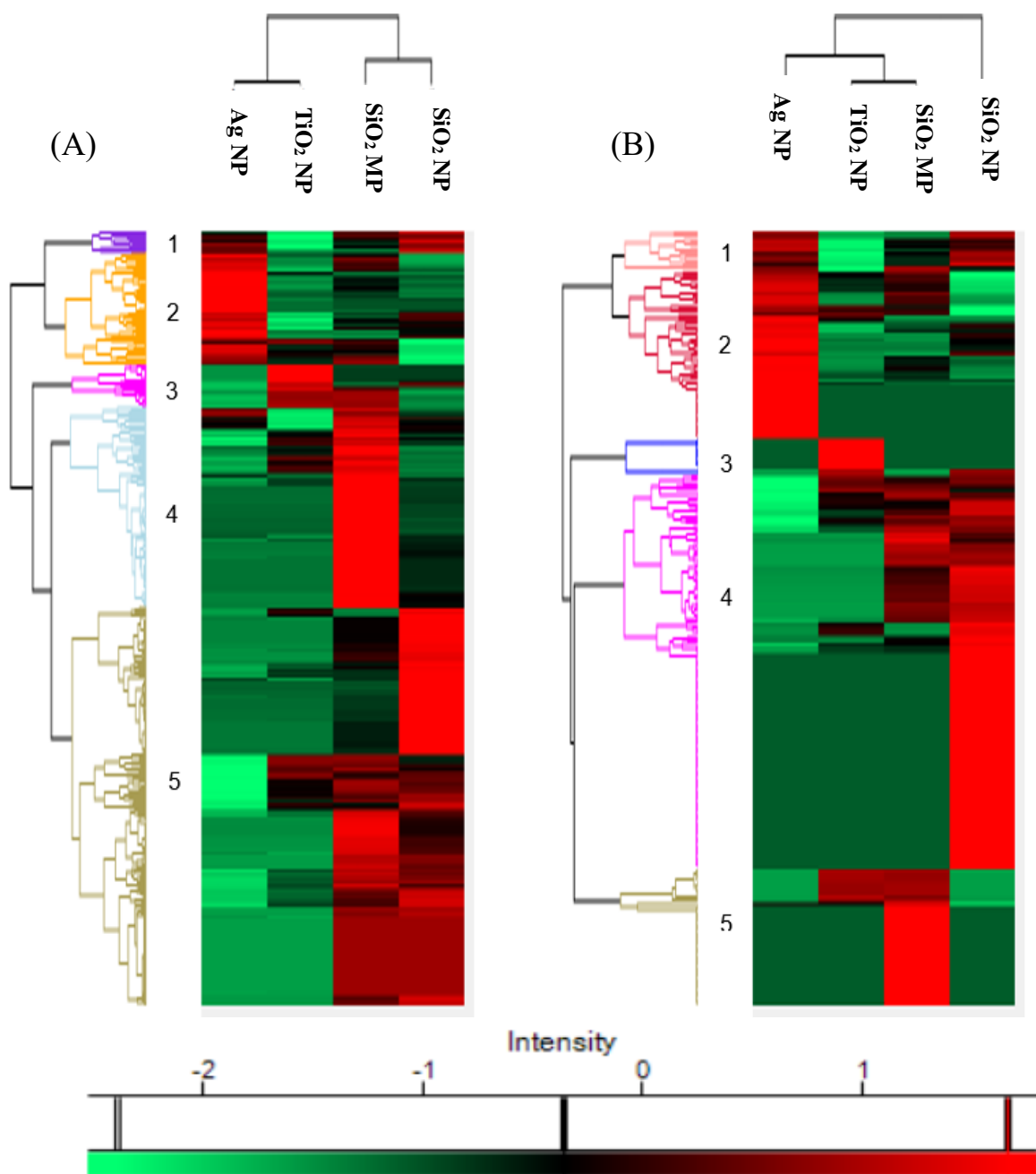


Figure 2.4 Hierarchical clustering of the salivary proteins formed around each dietary particle. (A) Heat map showing relative abundance of 506 differentially expressed genes corresponding to proteins identified on each dietary particle compared with human saliva. Color scheme is based on the z score values of fold change of individual proteins compared with whole saliva. (B): Heat map showing enrichment of proteins on each dietary particle compared with human saliva.

Apolipoproteins B-100, Annexin A2 and Annexin A11 were found to be enriched by all the particles. Notably, Ag NPs showed higher value of fold enrichment for Annexin proteins. On the other hand, SiO₂ NPs showed unique pattern of fold enrichment by adsorbing almost 11 unique proteins from the list of 20 most enriched proteins (Supplementary data: Table S1). Notably, only 8 proteins from the list of 20 most abundant proteins were shared by both SiO₂ NPs and SiO₂ MPs, suggesting the potential role of particle size in determining the types of proteins binding onto particles.

2.6.4 Comparative Analysis of the Protein Corona on Dietary Particles:

The top twenty most abundant salivary proteins from the protein corona formed on the 4 different dietary particles is listed in Table 2. Generally, the most abundant protein from different particles was almost same but with different relative ranking for their abundance.

Table 2.2: 20 most abundant salivary -coronal proteins identified in the protein corona of each dietary particle's following 1 hr of incubation with human saliva

S.No	Saliva	SiO ₂ NP	SiO ₂ MP	TiO ₂ NP	Ag NP
1	<i>Alpha-amylase 1</i>	Lysozyme C	<i>Lactotransferrin</i>	<i>Zymogen granule protein 16 homolog B</i>	<i>Zymogen granule protein 16 homolog B</i>
2	Polymeric immunoglobulin receptor	<i>Lactotransferrin</i>	<i>Alpha-amylase 1</i>	<i>Lactotransferrin</i>	<i>BPI fold-containing family A member 2</i>
3	<i>Prolactin-inducible protein</i>	<i>Myeloperoxidase</i>	<i>Zymogen granule protein 16 homolog B</i>	<i>Prolactin-inducible protein</i>	<i>Immunoglobulin heavy constant mu</i>
4	Serum albumin	<i>Polymeric immunoglobulin receptor</i>	<i>Polymeric immunoglobulin receptor</i>	<i>Alpha-amylase 1</i>	BPI fold-containing family B member 1
5	Cystatin-SN	<i>Prolactin-inducible protein</i>	Lysozyme C	<i>Polymeric immunoglobulin receptor</i>	<i>Polymeric immunoglobulin receptor</i>
6	<i>Zymogen granule protein 16 homolog B</i>	<i>Antileukoproteinase</i>	<i>Prolactin-inducible protein</i>	Lysozyme C	Myeloperoxidase
7	<i>Immunoglobulin heavy constant alpha 1</i>	Mucin-5B	<i>Immunoglobulin heavy constant alpha 1</i>	<i>Immunoglobulin heavy constant mu</i>	Actin, cytoplasmic 1
8	Mucin-5B	Deleted in malignant brain tumours 1 protein	Mucin-5B	Myeloperoxidase	<i>Alpha-amylase 1</i>
9	<i>Lactotransferrin</i>	<i>Immunoglobulin heavy constant alpha 1</i>	Serum albumin	<i>BPI fold-containing family A member 2</i>	<i>Immunoglobulin heavy constant alpha 1</i>
10	Lysozyme C	Lactoperoxidase	Cystatin-SN	Immunoglobulin kappa constant	Carbonic anhydrase 6
11	Cystatin-S	<i>Zymogen granule protein 16 homolog B</i>	Lactoperoxidase	<i>Immunoglobulin heavy constant alpha 1</i>	Alpha-actinin-4
12	Immunoglobulin kappa constant	<i>Alpha-amylase 1</i>	<i>Immunoglobulin heavy constant mu</i>	<i>Immunoglobulin kappa light chain</i>	Apolipoprotein B-100
13	<i>Immunoglobulin kappa light chain</i>	<i>Immunoglobulin heavy constant mu</i>	<i>Immunoglobulin kappa light chain</i>	<i>Immunoglobulin alpha-2 heavy chain</i>	Annexin A1
14	<i>Immunoglobulin alpha-2 heavy chain</i>	Protein S100-A9	<i>BPI fold-containing family A member 2</i>	Carbonic anhydrase 6	Protein disulfide-isomerase
15	Cystatin-SA	<i>BPI fold-containing family A member 2</i>	<i>Immunoglobulin alpha-2 heavy chain</i>	BPI fold-containing family B member 1	Annexin A6
16	Immunoglobulin heavy constant mu	<i>Immunoglobulin kappa light chain</i>	Myeloperoxidase	Cystatin-SN	<i>Immunoglobulin alpha-2 heavy chain</i>
17	Carbonic anhydrase 6	Cystatin-SN	Cystatin-S	Lactoperoxidase	<i>Immunoglobulin kappa light chain</i>
18	<i>BPI fold-containing family A member 2</i>	Actin, cytoplasmic 1	Immunoglobulin kappa constant	Apolipoprotein B-100	Protein-glutamine gamma-glutamyltransferase E
19	Lactoperoxidase	Pyruvate kinase PKM	Deleted in malignant brain tumors 1 protein	Deleted in malignant brain tumors 1 protein	<i>Lactotransferrin</i>
20	Zinc-alpha-2-glycoprotein	<i>Immunoglobulin alpha-2 heavy chain</i>	Carbonic anhydrase 6	Actin, cytoplasmic 1	<i>Prolactin-inducible protein</i>

*Common protein identified are highlighted in bold and Italized

Most abundant proteins included polymeric immunoglobulin receptor, prolactin inducible proteins, lactotransferrin, immunoglobulin alpha 2 heavy chain, BPI fold containing family A member 2. To characterize and compare the nature of proteins that are found in the top 20 abundant and enriched proteins on the particles surface, we grouped protein and for their molecular weight (MW) and isoelectric point (pI). Almost 70% of the corona proteins composed of those with molecular weight < 60KDa. Unlike other particles, Ag NPs had less proteins with mass <20 KDa and also had proteins with mass of 100-150 kDa (Figure 2.5A). We also compared the molecular weight and pI of most enriched proteins. Mostly, the enriched proteins on SiO₂ and TiO₂ particles had MW of 100-150 KDa (Figure 2.5B).

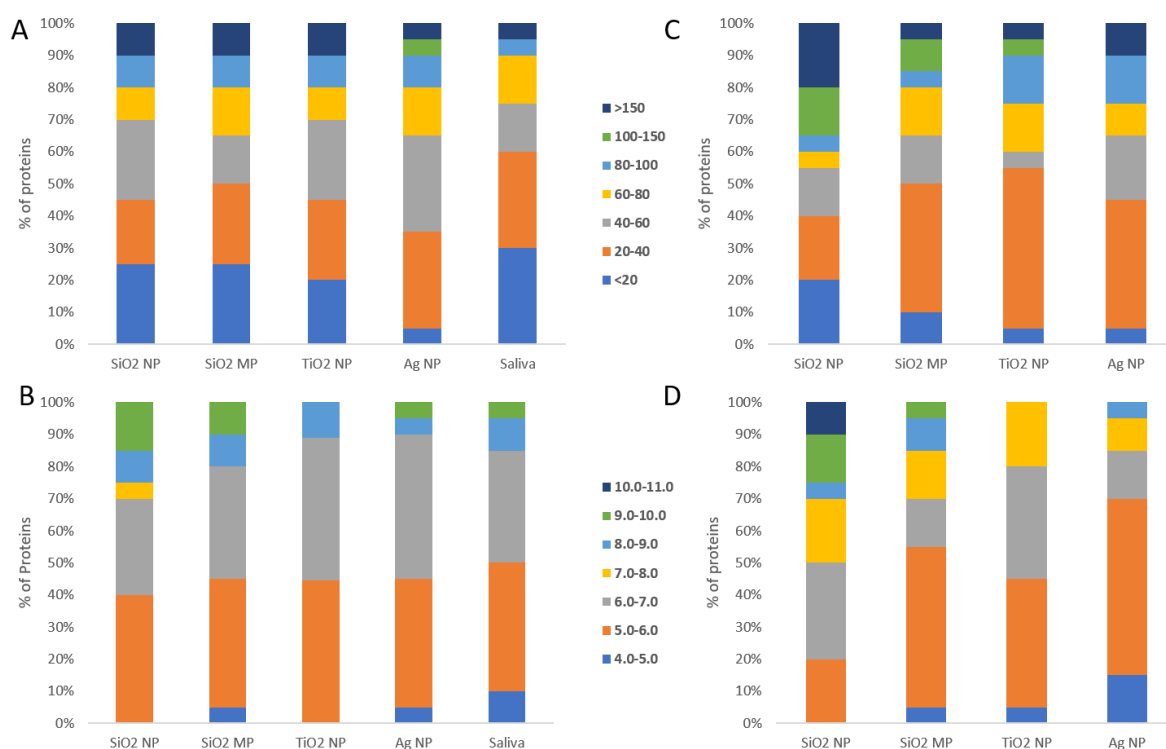


Figure 2.5 comparison of top 20 abundant (A & C) and enriched proteins (B & D) on the corona profiles based on MW & pI. graph (A & B): shows the classification of coronal Proteins according to their molecular weight (MW); graph (C&D): shows the difference between abundant and enriched coronal profiles on the particles based on the calculated isoelectric point (pI).

Figure 2.5 C & D represents the protein classification by pI for abundant and enriched coronal proteins of the dietary particles, respectively. Generally, 90% of the most abundant proteins present on the particles had their pI values less than 7 (Fig 2.5C). Notably, 50% of proteins enriched on SiO₂ NPs were with a pI value in the range of 7-11(Figure 2.5D). Overall, high molecular weight proteins with pI > 7 were enriched on the particles.

2.6.5 Functional Annotation of the Salivary Protein Corona:

We employed bioinformatics tools, such as Scaffold gene ontology (GO) and Panther database to classify the coronal proteins based on GO terms. Classes of proteins identified through GO term annotation are presented as stacked bar plot in figure 2.6.

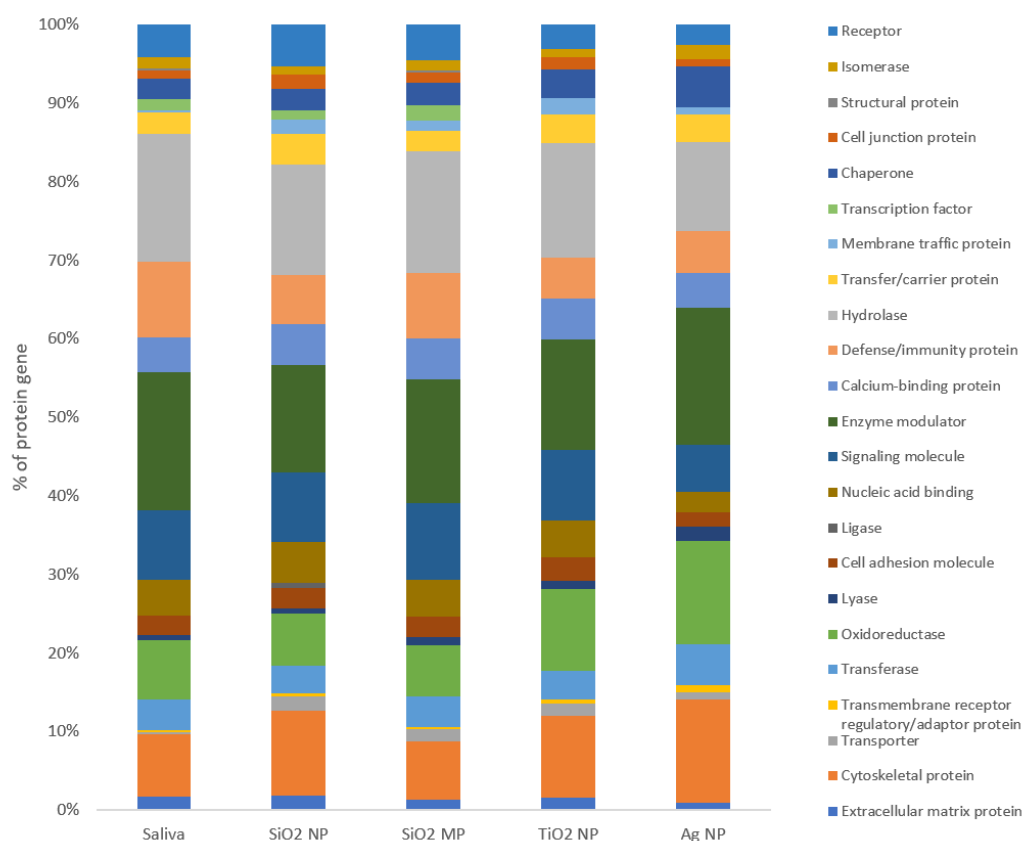


Figure 2.6 :Bioinformatic classification of identified salivary coronal proteins according to their protein class.

Enzyme modulator, hydrolase, proteins involved in host defence and immunity, signalling molecule, oxidoreductase and cytoskeletal proteins constituted ~60% of the coronal proteins. There were quantitative differences in the relative distribution of these protein classes among the tested particles. For instance, there was a two-fold increase in oxidoreductase class of proteins on Ag NPs while, the presence of oxidoreductase in other particles were comparable to that of saliva. Similarly, transcription factors were found only in SiO₂ particles. Other protein

classes such as transporter, calcium binding, and carrier protein were found in higher percentage on the tested particles compared to the whole saliva which in turn suggest the enrichment of these protein classes on the surface of particles.

2.6.6 Influence of Dietary Particles on the Enzyme Activities of α -amylase and Lysozyme in Human Saliva:

As the NP surface have the ability to modify the structure and therefore the function of the proteins, we hypothesized that activity of α -amylase and lysozyme will be influenced by the presence of dietary particles in human saliva. Interestingly, all the dietary particles showed statistically significant decrease in the enzyme activity as shown in figure 2.7 A.

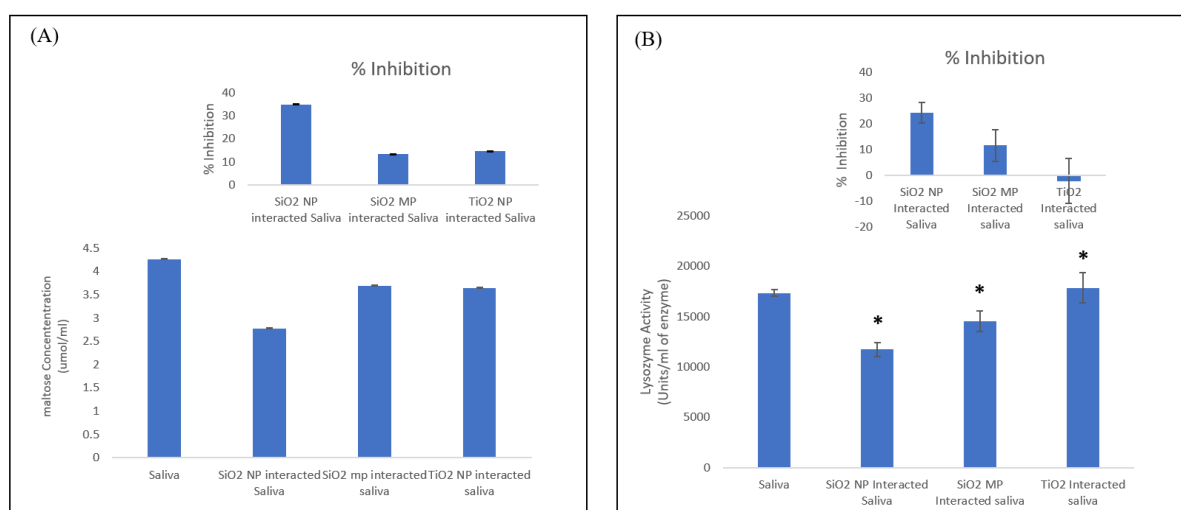


Figure 2.7 Influence of dietary particles on the enzyme activity of α -amylase and lysozyme in human saliva. Figure 7(A): α -Amylase activity by DNS assay with particle concentration of 2 mg/mL. The enzyme inhibitory activity is expressed as decrease in units of maltose liberated. Figure 7(B): Lysozyme activity by turbidimetric method with bacterial suspension concentration of *M. lysodeikticus* at 0.3mg/mL with particle concentration of 1.25 mg/ml. The enzymes are incubated in the substrate for 5 min.

Among the three dietary particles tested (SiO₂ NP, SiO₂ MP and TiO₂ NP), SiO₂ NPs exhibited higher inhibition (34.94%) as compared to whole saliva. SiO₂ MPs and TiO₂ NPs didn't show significant difference between them in the enzyme inhibition activity as shown in the figure inset 7a. The lysozyme function in saliva was found to be affected by the presence of SiO₂ particles (both NPs and MPs) but not by TiO₂ NPs (figure 2.7B). The % inhibition of lysozyme activity was 24.3, 11.58 for SiO₂ NPs and SiO₂ MPs, respectively.

2.7 Discussion:

We assessed the protein corona formed on human saliva interacted particles, as mouth is the port of entry for particles used as food additives. Our results showed qualitative and quantitative difference in the distribution of proteins present in the hard corona of different types of dietary particles tested. NPs of SiO₂ showed the highest amount of proteins adsorbed in comparison to other particles. Proteomic analysis showed the distinct type of gene clusters corresponding to proteins adsorbed on different particles. The functional annotation of proteins found associated with particles showed higher prevalence for those involved in metabolic and defence functions.

Inorganic particles used as food additives could get released from the food matrix and could interact with saliva during masticulation of food. Saliva serves pivotal function in enabling the smooth passage of food through digestive tract and is a major reservoir of digestive enzymes and proteins of relevance to oral hygiene [24, 25]. Therefore, it is crucial to understand the interactions of human salivary proteins with particles, including NPs that are used as food additives.

Several studies addressing the interaction of serum plasma with NPs have showed that the physicochemical properties of the particles such as size, shape, state of agglomeration and aggregation, and surface charge have significant influence on the formation and composition of protein corona [26, 27]. We observed agglomeration of particles when they were dispersed in saliva and PBS buffer. The increase in particle size when dispersed in saliva could be explained by the combined effect of the protein corona formation and the agglomeration of the particles due to the pH and ionic strength of the saliva [28]. Many studies have shown that protein corona could stabilize the particles in the solution [18, 29]. For instance, TiO₂ and Ag NPs dispersed in water and PBS (Phosphate Buffer Saline) quickly agglomerate from their original size of 20 to 50 nm to hundreds of nanometres while, in the human saliva the protein coating prevents the particles from forming large clusters. The net negative charge of particles reduced after incubation in saliva, suggesting the presence of protein corona. It should be noted that the type and relative abundance of proteins bound onto NP surface are determined not only by the physicochemical properties of NPs but also the properties of proteins in the biological fluid along with the micro-environment.

1D gel analysis of proteins associated with particle corona showed unique bands which were absent in the saliva control pointing towards the possibility of selective enrichment of certain proteins on particle surfaces. Further, protein profiling using LC-MS/MS showed that the type of protein bound onto particles is not primarily determined by their abundance in saliva. For instance, when the highly abundant mucin proteins were absent on Ag NPs, low abundant proteins such as lysozyme and lactoperoxidase were found to be enriched on particle surface. Thus, the difference in the abundance of proteins present in saliva and those retrieved from the particle surface suggest the selective enrichment of protein on particle surface. Apo-B100 lipoprotein, for example, showed significant enrichment on AgNPs with 64-fold increase in

comparison to saliva while it was 47 and 33 fold increase in the case of SiO₂ NPs and TiO₂ respectively which are congruent with other reported studies [30-32]. Similarly, Annexin A2, A11, A6 were found to be enriched on TiO₂ and Ag NPs. Studies have shown that particles with negative surface charge preferentially bind with proteins with net positive charge [8, 33, 34]. Accordingly, we also noticed that low abundant antimicrobial proteins displaying a positive charge (pI >7) such as Antileukoproteinase, myeloperoxidase, Lactotransferrin and lysozyme getting enriched on these particles with net negative charge. Interestingly, particles also showed a high prevalence of proteins with net negative charge in their corona. We attribute this preferential binding of negatively charged proteins on to the surface of negatively charged particles to Vroman's effect. According to Vroman's effect the initial binding of positively charged salivary proteins mask the negative surface of particles whereby allowing the binding of negatively charged proteins. Thus, while coulombic interactions play a major role in determining protein-particle interactions, studies have also shown metal specific binding of proteins. For instance, TiO₂ particles have shown to enrich phosphoproteins such as acidic PRPs (proline rich proteins), statherin, histatin-1, cystatins S and SA-III [35]. Similarly, we also observed an enrichment of proteins such as salivary proline-rich proteins, tubulin beta chain, deleted in malignant brain tumors 1 protein, fibrinogen gamma chain and collagen alpha -2(VI) on the surfaces of TiO₂ and SiO₂ particles. Another example for preferred binding of proteins on to metal surface was the enrichment of oxidoreductase on Ag NPs. Thiol group of cysteine molecules present in the active site of oxidoreductase is thought to mediate this preferred binding with AgNPs.

Generally, proteins associated with corona were identified to be majorly involved in cellular process & cell communication, metabolic process and response to stimulus. Almost 50 % of enriched proteins on SiO₂ NPs are involved in catalytic activity such as transferase, hydrolase

and enzyme regulator activity. As for Ag NPs the top enriched proteins are those involved mostly in hydrolase activity (33%). 67 % of the proteins found on TiO₂ NPs are those involved in cytoskeletal protein binding. Another major class of proteins found enriched on particle surfaces was apolipoproteins such as Apo B100, Apo AI, Apo E. The consequence of depleting Apolipoproteins from human saliva warrants further investigation, as these proteins play a major role in lipid metabolism.

When proteins adsorbed on to the surface of the particles, it may undergo structural rearrangement leading to conformational changes that will render the protein to become dysfunctional due to change in the secondary structure [36, 37]. Particles of SiO₂ (NPs and MPs), and TiO₂ NP caused partial inhibition of α -amylase and lysozyme activity of saliva. Among the tested particles SiO₂ NPs showed the highest percentage of inhibition. Generally, silica surfaces are regarded amenable for enzyme immobilization since silica surface chemistry has little effect on proteins. Therefore, the observed loss of enzyme activity when they were interacted with SiO₂ NPs is thought to be mediated by unique interaction of NPs of SiO₂, to cause conformational change in enzyme.

Digestion of amylose and amylopectin in the mouth is often assumed to be of minimal importance, as food stays in the mouth only for few seconds and the time given to the enzyme to act enzymatically in the mouth during mastication is believed to be vary with individuals for effective digestion. However, Studies have shown that considerable amount of starch hydrolysis happens in mouth during masticulation of food and that salivary amylase were protected from the acid inactivation in the stomach by partially digested starch [38, 39]. Therefore, binding of α -amylase to NPs of SiO₂ could compromise the action of α -amylase beyond the oral cavity. Further, the presence of NPs in small intestine could have similar effect

on pancreatic α -amylase. In short, our studies showed the selective enrichment of certain proteins including digestive enzymes and that these interactions could compromise enzyme activities. The mechanism of enzyme inactivation by SiO₂ NPs is currently addressed in a separate study.

2.8 Conclusion:

For the first time we captured the interaction of salivary proteome with dietary particles through a qualitative and quantitative approach. We observed a distinctive difference between each dietary particle on its protein corona composition with differential abundance and fold enrichment of significant salivary proteins. Further, we show that the interactions of particles with proteins could lead to compromised enzyme functions that are vital to the function of saliva.

2.9 Supplementary information

Table 2.3(S1): 20 most enriched proteins by fold change ≥ 2 .

S.No	SiO ₂ NP				SiO ₂ BP				TiO ₂ NP				Ag NP			
	Identified Proteins	Fold change by Saliva	pI	Molecular weight (kDa)	Identified Proteins	Fold change by Saliva	pI	Molecular weight (kDa)	Identified Proteins	Fold change by Saliva	pI	Molecular weight (kDa)	Identified Proteins	Fold change by Saliva	pI	Molecular weight (kDa)
1	<i>Apolipoprotein B-100</i>	33	6.57	516	<i>Apolipoprotein B-100</i>	51	6.57	516	<i>Apolipoprotein B-100</i>	47	6.57	516	<i>Apolipoprotein B-100</i>	64	6.57	516
2	C-C motif chemokine 28	23	10.23	14	<i>Annexin A2</i>	23	7.56	39	<i>Annexin A2</i>	18	7.56	39	<i>Annexin A2</i>	34	7.56	39
3	Histidine-rich glycoprotein	21	7.03	60	Histidine-rich glycoprotein	16	7.03	60	<i>Annexin A11</i>	15	7.53	54	<i>Annexin A6</i>	26	5.41	76
4	Apolipoprotein E	18	5.52	36	<i>Annexin A11</i>	14	7.53	54	Plastin-3	10	5.41	71	Apolipoprotein E	19	5.52	36
5	Slit homolog 3 protein	14	7.91	168	<i>Annexin A5</i>	12	4.93	36	<i>Annexin A6</i>	8.7	5.41	76	<i>Annexin A11</i>	15	7.53	54
6	Unconventional myosin-II	12	9.21	125	<i>Annexin A6</i>	11	5.41	76	<i>Annexin A5</i>	7.3	4.93	36	Calpain-1 catalytic subunit	15	5.49	82
7	Midkine	12	9.78	16	Apolipoprotein E	11	5.52	36	Guanine nucleotide-binding protein G(i) subunit alpha-2	7.3	5.34	40	<i>Annexin A5</i>	15	4.93	36
8	Guanine nucleotide-binding protein G(i) subunit alpha-2	11	5.34	40	Intelectin-1	11	5.48	35	Intelectin-1	7.3	5.48	35	Actin-related protein 2	11	6.29	45
9	Talin-1	11	5.77	270	Collagen alpha-2(VI) chain	9.3	5.85	109	Ras-related protein Rap-1b	7.3	5.65	21	Copine-3	11	5.6	60
10	Ras GTPase-activating-like protein IQGAP1	9.9	6.08	189	Chitinase-3-like protein 1	9.3	8.65	43	Integrin alpha-M	7.2	6.75	127	Endoplasmic	11	4.73	92
11	EH domain-containing protein 1	9.4	6.35	61	CD59 glycoprotein	8.1	5.18	14	Protein S100-A12	5.8	5.8	11	Tubulin alpha-4A chain	11	4.93	50
12	Histone H1.5	9.4	10.91	23	Transitional endoplasmic reticulum ATPase	8.1	5.14	89	Cell division control protein 42 homolog	5.8	6.16	21	CD59 glycoprotein	7.6	5.18	14
13	Angiogenin	8.5	9.73	17	Alpha-L-iduronidase	8.1	9.09	73	ADP-ribosylation factor 3	5.8	7.04	21	Intelectin-1	7.6	5.48	35
14	Integrin beta-2	8.4	6.54	85	Integrin alpha-M	6.8	6.75	127	Integrin beta-2	4.7	6.54	85	Ras-related protein Rap-1b	7.6	5.65	21
15	Collagen alpha-2(VI) chain	7.9	5.85	109	Guanine nucleotide-binding protein G(i) subunit alpha-2	6.8	5.34	40	Programmed cell death 6-interacting protein	4.4	6.14	96	Grancalcin	7.6	5.02	24
16	<i>Annexin A2</i>	7.6	7.56	39	Ras-related protein Rap-1b	6.8	5.65	21	Calpain-1 catalytic subunit	4.4	5.49	82	Transitional endoplasmic reticulum ATPase	7.6	5.14	89
17	<i>Annexin A11</i>	7.6	7.53	54	Extracellular matrix protein 1	6.8	6.19	61	Syntenin-1	4.4	7.04	32	<i>Annexin A4</i>	7.6	5.84	36
18	Beta-1,3-galactosyl-O-glycosyl-glycoprotein beta-1,6-N-acetylglucosaminyltransferase 3	7.6	8.53	51	Ras-related protein Rab-27A	6.8	5.09	25	<i>Annexin A4</i>	4.4	5.84	36	Extracellular matrix protein 1	7.6	6.19	61
19	Integrin alpha-M	7.2	6.75	127	Protein S100-A12	5.6	5.8	11	Extracellular matrix protein 1	4.4	6.19	61	Carbonyl reductase [NADPH] 1	7.6	8.55	30
20	Proline-rich protein 4	6.9	6.56	15	Kallikrein-10	5.6	8.61	30	Ras-related protein Rab-7a	4.4	6.32	23	Clathrin heavy chain 1	7.6	5.48	192

*Common proteins are Italized and unique proteins are highlighted in bold

2.10 Reference

1. Bhushan, B., *Introduction to nanotechnology*, in *Springer handbook of nanotechnology*. 2017, Springer. p. 1-19.
2. Hulla, J., S. Sahu, and A. Hayes, *Nanotechnology: History and future*. Human & experimental toxicology, 2015. **34**(12): p. 1318-1321.
3. Rashidi, L. and K. Khosravi-Darani, *The applications of nanotechnology in food industry*. Critical reviews in food science and nutrition, 2011. **51**(8): p. 723-730.
4. McCracken, C., P.K. Dutta, and W.J. Waldman, *Critical assessment of toxicological effects of ingested nanoparticles*. Environmental Science: Nano, 2016. **3**(2): p. 256-282.
5. Docter, D., et al., *The nanoparticle biomolecule corona: lessons learned - challenge accepted?* Chemical Society Reviews, 2015. **44**(17): p. 6094-6121.
6. Ke, P.C., et al., *A Decade of the Protein Corona*. ACS nano, 2017.
7. Barrán-Berdón, A.L., et al., *Time evolution of nanoparticle–protein corona in human plasma: relevance for targeted drug delivery*. Langmuir, 2013. **29**(21): p. 6485-6494.
8. Tenzer, S., et al., *Rapid formation of plasma protein corona critically affects nanoparticle pathophysiology*. Nature nanotechnology, 2013. **8**(10): p. 772.
9. Winzen, S., et al., *Complementary analysis of the hard and soft protein corona: sample preparation critically effects corona composition*. Nanoscale, 2015. **7**(7): p. 2992-3001.
10. Powell, J.J., et al., *Origin and fate of dietary nanoparticles and microparticles in the gastrointestinal tract*. Journal of Autoimmunity, 2010. **34**(3): p. J226-J233.
11. de Almeida, P.D.V., et al., *Saliva composition and functions: a comprehensive review*. J contemp dent pract, 2008. **9**(3): p. 72-80.
12. Humphrey, S.P. and R.T. Williamson, *A review of saliva: normal composition, flow, and function*. The Journal of prosthetic dentistry, 2001. **85**(2): p. 162-169.
13. Kaji, S.S., et al., *The Effect of TiO₂-Nanoparticle on the Activity and Stability of Trypsin in Aqueous Medium*.
14. Vertegel, A.A., R.W. Siegel, and J.S. Dordick, *Silica Nanoparticle Size Influences the Structure and Enzymatic Activity of Adsorbed Lysozyme*. Langmuir, 2004. **20**(16): p. 6800-6807.
15. Huynh, K.A. and K.L. Chen, *Aggregation kinetics of citrate and polyvinylpyrrolidone coated silver nanoparticles in monovalent and divalent electrolyte solutions*. Environmental science & technology, 2011. **45**(13): p. 5564-5571.
16. Dobrovolskaia, M.A., et al., *Interaction of colloidal gold nanoparticles with human blood: effects on particle size and analysis of plasma protein binding profiles*. Nanomedicine: Nanotechnology, Biology and Medicine, 2009. **5**(2): p. 106-117.
17. Lu, P.-J., et al., *Methodology for sample preparation and size measurement of commercial ZnO nanoparticles*. Journal of Food and Drug Analysis, 2018. **26**(2): p. 628-636.
18. Deng, Z.J., et al., *Differential plasma protein binding to metal oxide nanoparticles*. Nanotechnology, 2009. **20**(45): p. 455101.
19. McCall, R.L. and R.W. Sirianni, *PLGA nanoparticles formed by single-or double-emulsion with vitamin E-TPGS*. Journal of visualized experiments: JoVE, 2013(82).
20. Schipper, R., et al., *SELDI-TOF-MS of saliva: Methodology and pre-treatment effects*. Journal of Chromatography B, 2007. **847**(1): p. 45-53.
21. Lundqvist, M., et al., *Nanoparticle size and surface properties determine the protein corona with possible implications for biological impacts*. Proceedings of the National Academy of Sciences, 2008.
22. Shevchenko, A., et al., *In-gel digestion for mass spectrometric characterization of proteins and proteomes*. Nature Protocols, 2007. **1**: p. 2856.

23. Helal, R. and M. Melzig, *Determination of lysozyme activity by a fluorescence technique in comparison with the classical turbidity assay*. Die Pharmazie-An International Journal of Pharmaceutical Sciences, 2008. **63**(6): p. 415-419.
24. Loo, J., et al., *Comparative human salivary and plasma proteomes*. Journal of dental research, 2010. **89**(10): p. 1016-1023.
25. van't Hof, W., et al., *Antimicrobial defense systems in saliva*, in *Saliva: Secretion and Functions*. 2014, Karger Publishers. p. 40-51.
26. Docter, D., et al., *The nanoparticle biomolecule corona: lessons learned—challenge accepted?* Chemical Society Reviews, 2015. **44**(17): p. 6094-6121.
27. Zanganeh, S., et al., *Chapter 3 - Protein Corona: The Challenge at the Nanobiointerfaces A2 - Mahmoudi, Morteza*, in *Iron Oxide Nanoparticles for Biomedical Applications*, S. Laurent, Editor. 2018, Elsevier. p. 91-104.
28. Bihari, P., et al., *Optimized dispersion of nanoparticles for biological in vitro and in vivo studies*. Particle and Fibre Toxicology, 2008. **5**(1): p. 14.
29. Monopoli, M.P., et al., *Physical– chemical aspects of protein corona: relevance to in vitro and in vivo biological impacts of nanoparticles*. Journal of the American Chemical Society, 2011. **133**(8): p. 2525-2534.
30. Tenzer, S., et al., *Nanoparticle Size Is a Critical Physicochemical Determinant of the Human Blood Plasma Corona: A Comprehensive Quantitative Proteomic Analysis*. ACS Nano, 2011. **5**(9): p. 7155-7167.
31. Sanfins, E., et al. *Nanoparticle-protein interactions: from crucial plasma proteins to key enzymes*. in *Journal of Physics: Conference Series*. 2011. IOP Publishing.
32. Jeon, Y.-M., et al., *The effects of TiO₂ nanoparticles on the protein expression in mouse lung*. Molecular & Cellular Toxicology, 2011. **7**(3): p. 283.
33. Karmali, P.P. and D. Simberg, *Interactions of nanoparticles with plasma proteins: implication on clearance and toxicity of drug delivery systems*. Expert Opinion on Drug Delivery, 2011. **8**(3): p. 343-357.
34. Deng, Z.J., et al., *Plasma protein binding of positively and negatively charged polymer-coated gold nanoparticles elicits different biological responses*. Nanotoxicology, 2012. **7**(3): p. 314-322.
35. Salih, E., et al., *Large-scale phosphoproteome of human whole saliva using disulfide–thiol interchange covalent chromatography and mass spectrometry*. Analytical biochemistry, 2010. **407**(1): p. 19-33.
36. Treuel, L., *How protein adsorption shapes the biological identity of NPs—where do we stand*. J Phys Chem Biophys, 2013. **3**: p. e113.
37. Walkey, C.D. and W.C. Chan, *Understanding and controlling the interaction of nanomaterials with proteins in a physiological environment*. Chemical Society Reviews, 2012. **41**(7): p. 2780-2799.
38. Hoebler, C., et al., *Physical and chemical transformations of cereal food during oral digestion in human subjects*. British Journal of Nutrition, 1998. **80**(5): p. 429-436.
39. Mandel, A.L. and P.A. Breslin, *High endogenous salivary amylase activity is associated with improved glycemic homeostasis following starch ingestion in adults*. The Journal of nutrition, 2012. **142**(5): p. 853-858.

CHAPTER 3

Studies on the interaction of silica particles on the salivary α -amylase by multi-spectroscopic methods

Previous study showed that SiO₂ NPs adsorb more proteins in comparison to TiO₂ and Ag NPs. SiO₂ NPs were found to inhibit the salivary α -amylase and salivary lysozyme which was significantly higher when compared with other NPs. To further understand the mechanism of interaction, we continued our study which is detailed in chapter 3. We investigated the influence of SiO₂ particles in nano and micron size on the structure and function of salivary α -amylase.

This chapter is co-authored by Wut Hmone Phue, Ke Xu and Dr. Saji George. It is planned for submission in Journal of Trends in Food Science and Technology.

3. STUDIES ON THE INTERACTION OF SILICA PARTICLES ON THE SALIVARY α -AMYLASE BY MULTI-SPECTROSCOPIC METHODS.

3.1 Abstract:

We had observed significant enrichment of salivary proteins, including vital enzymes on SiO₂ particles and suspected that protein binding on to silica particles could compromise the structure and function of proteins function. Further studied were conducted on important salivary enzyme- α -amylase to assess the effect of its interaction with SiO₂ particles (nano and micron size) on both the enzyme activity and structure. Spectroscopy analysis (fluorescence spectroscopy, FTIR, CD) and enzyme kinetic assays were carried out to understand the effect of particles on the structure and function of a-amylase, respectively. The substrate affinity for α -amylase was found to be significantly reduced when they were interacted with NPs of SiO₂. The SiO₂ NP- α -amylase and SiO₂ MP- α -amylase complex exhibited non-competitive and competitive type of inhibition, respectively. Stern–Volmer plots confirmed the static type of quenching with strong quenching of the chromophore residues of the protein for SiO₂ NP - α -amylase complex followed by SiO₂ MP - α -amylase complex. Far-UV Circular Dichroism studies and FTIR Spectroscopy revealed conformational changes in the 2d structure of proteins. In short, binding of human salivary α -amylase on to food grade silica particles compromised their structure and function and the effect was more pronounced for SiO₂ particles in the ‘nano’ size range.

Keywords: SiO₂ NP (nano particle), SiO₂ MP (micron particle), Spectroscopy, α -amylase, protein conformation.

3.2 Résumé :

Nous avons observé un enrichissement significatif de protéines salivaires, incluant des enzymes vitales sur les particules de SiO₂ et avons soupçonné que la liaison des protéines aux particules de silice pourrait compromettre la structure et la fonction des protéines. Des études complémentaires ont été menées sur l'enzyme α -amylase afin d'évaluer les effets de son interaction avec les particules de SiO₂ (de taille nano et micro) sur l'activité et la structure enzymatique. Une analyse spectroscopique (spectroscopie de fluorescence, FTIR, CD) et des tests cinétiques enzymatiques ont été effectués afin de comprendre l'effet de particules sur la structure et la fonction d' α -amylase, respectivement. L'affinité du substrat pour l'enzyme α -amylase s'est trouvée réduite lors de ses interactions avec les NPs de SiO₂. Les complexes NP- α -amylase et MP- α -amylase exhibaient respectivement des types d'inhibition non-compétitives et compétitives. Des graphiques Stern-Volmer confirmaient le type de désactivation statique avec une désactivation forte des résidus de chromophores de la protéine pour le complexe NP - α -amylase de SiO₂ suivi du complexe SiO₂ MP- α -amylase de SiO₂. Des études poussées en spectroscopie de dichroïsme circulaire UV et la spectroscopie FTIR ont révélé des changements de conformation dans la structure 2D des protéines. Bref, la liaison de α -amylase de la salive humaine sur le silice de qualité alimentaire compromettait leur structure et leur fonction. Cet effet était plus prononcé pour les particules de SiO₂ de taille 'nano'.

Mots clés : SiO₂ NP (nano particules), SiO₂ MP (micron particules), spectroscopie, α -amylase, conformation de protéine.

3.3 Introduction:

The new application of nanosized particles in food and nutraceutical industry for improving stability, quality, bioavailability of active ingredients and overall function of the final product are increasing. However, this growing trend of using engineered NPs in food and consumer

products undeniably leads to human exposure through oral route while their health effects remain unclear [1] [2]. For instance, the safety of SiO₂ particles- a high volume particles commonly used as food additive for several decades, is debatable [3]. For instance, regulatory toxicology team couldn't extrapolate the results from the available chronic study to confirm the ADI for the SiO₂ particle due to the limitations and knowledge gaps in characterizing the particles and simulating the human exposure conditions. Use of SiO₂ in food inadvertently will lead to human exposure. The passage of SiO₂ NPs to gastrointestinal tract may lead to potential health hazards [4, 5]. However, studies addressing the interaction of NPs with proteins of relevance to gastro-intestinal system are grossly missing in the literature [2].

Human salivary α -amylase is the most abundant enzyme in human saliva with single polypeptide chain of ~475 residues and 2 sulfahydryl groups and 4 di-sulfide bridges. Salivary amylase initiates the digestion of complex carbohydrates in the oral cavity, where starch molecules gets partially digested in to oligosaccharides, maltose and glucose [8]. A compromise in its function may create a health concern over time since it could possibly influence the nutrient [9].

In this study we chose salivary α -amylase enzyme to understand the interaction and mechanism of inhibition of salivary α -amylase by nano and micron sized particles of SiO₂ (SiO₂ NP and SiO₂ MP). We monitored enzyme kinetics of native and SiO₂ interacted human salivary α -amylase and measured the structural alteration induced by particles using different spectroscopic techniques such as Fluorescence quenching, FTIR and CD. Though, SiO₂ NP and SiO₂ MP has similar surface chemistry, we observed a difference between the nano and micron sized SiO₂ particles on the activity and stability of the α -amylase enzyme.

3.4 Materials and Methods:

3.4.1 Chemicals and Reagents:

All chemicals and reagents were of analytical grade. α -amylase (From human saliva) > 100 U/mg were purchased from Lee BioSolutions (Maryland Heights, USA). Starch from potato, 3,5-Dinitrosalicylic acid were purchased from Sigma Aldrich (St. Louis, Missouri, United States). The silicon dioxide particles used in this study are as follows, Food grade silicon dioxide particles (SiO_2) in nano size (AEROSIL 200F) and micron size (SIPERNAT 22) obtained from Evonik Corporation (NJ, United States).

For all the experiment the stock solution and buffer (PBS buffer -0.01 M, pH 7.4) were prepared according to the standard laboratory procedures using Milli-Q reagent grade water (MilliQ, Millipore, Canada).

3.4.2 Physical Characterization:

The shape and size of the silicon dioxide particles (SiO_2 NP and SiO_2 MP) was observed by Scanning Electron Microscopy (SEM). For SEM analysis (Hitachi, SEM-SU8230, Japan) samples (5 μl of 50 ppm NP dispersion) were dropped on the SEM stub, dried at room temperature for overnight and were examined at 50 KV accelerating voltage without coating [10]. The particle size range, polydispersity index (PDI) and surface charge of particles were characterized by Dynamic Light Scattering (DLS) and zeta potential measurement in Nanobrook omni instrument (Brookhaven's, New York) at 25°C at a concentration of 50 $\mu\text{g/mL}$. Samples prepared for the DLS were loaded in to a pre-rinsed folded capillary cell for the zeta potential measurement with an applied voltage of 100 V.

3.4.3 Preparation /Interaction of Silicon Dioxide Particles with α -amylase:

A stock solution of 1000 U/mL was prepared in 20mM PBS buffer pH 7.4 and diluted with the same buffer for the working stock which is 200U/mL. Depending on the experiment protocol

the concentration of the enzyme was either kept constant and or varied. The reaction mixture was equilibrated for the optimal incubation time at 37 °c for 1 h.

3.4.4 Effect of SiO₂ Particles on Enzyme Kinetics of α -amylase by DNS Method:

Determination of reducing sugars was carried out by dinitro salicylic acid method (DNS). For this, 10% (W/V) soluble potato starch solution was prepared by dissolving 5g of potato starch in 50 mL of 0.02M sodium phosphate buffer (pH 6.9 with 0.006M of sodium chloride). The resulting solution was heated directly on a hot plate using constant stirring, bring to boil and maintain the solution at that temperature for 15 min to enhance the solubility of the starch solution. DNS reagent was prepared by dissolving 1 g of 3,5-dinitrosalicylic acid in 50 mL Milli-Q water. It was then mixed with sodium potassium tartrate tetrahydrate solution prepared in 2N sodium hydroxide, heated on a hot plate at 70°C and made up to 100 mL with Milli-Q water. The working solution of standard enzyme α -amylase (2 activity units/mL) was prepared from stock solution(1000U/mL) in PBS buffer and used to hydrolyse the starch. Equal amount of SiO₂ particles and α -amylase enzyme (40 μ l with total volume of 80 μ L) were added in the 96 well microplate and incubated at 37°C for 1hr. Subsequently, 20 μ L of Starch solution was added to the wells, incubated for 10 min at 37 °C and the reaction was terminated by adding 100 μ L of DNS reagent and keeping the plate in boiling water bath maintained at 100°C for 15 min. The plate was cooled to room temperature and the absorbance at 540 nm was measured for each well using a plate reader (Spectra max i3x, Molecular Devices, USA).

Particles interacted α -amylase was incubated with increasing concentration of soluble starch (5-80 mg/mL) and the enzyme activity was measured as a function of time. The values obtained were used for preparing Lineweaver- Burk plot from which V_{\max} and K_m values were calculated. The type of enzyme inhibition when interacted with particles was determined by fitting the kinetic data in to Dixon plot graph. Here, the kinetic parameters were obtained by

incubating the particles interacted α -amylase with various concentration of inhibitors (SiO_2 Particle from 2-16 mg/mL) and starch solution (from 5-80 mg/mL) while, the concentration of α -amylase kept constant at 2 activity units/mL.

3.4.5 Fluorescence Spectroscopy:

Samples for fluorescence spectroscopy was prepared by mixing 100 μl of α -amylase (10 activity U/mL) with 30 μl of increasing concentration of SiO_2 NP and SiO_2 MP from 0.2 – 1.0 mg/mL. The resulting mixture was incubated at 37 °C for 1 hr. Fluorescence measurements were obtained using a plate reader (Spectra max i3x plate reader (soft max pro 7.0.3, Molecular Devices, USA). The emission spectra were recorded in the range of 320-600nm upon excitation at 280 nm, using 10 nm/10 nm slit widths, and each spectrum was the average of three scans.

The binding constant and number of binding sites was obtained by Stern -Volmer equation:

$$\frac{I_0}{I} = 1 + K_q \tau_0 [Q] = 1 + K_{sv} [Q] \text{ -----Equation 1}$$

Where I_0 and I represent the fluorescence intensities in the absence and the presence of the quencher (SiO_2 Particles) respectively, K_{sv} is the dynamic quenching constant and the Q is the concentration of the quencher. The slope of the fitted data to the equation will give the value of K_{sv} . k_q is the bimolecular quenching rate constant, and τ_0 is the biomolecular fluorescence lifetime in the absence of quencher, which is considered to be 2.97 ns for α -amylase[11].

The number of binding constant (K) and number of binding sites (n) between the quencher and the α -amylase can be obtained by the equation mentioned below,

$$\log \frac{I_0 - I}{I} = \log K + n \log [Q] \text{ -----Equation 2}$$

Where I_0 and I represent the fluorescence intensities in the absence and the presence of the quencher (SiO_2 Particles) respectively, K and n represents the binding constant and number of

binding sites and Q represents the quencher concentration (SiO₂ Particles). The values of K and n was obtained by linear fitting the data with the equation where the slope of the line gives n and y intercept gives the values of K [12].

3.4.6 Far- UV Circular Dichroism Spectroscopy:

Circular dichroism (CD) spectra of pure α -amylase and those interacted with SiO₂ Particles were recorded using JASCO J-150 CD Spectrophotometer. A quartz cuvette cell with a path length of 1mm was used for holding samplings for measurement in the Far-UV CD spectra (185-260nm). Three scans with a scan speed of 20nm/min were performed and the obtained values were averaged. A spectrum of blank solution was subtracted and smoothed from the spectra of pure and SiO₂ particles interacted enzyme by using the spectra analyser software (JASCO J-815 CD Spectrometer, Maryland, USA). The secondary structure content was measured using Dichroweb software where, Contin-LL (Provencher & Glockner Method) and reference set 7 (optimized for 190-240 nm) were used. The results were expressed in millidegrees (mdeg) and the value of mean residue weight (MRW) was obtained using the equation, $MRW = \text{Molecular weight} / (\text{number of residues} - 1)$ wherein MRW value for α -amylase is 111.919 Daltons was used for calculating the secondary structure content [13]. The concentration of the concentration of α -amylase and the SiO₂ Particles in the CD study was 100 U/ml and 1mg/mL .

3.4.7 FTIR Analysis of Protein Structure:

The FTIR spectra were recorded on FTIR spectrometer - α -alpha -P from Bruker, which is equipped with germanium attenuated total reflection (ATR) accessory. All spectra of the samples were taken via the ATR method and the spectra were read between 650 to 4000 cm⁻¹,

with a resolution of 4 cm⁻¹ and 120 scans. An equal volume of 10 µl of pure protein α -amylase (250 U/mL) and the SiO₂ particles(1mg/mL) mixtures were pre incubated (37°C for 1 hr) and the incubated samples (20 µl) were dropped on the ATR probe and let it dry for 10 min. Subsequently, the spectra of the samples were recorded thrice and averaged [14].

3.5 RESULTS:

3.5.1 Particle Characterization:

The SiO₂ NPs and MPs used in this study were characterized prior to their interaction with the enzyme α -amylase to assess their size and shape using SEM as shown in the Figure 3.1. According to the suppliers, the primary particle sizes of SiO₂ NP and SiO₂ MP were 12nm, and 110 µm respectively. However, SEM analysis showed that size of primary particles constituting the aggregates are 25 nm and 70 nm for SiO₂ NP and SiO₂ MP respectively.

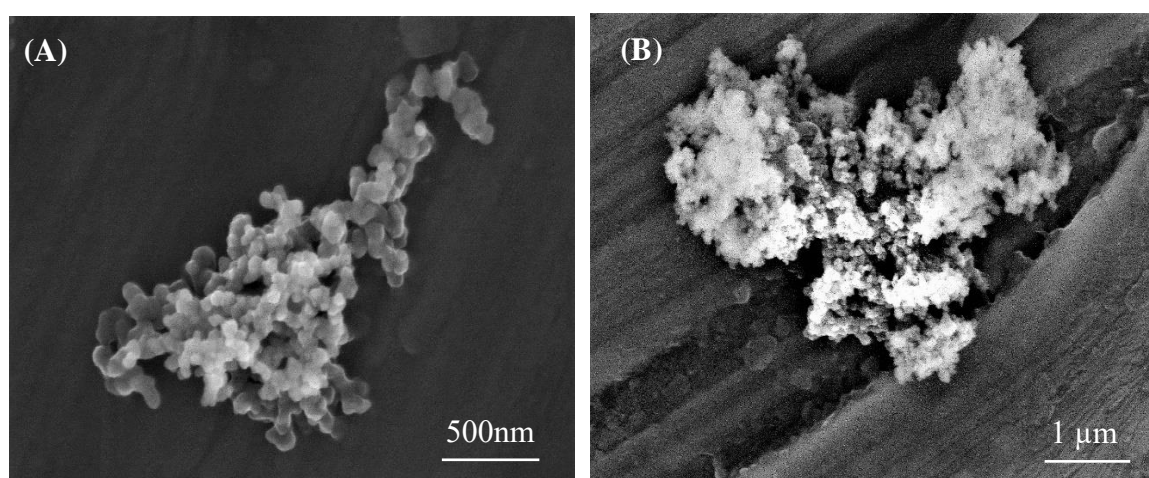


Figure 3.1 SEM image of food grade silicon dioxide particles obtained after drying the NP dispersion (50 ppm) on the SEM stub. (A) SiO₂ NP and (B) SiO₂ MP.

A significant decrease in particle size was observed for SiO₂ MPs in water and buffer due to the deagglomeration of the particles. Particles exhibited negative surface charge for both nano and micron size and no significant difference in the surface charge and PDI of the particles which are dispersed in water and PBS buffer (Table 3.1).

Table 3.1 Physical characterization of SiO₂ particles suspended in water and PBS buffer.

SiO ₂ Particles	Suspended in water			Suspended in PBS		
	Effective diameter by number (nm)	PDI	Zeta potential (mV)	Effective diameter by number (nm)	PDI	Zeta potential (mV)
SiO ₂ NP	50.53±15.10	0.32±0.082	-25.95±0.788	55.62±16.94	0.37±0.20	-26.47±5.62
SiO ₂ MP	41.78±4.05	0.34±0.11	-20.13±2.63	41.96±24.10	0.25±0.03	-28.54±2.76

Table 1: Summarize the physical characterization of the SiO₂ particles used in the experiment.

Effective diameter by number in (nm); Poly dispersity index-PDI; and Zeta potential (ZP) in mV of SiO₂ NP and SiO₂ MP particles measured when dispersed in water and PBS at a particle concentration of 20µg/mL. Values are mean ± SD from three independent experiment.

3.5.2 Enzyme Inhibition Kinetics:

A graphical method was used to determine the type of inhibition and the dissociation constant (K_i) for an enzyme-inhibitor complex using Dixon plot. The effect on the enzyme rate of α -amylase were determined at increasing substrate concentration from 1-10 mg/mL and over a range of inhibitor (SiO₂ NP and MP particles) concentration from 2 – 16 mg/mL. Kinetic parameters were determined from Michaelis -Menton plot and Dixon plot. It was observed that, the K_m values for α -amylase interacted with SiO₂ NP (0.0334M), SiO₂ MP (0.0375 M) was higher than that of free enzyme (0.0237 M). V_{max} values for free α -amylase and SiO₂ NP and SiO₂ MP interacted α -amylase are 5.5685 µmol/min/mL, 5.2261 µmol/min/mL and 5.6675 µmol/min/mL respectively (Figure 3.2 (C)). The V_{max} values decreased for SiO₂ NP interacted α -amylase while there is no significant difference between V_{max} values for free α -amylase and SiO₂ MP interacted α -amylase.

The type of inhibition for the free α -amylase and SiO_2 particle interacted α -amylase was obtained through Dixon plot as shown in Figure 3.2(A) & (B). The inhibitor constant K_i is an indication of how potent an inhibitor on the enzyme activity and it's the concentration required to produce half maximum inhibition.

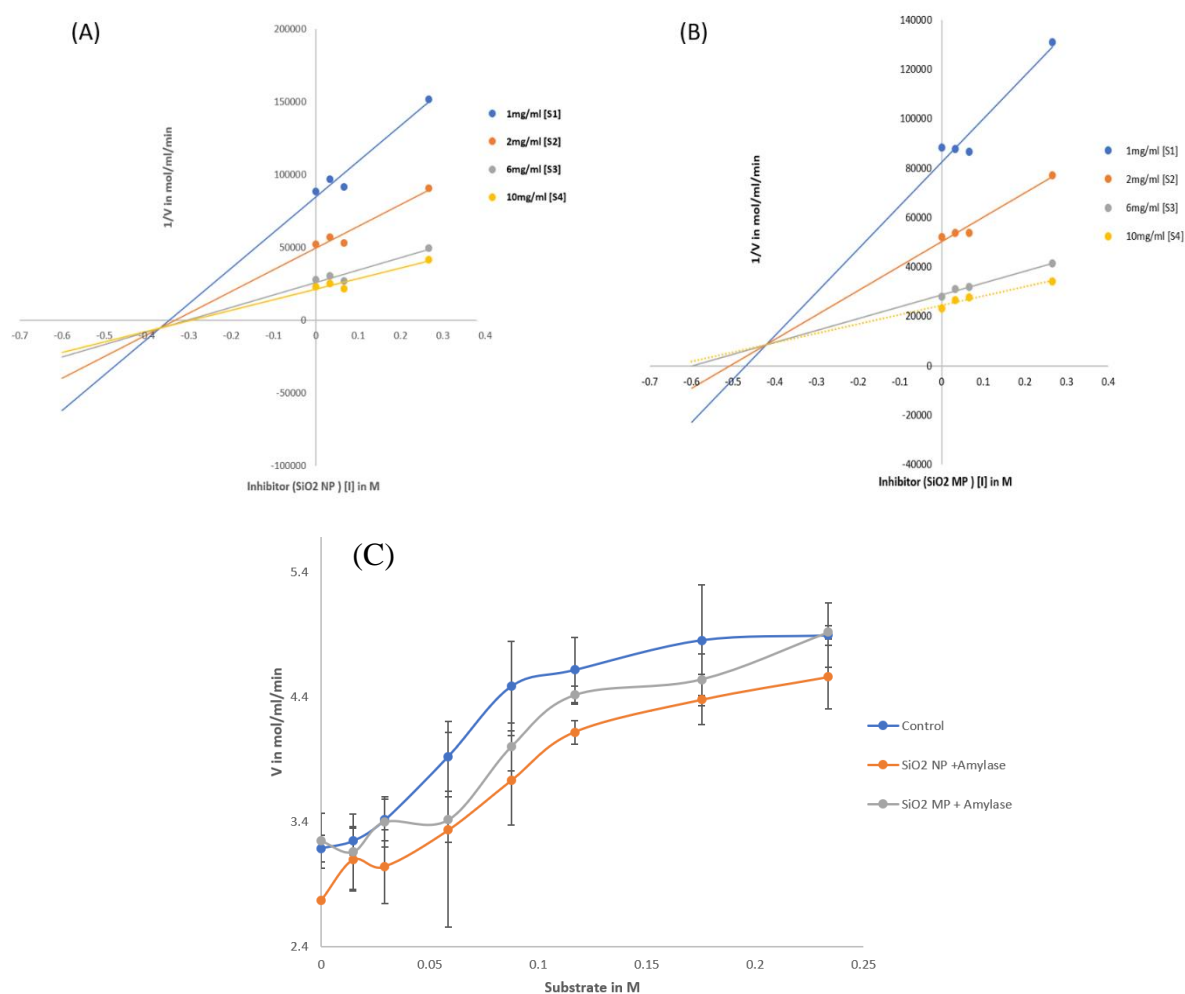


Figure 3.2 Dixon plot for the inhibition kinetic study with Starch concentration: (A) α -amylase interacted with SiO_2 NP ;(B) α -amylase interacted with SiO_2 MP. (C) Michaelis-Menton plot for K_m and V_{max} values of α -amylase and α -amylase interacted with SiO_2 particles in the presence of different concentration of soluble starch.

From the graph 3.2(A), the SiO₂ NP interacted α -amylase showed non-competitive inhibition as the inhibition curves obtained with different substrate concentrations in to a single straight line converging in the third quadrant at $-K_i$ and $-I$ with the K_i value of 0.45M. α -amylase interacted with SiO₂ MP showed a competitive inhibition as the lines converge above the x - axis and the value of $[I]$ where they intersect is $-K_i$ representing the pattern of competitive inhibition with K_i value of 0.35M (Figure 3.2 (B)).

SiO₂ Particle -Protein Interaction and Protein Modification Studies:

3.5.3 Fluorescence Quenching Studies of α -amylase in the Presence of SiO₂

Particles:

The fluorescence spectroscopy experiments were designed to assess structural changes of α -amylase in the presence of varying concentration of SiO₂ particles. The α -amylase provides strong fluorescence intensity at 360 nm when excited at 280 nm. The quenching effect was observed with gradual increase in the concentration of SiO₂ particles as shown in the figure 3.3(A) and 3.3(C) for NP and MP respectively. The Trp fluorescence was quenched significantly by SiO₂ NP as compared to the SiO₂ MP. To determine the nature of quenching mechanism of the fluorescence emission of α -amylase upon interaction with SiO₂ particles, the Stern–Volmer (SV) equation has been applied as mentioned in the materials & methods section. The quenching effect of the SiO₂ particles on the fluorescence emission of the α -amylase was also found to be concentration dependent as determined by the Stern-Volmer equation and the fluorescence data was plotted to fit in a linear way to confer the state of quenching process as static. Mostly, static type of quenching occurs in the interaction of α -amylase with SiO₂ particles. From SV linear plot, the K_{sv} are calculated for SiO₂ NP and MP interacted α -amylase and found to be 58.315 M⁻¹ and 5.599 M⁻¹.

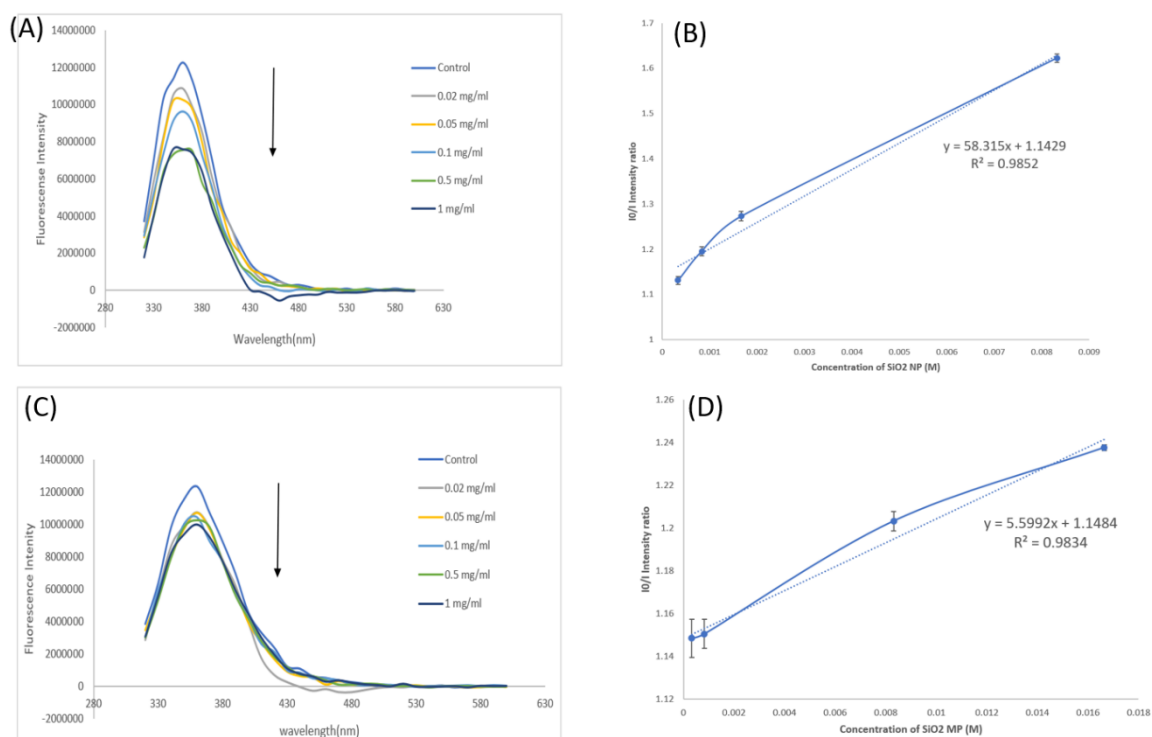


Figure 3.3 Fluorescence spectra of α -amylase in the presence of SiO₂ particles with increasing concentration from 0 to 1 mg/mL, while the enzyme concentration was kept constant, representing the steady state quenching process: (A)& (B): Fluorescence spectra and Stern-Volmer plot of α -amylase interacted with SiO₂ NP with increasing concentration ; (B) Fluorescence spectra and Stern-Volmer plot of α -amylase interacted with SiO₂ MP with increasing concentration.

The biomolecular quenching rate constant K_q for α -amylase interacted with SiO₂ NP and MP are $19.634 \text{ (M}^{-1} \text{ s}^{-1}\text{)}$ and $1.895 \text{ (M}^{-1} \text{ s}^{-1}\text{)}$ respectively. Upon interaction of SiO₂ particles with the α -amylase surface, the binding constant (k_b) and number of binding sites per protein molecule (n) for NP-Protein complex can be determined based on the equation 2. The values of K_b and n for α -amylase upon interaction with varying concentrations of SiO₂ particles were determined from the intercept and slope of $\log [I_0 - I/I]$ versus $\log [Q]$ plots at 298K as shown in Figure 3.4.

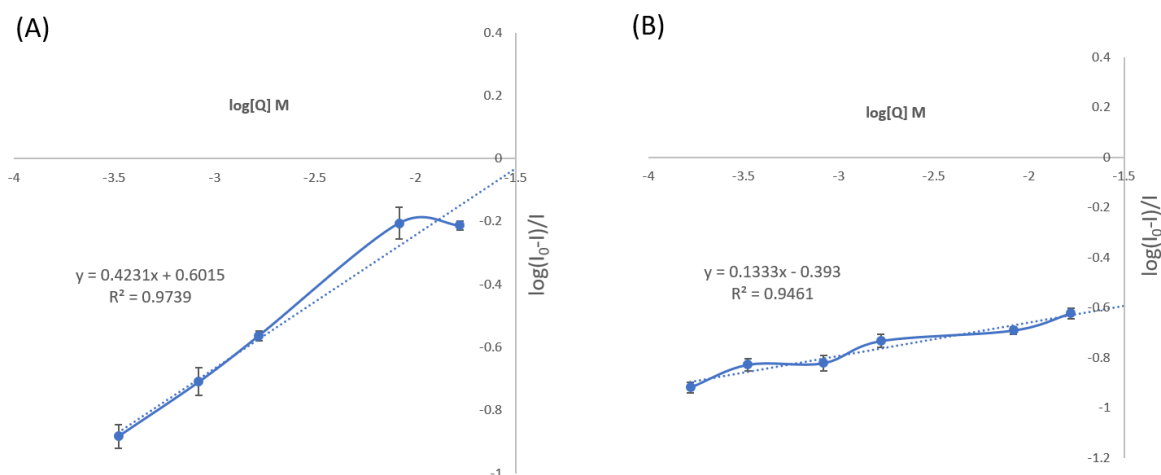


Figure 3.4 Double -logarithmic plots representing the binding constant (K) and number of binding sites (n). (A) α -amylase interacted with SiO₂ NP (B) α -amylase interacted with SiO₂ MP.

The binding constant for SiO₂ NP and SiO₂ MP interacted α -amylase are 0.6015 (M⁻¹) and 0.393 (M⁻¹) and the number of binding sites is 0.423 and 0.133 respectively. It is quite evident that, SiO₂ NP interacted α -amylase has higher binding constant and number of binding sites as compare to α -amylase interacted with SiO₂ MP.

3.5.4 FTIR Analysis:

The FTIR spectra was investigated for the free α -amylase and SiO₂ NP and SiO₂ MP particle interacted α -amylase to identify the structural changes in enzyme because of interaction with SiO₂ particles. The specific stretching and vibrations of the peptide backbone in amide I, II, III band regions give information about different types of secondary structures which includes α -helix, β -sheets, turns, and unordered structures. In addition, Amide I band (covering the infrared band region due to the stretching vibration of C=O and C-N of the amide group

covering approximately between 1600 and 1700 cm^{-1}) is the most sensitive region for probing changes in protein secondary structure.

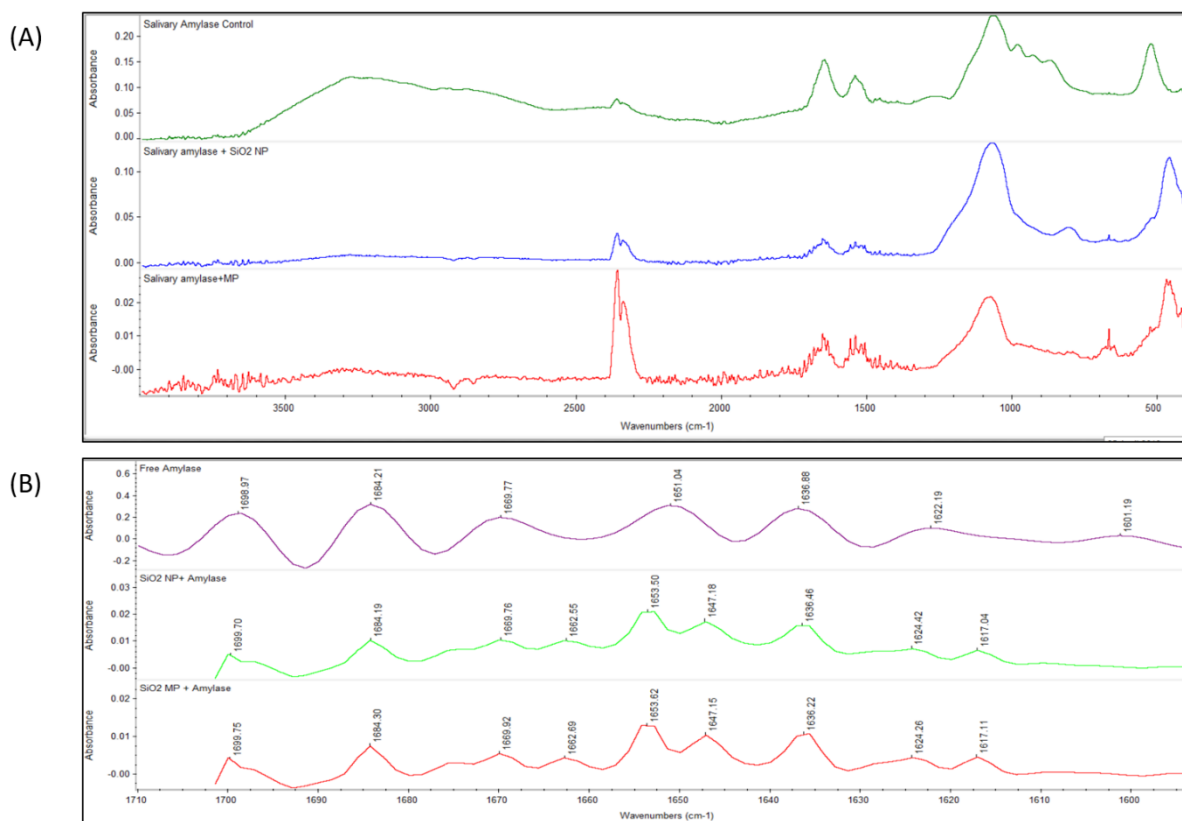


Figure 3.5 FTIR spectra of free α -amylase and SiO₂ interacted α -amylase. (A) FTIR spectra of free α -amylase and SiO₂ NP and MP particle interacted α -amylase and (B) Amide 1 region of α -amylase and SiO₂ particle interacted α -amylase.

As shown in the figure 3.5(A), the original FTIR spectra was different from the free α -amylase spectra, especially in the amide I region from 1600- 1700 cm^{-1} (Figure 3.5(B)) observed obvious change in the shape and peak position of the SiO₂ interacted particles compared to free α -amylase.

The peak at 1651.04 cm^{-1} in the amide I region indicated a higher content of α -helix structure for free α -amylase. However, for SiO₂ particle interacted α -amylase, the peak got shifted with decrease in the peak intensity for SiO₂ NP -A-amylase complex (1653.52 cm^{-1}) followed by

SiO₂ MP α -amylase complex (1653.50 cm⁻¹). Similar trend was observed for β -sheet structure in the Amide I region at 1622.9 cm⁻¹ and 1636.88 cm⁻¹. While, there was no significant shift in the peak at 1636.88cm⁻¹ (Figure 3.5B). The observed peak got shifted to 1624.26cm⁻¹ and 1624cm⁻¹.

The observed peak for the turns remains unchanged for free α -amylase and SiO₂ particle treated α -amylase. However, significant decrease in peak intensity was observed for SiO₂ NP - α -amylase complex followed by SiO₂ MO - α -amylase complex. It is quite observant that, SiO₂ interacted α -amylase underwent higher decrease in the peak intensity as compared to SiO₂ MP with notable peak shift in some region in the Amide I as mentioned above.

Amide III peak were observed in free α -amylase at 1269.04cm⁻¹ whereas it was completely disappeared upon interaction on SiO₂ NP and MP interacted α -amylase.

3.5.5 CD Analysis to Study the Changes in the Secondary Structure of α -amylase upon Interaction with SiO₂ Particles:

The Circular dichroism (CD) spectroscopy was used to determine the secondary structural change of α -amylase upon interaction with SiO₂ NP and MP particles. The CD spectra of free α -amylase and in the presence of SiO₂ particle of NP and MP were monitored in Far -UV range (185-260nm). The typical pattern of α -helical protein with negative band at 222nm and 208 nm and a positive band at 193 nm secondary structure pattern [15] was observed here, as shown in Figure 3.6.

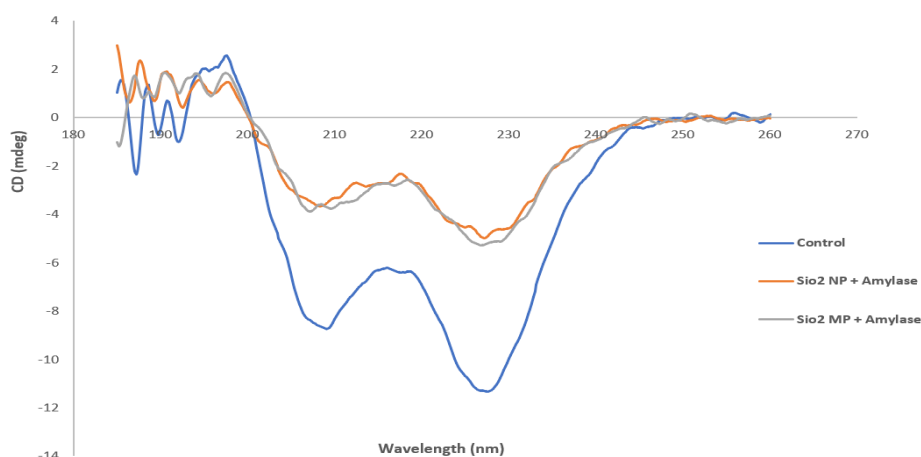


Figure 3.6 Far-UV CD spectra representing the changes in the secondary structure of the α -amylase and the α -amylase interacted with SiO₂ NP and MP particles. The concentration of the concentration of α -amylase and the SiO₂ Particles in the CD study was 100U/mL and 1mg/mL respectively.

Upon interaction with SiO₂ particles, the two-negative peak in the CD spectra (208 and 222nm) and one positive peak at 193nm of α -amylase was decreased which clearly indicates a loss in the α -helical structure. However, there is no significant difference between the SiO₂ NP and SiO₂ MP. The percentage change in the helical content for the SiO₂ NP and SiO₂ MP interacted α -amylase from free α -amylase was 64.54 and 58.72 percent. Whereas, total strands change was observed to be 3.31 and 4.05 percent for SiO₂ NP and SiO₂ MP interacted α -amylase. The change in turns percentage were 1.03 and 1.54 for SiO₂ NP and SiO₂ MP interacted α -amylase respectively. Also, the 208 nm negative and 193nm positive peak for helical structure was slightly shifted for SiO₂ particle interacted α -amylase with a decrease in the intensity of the peak while no significant peak shift was observed at the dichoric band (222 nm) associated with α -helical structure. The peak position at dichoric band didn't shift for α -amylase interacted with both NP and MP of SiO₂ particle. However, a significant decrease in the peak intensity was observed for both the α -amylase-SiO₂ particle complex.

3.6 Discussion:

The main aim of this study was to investigate the differences between the SiO₂ particle at nano and micron size while interacting with salivary enzyme and to see its influence on the enzyme function and structure. We observed α -amylase treated with SiO₂ NP showed higher rate of inhibition on the enzyme activity as compared to amylase treated with SiO₂ MP. Further, our spectroscopic studies confirmed that, change in the protein structure was significant when interacted with SiO₂ NPs, while SiO₂MPs showed less effect on the change in the conformation of the protein structure.

As revealed by Michaelis-Menten constant K_m ; V_{max} and K_i using Lineweaver-Burk plot and Dixon plot, differences in mechanism of enzyme inhibition was observed when α -amylase was interacted with particles of same core chemistry but different sizes (Figure: 3.2). K_m is the measure of the substrate affinity for the enzyme and it change in response to the conformational change of protein upon interaction with SiO₂ particles. Higher values of K_m indicate lower substrate affinity for the enzyme due to the conformational changes[16, 17]. Our results showed higher K_m values for SiO₂ particle interacted α -amylase which suggest conformational change resulting in the lower affinity for the substrate as compared to the free enzyme α -amylase. The decrease in the V_{max} value represent the influence of interaction of SiO₂ particles on the structure of the enzyme, which resulted in reduced or affected enzyme activity. The similar observation with decreased V_{max} and higher K_m was observed in immobilized α -amylase by NPs [18, 19]. Thus the reduction in the enzyme activity could be due to the limited accessibility of the substrate to the active site and structural changes in the enzyme upon interaction with SiO₂ particles.

Moreover, SiO₂ NP interacted α -amylase found to exhibit non- competitive mode of inhibition where both substrate and the inhibitor bind to the enzyme at completely independent active site. Whereas, SiO₂ MP interacted α -amylase showed competitive type of inhibition ,where the V_{\max} remains unchanged with different K_m values .This phenomenon found to be in line with our results showing higher K_m value for SiO₂ MP interacted α -amylase as compared to free α -amylase [20].

Further, the difference in fluorescence quenching and its intensity between α -amylase and SiO₂ particle interacted α -amylase showed significant difference especially the extent of quenching for SiO₂ NP- α -amylase complex was higher as compared to SiO₂ MP interacted α -amylase. Thereby, this phenomenon indicating a change in the environment of Trp residues due to the strong interaction of protein and SiO₂ particles. The enzyme inhibition assay was found to be in line with the quenching data that higher quenching effect of SiO₂ NPs corresponds to stronger inhibition of the α -amylase. Several studies have showed the anti- α -amylase activity by AgNPs, SNPs but not much with the SiO₂ NPs [17]. However , some studies were found on immobilizing α -amylase enzyme with modified magnetic NPs to increase the thermal stability and enzyme activity of α -amylase[21, 22].

The quenching data suggest, the natural chromophore residues of α -amylase can't be quenched by the combination of dynamic and static mode as the Stern-Volmer plot fitted linear for SiO₂ NP and SiO₂ MP interacted α -amylase. Hence it suggests the either dynamic or static type of quenching occurred. Moreover, the biomolecular quenching constant value found to be higher than the value of typical dynamic quenching mechanism which confirms the complex-controlled mechanism between the quencher and the and the protein [23, 24].

The higher fluorescence quenching constant for SiO₂ NP interacted α -amylase describes its strong affinity for the Trp compound, and showed stronger binding affinity to α -amylase than SiO₂ MP. This phenomenon would be due to the hydrophobic interaction involved between

the quencher and the protein surface which is a consistent observation with respect to static type of quenching mechanism [25]. Moreover, the quenching effect of SiO₂ NP found to be concentration dependant whereas, there was no significant quench in the fluorescence with increasing concentration of SiO₂ MP .

Effect of SiO₂ particle binding on the secondary structure of the enzyme α -amylase

The results obtained from CD and Far-UV FTIR confirmed the change in the secondary structure of the protein upon interaction with the SiO₂ particles. Where, SiO₂ NPs showed greater increase in the protein conformation as of the enzyme as compared to SiO₂ MPs. This can be supported by clear observation of peak shift and decrease in peak intensity at specific regions as mentioned below.

The shift in the peak intensity for N-H stretching at 3277.236cm⁻¹; C=O stretching at 1600-1700cm⁻¹ (Amide I region) ; C-H stretching and N-H bending at 1480-1575cm⁻¹ found to be shifted with a noticeable decrease in peak intensity for SiO₂ NP interacted α -amylase followed by SiO₂ MP interacted α -amylase as compared to the free enzyme. Thereby indicating the strong binding interaction of α -amylase and SiO₂ particles which induced secondary structure conformation in the protein enzyme. Similar observation of peak shift was even reported in several studies [17, 26]. It is also evident from the CD spectra that, the intensity of the negative ellipticities of α -amylase decreased upon interaction with SiO₂ Particles suggesting the formation of complex between SiO₂ particles and α -amylase. From the overall observation of enzyme kinetics and spectroscopic studies, in order to understand the effect of SiO₂ particles on the protein enzyme.

The mechanism of interaction of SiO₂ particles with α -amylase enzyme was found to be varied with respect to change in the particle size (NP and MP). This shows that, although they have

similar surface chemistry, the change in the other physicochemical properties can greatly influence the binding interaction of the particles on to the protein enzyme. This observation was noted in the previous studies where, size of the particle plays a significant role in influencing the structure and enzyme activity due to the contribution of the surface curvature[27]. The loss in the α -helical content found to be strongly dependent on size of the SiO_2 particles where the greater loss of secondary structure found to be observed for α -amylase adsorbed on to SiO_2 NPs. The same phenomenon was also observed with lysozyme and SiO_2 particles and several others[27]. There, NPs tends to cause unfolding of adsorbed proteins as compared to the micron particles.

As Several studies had reported the presence of nano sized particles in the food additive E551, which is a common food additive in most of the food products. This could lead to the intake of nanosilica through dietary exposure. Hence, its essential to identify the gaps in the knowledge associated with the interaction of nanosilica in the GIT and its possible uncertainties and outcomes. [28, 29]. Moreover, from our observation and results obtained from this study, the carbohydrate digestion including other digestive enzymes for nutrient absorption may possibly compromise its functions due to the binding interaction of such NPs on to the protein enzymes.

3.7 Conclusion:

In this study, the interaction of α -amylase and SiO_2 particles were investigated in detail. The results suggested that the relative inhibitory activity of α -amylase treated with SiO_2 NPs found to be higher than the α -amylase treated with SiO_2 MPs. Thereby inhibiting the starch hydrolysis by non-competitive and competitive mode of inhibition for α -amylase interacted with SiO_2 NP

and SiO₂ MP respectively. Further, spectroscopic studies revealed that the protein structure of SiO₂ NP interacted α -amylase found to be changed greatly as compared to SiO₂ MP interacted α -amylase. Thereby, SiO₂ NPs could be a potent α -amylase inhibitor where, it has significant possibility to interrupt the process of starch digestion.

3.8 Reference

1. Murugadoss, S., et al., *Toxicology of silica nanoparticles: an update*. Archives of toxicology, 2017. **91**(9): p. 2967-3010.
2. McCracken, C., P.K. Dutta, and W.J. Waldman, *Critical assessment of toxicological effects of ingested nanoparticles*. Environmental Science: Nano, 2016. **3**(2): p. 256-282.
3. Younes, M., et al., *Re-evaluation of silicon dioxide (E 551) as a food additive*. EFSA Journal, 2018. **16**(1).
4. Setyawati, M.I., C.Y. Tay, and D.T. Leong, *Mechanistic investigation of the biological effects of SiO₂, TiO₂, and ZnO nanoparticles on intestinal cells*. Small, 2015. **11**(28): p. 3458-3468.
5. Powell, J.J., et al., *Origin and fate of dietary nanoparticles and microparticles in the gastrointestinal tract*. Journal of Autoimmunity, 2010. **34**(3): p. J226-J233.
6. Docter, D., et al., *The nanoparticle biomolecule corona: lessons learned - challenge accepted?* Chemical Society Reviews, 2015. **44**(17): p. 6094-6121.
7. Ke, P.C., et al., *A Decade of the Protein Corona*. ACS nano, 2017.
8. Butterworth, P.J., F.J. Warren, and P.R. Ellis, *Human α -amylase and starch digestion: An interesting marriage*. Starch-Stärke, 2011. **63**(7): p. 395-405.
9. Bergin, I.L. and F.A. Witzmann, *Nanoparticle toxicity by the gastrointestinal route: evidence and knowledge gaps*. International journal of biomedical nanoscience and nanotechnology, 2013. **3**(1-2): p. 10.1504/IJBNN.2013.054515.
10. McCall, R.L. and R.W. Sirianni, *PLGA Nanoparticles Formed by Single- or Double-emulsion with Vitamin E-TPGS*. Journal of Visualized Experiments : JoVE, 2013(82): p. 51015.
11. Castanho, M.A. and M.J. Prieto, *Fluorescence quenching data interpretation in biological systems: the use of microscopic models for data analysis and interpretation of complex systems*. Biochimica et Biophysica Acta (BBA)-Biomembranes, 1998. **1373**(1): p. 1-16.
12. Ernest, V., et al., *Studies on the effect of AgNP binding on α -amylase structure of porcine pancreas and Bacillus subtilis by multi-spectroscopic methods*. Journal of Luminescence, 2014. **146**: p. 263-268.
13. Sreerama, N. and R.W. Woody, *Estimation of protein secondary structure from circular dichroism spectra: comparison of CONTIN, SELCON, and CDSSTR methods with an expanded reference set*. Analytical biochemistry, 2000. **287**(2): p. 252-260.
14. Shang, L., et al., *pH-dependent protein conformational changes in albumin: gold nanoparticle bioconjugates: a spectroscopic study*. Langmuir, 2007. **23**(5): p. 2714-2721.
15. Holzwarth, G. and P. Doty, *The ultraviolet circular dichroism of polypeptides1*. Journal of the American Chemical Society, 1965. **87**(2): p. 218-228.
16. Kalantari, M., et al., *Lipase immobilisation on magnetic silica nanocomposite particles: effects of the silica structure on properties of the immobilised enzyme*. Journal of Materials Chemistry, 2012. **22**(17): p. 8385-8393.
17. Jiang, S., et al., *In vitro inhibition of pancreatic α -amylase by spherical and polygonal starch nanoparticles*. Food & function, 2018. **9**(1): p. 355-363.
18. Abdel-Naby, M.A., et al., *Immobilization of Bacillus subtilis of its enzymatic properties*. Microbiol. Res, 1998. **153**: p. 1-000.
19. Bindu, V., A. Shanty, and P. Mohanan, *Parameters Affecting the Improvement of Properties and Stabilities of Immobilized α -amylase on Chitosan-metal Oxide Composites*. International Journal of Biochemistry and Biophysics, 2018. **6**(2): p. 44-57.
20. Yoshino, M. and K. Murakami, *A graphical method for determining inhibition constants*. Journal of enzyme inhibition and medicinal chemistry, 2009. **24**(6): p. 1288-1290.

21. Rasouli, N., N. Sohrabi, and E. Zamani, *Influence of a novel magnetic recoverable support on kinetic, stability and activity of beta-amylase enzyme*. Physical Chemistry Research, 2016. **4**(2): p. 271-283.
22. Ernest, V., et al., *Silver nanoparticles: a potential nanocatalyst for the rapid degradation of starch hydrolysis by α -amylase*. Carbohydrate research, 2012. **352**: p. 60-64.
23. Soares, S., N. Mateus, and V. De Freitas, *Interaction of different polyphenols with bovine serum albumin (BSA) and human salivary α -amylase (HSA) by fluorescence quenching*. Journal of Agricultural and Food Chemistry, 2007. **55**(16): p. 6726-6735.
24. Fraiji, L.K., D.M. Hayes, and T. Werner, *Static and dynamic fluorescence quenching experiments for the physical chemistry laboratory*. Journal of chemical education, 1992. **69**(5): p. 424.
25. Sun, L., M.J. Gidley, and F.J. Warren, *The mechanism of interactions between tea polyphenols and porcine pancreatic alpha-amylase: Analysis by inhibition kinetics, fluorescence quenching, differential scanning calorimetry and isothermal titration calorimetry*. Molecular nutrition & food research, 2017. **61**(10): p. 1700324.
26. Miles, A.J. and B.A. Wallace, *Circular dichroism spectroscopy of membrane proteins*. Chemical Society Reviews, 2016. **45**(18): p. 4859-4872.
27. Wu, Z., B. Zhang, and B. Yan, *Regulation of enzyme activity through interactions with nanoparticles*. International journal of molecular sciences, 2009. **10**(10): p. 4198-4209.
28. Dekkers, S., et al., *Presence and risks of nanosilica in food products*. Nanotoxicology, 2011. **5**(3): p. 393-405.
29. Athinarayanan, J., et al., *Presence of nanosilica (E551) in commercial food products: TNF-mediated oxidative stress and altered cell cycle progression in human lung fibroblast cells*. Cell biology and toxicology, 2014. **30**(2): p. 89-100.

GENERAL CONCLUSION:

For the first time we captured the interaction of salivary proteome with dietary particles through a qualitative and quantitative approach. We observed a distinctive difference between each dietary particle on its protein corona composition with differential abundance and fold enrichment of significant salivary proteins. Further, we show that the interactions of particles with proteins could lead to compromised enzyme functions that are vital to the function of saliva. In continuation to that, we wanted to understand the mechanism of interaction of SiO₂ NPs with significant salivary enzyme, α -amylase. Our results suggested that the relative inhibitory activity of α -amylase treated with SiO₂ NPs found to be more efficient than the α -amylase treated with SiO₂ MPs. Further, spectroscopic studies revealed that the protein structure of SiO₂ NP interacted α -amylase found to be changed greatly as compared to SiO₂ MP interacted α -amylase. Thereby, SiO₂ NPs could be a potent α -amylase inhibitor where, it has significant possibility to interrupt the process of starch digestion. Furthermore, our results suggest that the reactivity of NP surface and its physico chemical properties will play critical role in the bio-nano interface of the human gastro intestinal tract.

FUTURE PRESPECTIVES:

The next step of this study is to see, how the food matrix transforms the physico chemical properties of the NPs and influence their fate during the bio-nano interaction in the GIT system. Moreover, when proteins adsorbed on to the surface of the particles, it may undergo structural rearrangement leading to conformational changes and thereby this will render the protein to become dysfunctional due to the changes in the secondary structure. This observation calls for deeper understanding to study the enzyme dysfunctions and the nutritional uptake mechanism in the digestive system in the presence of dietary NPs. The future perspective of this study is

to better understand the behaviour and influence of ingested NPs that entering the GIT system through dietary exposure.